Conservation Strategies That Address Habitat Loss and Fragmentation: Implications for Forest Cover Change and Wildlife Behavior

By

AMY C. COLLINS
DISSERTATION

Submitted in partial satisfaction of the requirements for the degree of

DOCTOR OF PHILOSOPHY

in

Ecology

in the

OFFICE OF GRADUATE STUDIES

of the

UNIVERSITY OF CALIFORNIA

DAVIS

Approved:

Dr. Dirk H. Van Vuren, Chair

Dr. Eric Post

Dr. Gail L. Patricelli

Committee in Charge

2020

Acknowledgements

I owe this achievement, and my subsequent career that comes from it to the following people. Firstly, my supervisor, Dirk Van Vuren, who enabled me to reach my full potential in graduate school. His energy that he put into my training was truly exceptional. He taught me how to be a scientific writer, how to navigate the academic environment, and how to be a better person. I won’t ever be able to thank him enough.

My PIs and co-authors Tim Caro, Monique Borgerhoff Mulder and Fraser Shilling for giving me the opportunity to work on such fantastic, applied conservation projects in America and Africa. I learnt so much. Thanks also to the awards that made this research possible: the Helene M. Overly Memorial Graduate Scholarship, Walter and Elizabeth Howard Wildlife Management Award, Henry A. Jastro Research Scholarship Award, National Center for Sustainable Transportation-NCST Federal Research Grant and Dissertation Grant, UC Davis Corporate Affiliate Fellowship Award, and the Rafe Sagarin Fund for Innovative Ecology Award.

My committee members, Eric Post and Gail Patricelli. Their intellectually stimulating conversations, editorial talent and fabulous mentorship progressed this work into three chapters that I am truly proud of.

Mark Grote, you are an absolute genius, and I have appreciated every minute that we got to work together. Working with you was always a fun journey, and you are an incredibly gifted teacher to boot.

To the communities on Pemba who welcomed us into their homes and showed us all of the hard work they have been doing to help Pemba's forests. Thank you. A huge thanks to the research assistants who I had the pleasure of working alongside for my second and third chapters: Annabelle Louderback-Valenzuela, Ben Banet, Harrison Knapp, Jeff Scott, Mia Guarnieri, Rachel Alsheikh, Parisa Farman, Tricia Nguyen, Vivian Lei, Mia Macneill, Pao Parez, Rich Codington, Jamie Bourdon, Collin Raff, Catherine Le, Dave Waetjen.
. You are all such hard workers, and I had so much fun in the field and/or watching animal videos with you. I'm so excited to see where your careers take you next. Thanks to the wildlife themselves for allowing me to enter their space and capture their behaviour on camera. In particular, to the three mountain lions that I encountered – thanks for being such inspirations.

To the UCD GGE community, you are all an incredible group of people, and I have engaged in such fun, scientific conversations with you all. To the support groups at Davis: geospatial ran by Michele Tobias, WFCB, Davis R Users Group, wildlife journal club, SCB, and the people I TA'ed with – Rachel Wigginton and Nicole Naar were particularly amazing teachers and role models. To my labmates, Jay Riggio, Aviva Rossi, Ellie Bolas, Summer Schlageter, thank you for all of your amazing input along the way, and hilarious office banter.

To my collaborators and mentors in England, Ben Collen and Monni Böhm. Without Ben and Monni I would not have gotten my first real break in applied conservation, would not have gone to grad school in London and America, and published my first first-author paper. Ben's passing away in my third year hit Monni, myself and the ZSL community hard. Losing someone who was so young, and inspirational, was devastating. Ben will always hold that special place of mentor, intellectual genius, and friend. Cheers to Ben.

My amazing group of incredibly smart friends who made me feel at home in a foreign country, and offered me a tremendous support network: Taylor, Luke, Jordan, Madeline, Chris, Kate, Ryan, Joanna, Lily. To everyone who I played frisbee with, I’ve never had so much fun playing a sport (except netball, but they don’t have that in the US). To Rob and Ken for our fun WFCB lunches together. To Eric, Emily, Sarah, Moose, for being the most banterous bunch of balboans. You took board games to a new level. And I of course have to mention all of my besties back in the UK, who offered such fun book club chats: Sam, Layla, Annabel, Hannah, Dee, Nina, Maddy. I miss you all dearly.

Completing a PhD is incredibly hard. Completing a PhD during a global pandemic is damn near impossible. The last 9 months, I had one person in particular who helped me through this seemingly impossible task. Jackie Aliperti offered her support to me every. Day. Her cat memes, jokes, advice and friendship gave me the confidence to get through the bad days and really celebrate the good days. The fact that we were synced up essentially to the day with our work schedules meant that I got to enjoy this wild ride with someone else on board. Jackie you’re my hero, my cat in sparkly emojis, and my dearest friend.

I am so grateful for the love and support from my family, particularly as doing this PhD has meant living on the other side of the world to them for the past five years. Thank you to Mum, Dad, my sister Lucy, my brother-in-law Lee, and my nephews for supporting me in my decision to study abroad. Thanks for keeping me sane and connected to the real outside world. Thanks for encouraging me to think big and think outside the box. I also want to extend this thanks to my new in-law family, Bruce, Mary Ann, Michele, Kristina, Yuriy and Jon. Your support has been incredibly heart-warming, I've loved learning the American ways of life off of you all and have been especially grateful to call you family in the last few Covid-y months.

To my immediate family – Cassie and Lily. Every day you do something bizarre and weird, and I never grow tired of hanging out with you both. You may only be a dog and a cat, but your fluffy, cute little faces add an extra level of entertainment to each day.

Finally, John Mola. Without you by my side, would this have been as an hilarious adventure as it was? Would I have kept my cool during the stressful times? Would I have challenged myself as much as I did? Definitely not. Your support knows no bounds and I feel incredibly honoured to call you my life partner.

Introduction

Abstract

Habitat loss and fragmentation is currently the primary driver of biodiversity decline. Community forest management and wildlife crossing structures are two common conservation strategies applied to mitigate habitat loss and fragmentation. Community forest management is an approach that enables local communities to participate in forest management in order to reduce deforestation, and crossing structures are intended to mitigate the negative impacts of roads in fragmenting the landscape. To implement efficient design, their effectiveness needs to be examined using rigorous and appropriate methods. Herein, I assess the efficacy of each in the context of counterfactual assessments and baseline conditions. Using Pemba Island, Tanzania, as a case study, I monitor Community forest management, and use unprotected areas as the baseline. For wildlife crossing structures I examine structures along California highways, and use adjacent wildland areas absent of roads as the baseline. I employ methods such as remote sensing and hierarchical modeling to decipher forest cover change, wildlife movement, and behavioral responses within a fragmented habitat. I focus on particular anthropogenic stressors that may contribute to the efficacy of Community forest management and wildlife crossing structures, such as human population density, and light and noise pollution. The results offer solutions to the broader conservation community in how to evaluate the conservation tools we are currently utilizing. Furthermore, results guide the decision-making process for wildlife managers, practitioners, and agencies specific to these case studies and future conservation projects.

In my first chapter, I evaluate the Reduced Emissions in Deforestation and Degradation (REDD+) program, that uses payments for ecosystem services as incentives to communities managing and protecting forests. Given the relatively recent addition of REDD+ to the conservation toolkit, evaluation of outcomes from ongoing REDD+ projects is important**.** I examined whether the REDD+ program on Pemba, Tanzania, impacted forest cover change between 2001 – 2018. I controlled for confounding variables and the non-random selection of REDD+ areas by using a statistical matching procedure. The Pemba REDD+ program had no discernible effect on forest cover change during the eight years after initiation. Likewise, I did not detect an effect of environmental or sociological covariates on forest cover. However, REDD+ areas that did better than predicted consisted of small islands accessible only by boat. My findings suggest reducing deforestation through REDD+ is not certain, yet patterns of success at the local level must be recognized, and affordable monitoring should continue as replanting efforts take time to manifest. In addition, examining forest outcomes of REDD+ using high-quality data and appropriate statistical methods is necessary.

In my second and third chapters, I evaluate crossing structures that provide a safe route for wildlife to navigate across roads. The efficacy of wildlife crossing structures might be affected by the exposure of animals to increased noise and artificial light at night produced by vehicles. Therefore, I tested two hypotheses as to how wildlife perceives noise and light, 1) as a risk, contributing to a ‘Landscape of Fear’, or 2) as a refuge, or ‘Human Shield’. Wildlife can respond to fearful stimuli in four ways; spatial avoidance, temporal avoidance, increased anti-predator behavior and altered group sizes. In chapter 2, I examine alterations to spatial and temporal patterns in response to traffic noise and light pollution. I examined species richness (spatial response) and visitation rates (spatial response) of mule deer (prey), bobcats (predator) and coyotes (predator), as well as increased nocturnality (temporal response) in mule deer, bobcats, and coyotes at 26 crossing structures across California, USA, using camera traps. At higher levels of noise pollution, I found that species richness declined, mule deer and bobcat visitations declined, and mule deer nocturnality increased. In response to light pollution, I observed spatial avoidance by bobcats and coyotes and greater nocturnality for all three species. These results suggest that anthropogenic noise and light disturbance contribute to a Landscape of Fear across different trophic levels. However, species richness and deer visitations increased at high levels of light pollution, suggesting a Human Shield of light. These findings indicate wildlife are avoiding anthropogenic noise and light pollution via altering spatiotemporal patterns, and that a Landscape of Fear and Human Shield are non-mutually exclusive mechanisms used to lower predation risk. Species-level differences are likely attributed to trophic level and sensory systems. Using these results, I make recommendations for transportation sectors to better equip crossing structures with appropriate mitigation features.

In chapter 3, I examine the third and fourth response to fearful stimuli - altered anti-predator behavior and group sizes, and incorporate a multi-scale framework to identify differences in fear responses across spatiotemporal scales. Anthropogenic noise pollution is pervasive across the landscape and can be present at three temporal scales; instantaneous, (occurring sporadically over the shortest time scales e.g. milliseconds), acute (more persistent than instantaneous e.g. minutes), and chronic (weeks, years). Instantaneous noise could induce a startle response, whereas acute and chronic noise could alter anti-predator behavior such as vigilance and group size. We examined whether these three levels of anthropogenic noise pollution invoke a Landscape of Fear, ‘habituation’, or Human

Shield response in mule deer (*Odocoileus hemionus*) and coyotes (*Canis latrans*) at highway crossing structures. We placed six camera traps at crossing structure entrances for a period of ~ two months across California to monitor decision-making (flight away from crossing structure or entry into crossing structure) and anti-predator behavior (vigilance, running, foraging, group size). Mule deer and coyotes demonstrated a Landscape of Fear response to instantaneous (2 seconds of noise) and chronic noise (1 week). For acute noise (~20 seconds), mule deer responded positively, most likely using crossing structures as a Human Shield, and coyotes demonstrated no alteration in response, thus likely habituating to localized noise. Our results are the first to demonstrate variations in fear response to anthropogenic noise disturbance across spatiotemporal scales. This dynamic response to fear could alter natural predator-prey interactions and scale up to ecosystem-level consequences such as trophic cascades.

Table of Contents

Chapter 1: Determining the efficacy of community-based forest management in Pemba, Tanzania

Amy C. Collins, Monique Borgerhoff Mulder, Mark N. Grote, Aniruddha Ghosh, James Thorne, Tim Caro

1. Introduction

Globally, approximately 5 million ha of forest are lost annually to human activity (Curtis et al. 2018), with consequences for biodiversity, ecosystem services, and community livelihoods (Barraclough and Ghimire 1995, Thompson et al. 2012). To reduce forest loss and avoid a 'tragedy of the commons', decentralization initiatives such as Community Forest Management (CFM) have been implemented (Ostrom 2015). For developing countries in particular, CFM offers a solution to the high financial cost to governments of patrolling protected areas, lowers animosity between villagers and park managers, and benefits from locally acquired ecological and technological knowledge (Blaikie 2006, Hayes 2006). Yet case studies have shown that some community-managed areas are underperforming, for reasons such as outside organizations bypassing local governance and community leaders profiteering (Roe et al. 2009).

A subset of the CFM initiative is the Reduced Emissions in Deforestation and Degradation (REDD+) program, which uses payments for ecosystem services, such as carbon credits, as incentive structures to communities managing and protecting forests. REDD+ projects have been in progress since the program's introduction in 2007 at the 13th Conference of Parties. From 2010 to 2015, $796 million USD have been received annually in funding pledges

(Norman and Nakhooda 2015, Simonet et al. 2015). As a program that has attracted a lot of funding (90% of which comes from the public sector), it has also attracted its share of scrutiny (Sunderlin et al. 2015). Given the relatively recent addition of REDD+ to the conservation toolkit, evaluation of outcomes from ongoing REDD+ projects is important to enable such projects to alter management approaches if needed, and to prioritize future direction of funding and REDD+ project design.

Prior research addressing the efficacy of CFM, including some REDD+ examples, did not include the time period before the CFM project had commenced, nor include comparisons with outcomes at unmanaged sites, and meta analyses were based on studies that varied in methodologies (Hayes 2006, Eklund et al. 2016). In the last several years, efforts to assess efficacy of CFM projects have emphasized standardizing methods and quantifying the baseline condition for the potential outcome(s) of interest. The baseline condition includes I) a *temporal baseline of condition*, obtained by collecting data leading up to implementation of REDD+; and II) a *spatial baseline of condition*, obtained by comparing formal REDD+ sites to unmanaged or informally managed control sites using a matching procedure (Pressey et al. 2015). Obtaining a spatiotemporal baseline of condition adjusts for any regional-scale factors, such as shifts in the market price of timber, that would influence the outcome(s) in question. Knowledge of the spatiotemporal baseline of condition also enables us to account for forest areas that were strategically selected for inclusion in the REDD+ program. For example, areas with pre-existing low levels of anthropogenic disturbance are often chosen for protection, and become recognized as ‘residual reserves’ (Margules and Pressey 2000). Such non-random selection of low-disturbance areas has the potential for community-managed areas to exhibit an inflated success rate (Margules and Pressey 2000).

Forest cover change has been used as an ecological metric of performance when assessing REDD+, in part as this is required to calculate carbon credit payments. Quantifying forest cover change also enables REDD+ projects to causally link the project outcome to factors that may be driving forest cover change, such as biological characteristics (e.g. rainfall or soil type), or sociological processes (e.g. land tenure rights or human density) (Sunderlin et al. 2015). Although quantifying forest cover change using satellite imagery enables us to capture a spatiotemporal baseline of condition with relative ease, studies evaluating forest cover change in REDD+ projects via satellite imagery are still lacking (Bowler et al. 2012, Hajjar and Oldekop 2018).

On Pemba Island, Tanzania, a REDD+ program was launched in 2010 with the goal of reducing carbon emissions, poverty, and gender inequality. Eighteen of the 121 administrative units or “wards” on Pemba agreed to participate, and they signed Community Forest Management Agreements (CoFMAs; Figure 1.1). Studies have examined the socioeconomic and political elements of the REDD+ program on Pemba via household surveys (Sunderlin et al. 2015, Andrews et al. 2020) and elucidated the proximate causes that drive forest removal: extraction for fuelwood, construction materials, and medicine, and land conversion to agriculture and salt ponds (Siex 2011, Fagerholm 2012, Terra Global Capital 2014). However, the extent of forest cover change on Pemba, and ultimate factors that potentially drive forest cover change, have not been examined.

Here, we use satellite imagery to generate a spatiotemporal baseline of forest condition for all wards across Pemba from 2001 to 2010 and examine the efficacy of CoFMA status from 2010 to 2018 under the program of REDD+. We first determine to what extent forest cover has altered on Pemba from 2001-2010 and from 2010-2018. Second, we ask whether socio-ecological factors other than CoFMA status may affect forest cover change. Third, we test for the possibility of the 'residual reserve' phenomenon by examining the statistical evidence for non-random selection of wards for participation in the REDD+ program. Finally, using a matching procedure to create statistical quasi-controls for CoFMAs, we examine whether CoFMA status under the REDD+ program has had an effect on forest cover change at the ward level.

2. Methods

2.1. REDD+ in Pemba

Pemba is a 920-km^2 island that has experienced roughly 95% forest loss in the last 200 years owing to the human extraction of trees, and more recently to climate change (Siex 2011, Punwong et al. 2013). The island contains a number of isolated forest patches recognized as forming part of the threatened Coastal Forests of Eastern Africa Hotspot (CEPF 2010). The forest types on Pemba vary from coral rag forest, to mangrove forest and high forest (Siex 2011). Pemba also contains three long-standing government-owned Forest Protected areas in the northern region.

The REDD+ program on Pemba, referred to locally as HIMA (*Hifadhi ya Misitu ya Asili ya jamii*), was achieved collaboratively by the Tanzanian Department of Forestry and Non-Renewable Natural Resources (DFNRNR), Royal Norwegian Embassy, JUMIJAZA (*Jumuiya ya*

Uhifadhi wa Misitu Asili-Zanzibar), and Care International. The 18 wards that agreed to participate received an initial start-up fund from REDD+, which communities invested into replanting programs, ecotourism, environmental education, monitoring, and enforcement. However, no ward has received carbon payments since project inception (Andrews and Borgerhoff Mulder 2018, Andrews et al. 2020). As the CoFMAs are designated following the approximate boundaries of wards, the ward is the appropriate unit of analysis for this study.

2.2 Forest Cover Change

i) *Satellite imagery*

To quantify forest cover change within each ward between 2001 and 2018, corresponding to nine years before through eight years after initiation of the Pemba REDD+ program, we analyzed a collection of Landsat 5, Landsat 7, and Landsat 8 satellite images. Landsat imagery was used because it is open source, spans the entire temporal period of the study, has a high spatial resolution (30 m)^2, and has bi-weekly data availability (Cohen and Goward, 2004). A two-year composite image was produced to represent three time periods of interest: 2001 (May 2000 – May 2002) and 2010 (October 2009 – October 2011) from a combination of Landsat 5 and 7 ETM+ imagery, and 2018 (January 2017 - January 2019) from Landsat 8 OLI imagery. All images were top-of-atmosphere reflectance, orthorectified, and had water, cloud, and shadow pixels removed via the mask *CFMASK* in Google Earth Engine version 7.3.2 (Foga et al. 2017, Gorelick et al. 2017). Each pixel in the resulting composite image represented the median, minimum, maximum, and standard deviation value for visible, Near Infrared (NIR), and Normalized Difference Vegetation Index (Near Infrared and Red) bands computed from the input imagery.

ii) Training data

To provide training data for the classification of forest and non-forest cover on Pemba, 440 training data locations were identified through visual inspection of Google Earth Imagery from Pemba for the years 2001, 2010 and 2018. We purposefully selected 440 training data locations using the following criteria: i) each location represented either forest (mangrove; coral rag forest; high forest) or non-forest (agriculture; urban development; bare land; coral rag shrub land; agroforestry) within a 60-m radius buffer ii) forest and non-forest classes were proportionally represented across all training data locations, and iii) locations were evenly distributed across the island. Land cover class at each of the 440 training data locations was determined for 2001, 2010, and 2018 imagery to account for any changes occurring over that period.

To inform visual inspection, prior to obtaining the 440 training data locations, we collected waypoints via a GPS device (Garmin eTrex 20 GPS handheld unit; n = 460) from a field survey in June – July 2015, and classified each one as forest or non-forest. We then cross-referenced 2015 Google Earth Imagery with each waypoint. Many of these waypoints represented locations that were not homogenous for one land use class within a satellite image pixel, and were clustered near villages as a result of limited accessibility in the field; therefore, we opted to exclude the waypoints obtained in the field survey from being used as training data locations in the subsequent landcover classification.

iii) Landcover classification

Images were classified as forest or non-forest for 2001, 2010, and 2018 using a *Random Forest* supervised classification in Google Earth Engine (Gorelick et al. 2017). We randomly assigned 70% of the training data locations to train the Landsat 5, 7 (2001; 2010) and

Landsat 8 (2018) composite data, and used the remaining 30% for post-classification accuracy assessment (Stehman 1997, Hijmans and van Etten 2012). Overall accuracy reported in the confusion matrix of the classified images was >90% for all images and demonstrated excellent agreement with the kappa coefficient (Table S1.1), supporting the suitability of this approach. Potential sources of error in classifications may be attributed to cloud cover distorting satellite imagery and a Scan Line Corrector error on Landsat 7.

To reduce noise (unclassified pixels) generated by the cloud mask, we applied a post-classification 15-m^2 smoothing function, *focal_median*, to each image via Google Earth Engine (Meng et al. 2009, Fuentes et al. 2019). The classified images were clipped to the 121 wards across Pemba, including the 18 CoFMAs. Shapefiles of ward areas were obtained from Global Administration Areas V3.6 (GADM 2018). Shapefiles of government forest protected areas were obtained from the National Bureau of Statistics (United Republic of Tanzania). Due to the different protection status of forests within the government forest protected areas, these areas were excluded from spatial analysis. Within each ward, total area (m^2) of forest and non-forest was quantified for the three years of interest (2001, 2010, 2018) by *zonal statistics* in QGIS (QGIS Development Team, 2018). As a result of the number of cloudy pixels differing for each year of imagery, forest area was divided by total area (forest + non-forest) to obtain a percent of the ward that was forest for each year (Table S1.2).

To calculate the ward-level annual rate of forest change before (2001-2010) and after (2010-2018) the implementation of COFMAs, we used the Compound Interest Law, as per the Food and Agriculture Organization of the United Nations (FAO: MacDicken et al. 2016). Calculations are completed within RStudio V1.1.3 (RStudio Team 2015).

2.3 Socio-ecological factors

To test whether factors other than REDD+ participation could influence the rate and/or direction of forest cover change on all Pemba wards, we collected data associated with i) productivity potential and ii) remoteness and opportunity cost at the ward level. We posited that areas that are highly productive and fertile could impact forest cover change either positively, by promoting tree growth and regeneration, or negatively, by encouraging farmers to remove native forest and plant crops. Remote areas may incur high travel costs (opportunity costs) by vehicle or boat for distribution of illegally harvested timber, which could disincentivize local communities to extract resources, with positive implications for forest cover change. Conversely, remote areas may lack, or be perceived to lack, enforcement and patrolling, with negative implications for forest cover change.

i) Productivity Potential Covariates

We examined precipitation, elevation, slope, and soil type as geographic variables that have the potential to influence vegetation productivity in Pemba (Figure 1.2a - d). We obtained precipitation (mm) for the wettest month (April) from the WorldClim version 2 database (Fick and Hijmans 2017). WorldClim contains the median precipitation from 1970-2000 for 30 seconds (~1km^2) spatial resolution. We acquired data for digital elevation and derived slope from the NASA Shuttle Radar Topographic Mission at a resolution of 1 arc-second (30m^2) through Google Earth Engine (Farr et al. 2007). We obtained soil data from the Soil and Terrain database for Southern Africa (SOTERSAF version 1.0), compiled by the

International Soil Reference and Information Centre (ISRIC; www.isric.org). The spatial resolution of the SOTERSAF data is 1 km, and the temporal coverage is 1950 - 2000. The three soil types that span Pemba are Hypoluvic Arenosols, Eutri-humic Regosols, and Ferralic Cambisols. Using these data, in QGIS we extracted the ward-level median precipitation for April, elevation, slope, and modal soil type.

ii) Remoteness or Opportunity Cost Covariates

We examined ward area, human population density (2012), human population growth rate for 2002 - 2010, distance to road, distance to coast, distance to the city of Wete (the central location for Pemba's government offices and law enforcement), and proportion of ward area that had intact forest prior to REDD+ implementation in 2010 as variables that would potentially affect remoteness or opportunity cost of deforesting within a ward (Figure 1.2e - i). Ward boundary and size were obtained from Global Administration Areas V3.6 (GADM 2018). Ward-level human population density (people/km^2) for 2012, and population growth rate (% annual increase) for 2002-2010, were obtained from the 2002 and 2012 Tanzania Population and Housing Census, Tanzania National Bureau of Statistics (Salerno et al. 2014). We used a combination of primary and secondary road maps compiled by Zansea (Zansea; www.suza.ac.tz/zansea-website) to calculate the per-pixel Euclidean distance to road (km), a map of the Pemba boundary (GADM) to calculate the per-pixel Euclidean distance to coast (km), and the location of Wete to calculate the per-pixel Euclidean distance to Wete using the *proximity* tool in QGIS. For each ward, we then calculated the median Euclidean distance.

To investigate the relationship between forest cover change after CoFMA establishment (2010-2018) and covariates measuring remoteness or productivity, we fit a robust spatial autoregressive model using the *stsls* function in the *spdep* package (Bivand and Wong 2018). We opted to use a spatially explicit model due to the spatial structure in the units of analysis, and the susceptibility of wards to *leakage* – when resource extraction is prohibited in one ward, the extraction pressure shifts to the nearest ward (Bowler et al. 2012). A list of wards and their associated neighboring wards can be found in Table S1.3.

2.4 Evidence of non-random selection of CoFMA wards and matching analysis

To examine the statistical evidence for non-random selection of CoFMA wards, which could inflate estimates of success - and to enable an appropriate match of CoFMA wards to control wards, we conducted covariate matching using all socio-ecological covariates listed above. We first removed control wards that contained zero forest in 2010 (n=2). The resulting dataset had 119 wards total, of which 98 were control wards, which served as a pool of possible matches for the 18 CoFMA wards (Table S1.2).

We then matched each CoFMA ward to five control wards on their covariate similarity ("covariate matching") using Mahalanobis Distances via the *matchIt* package (Ho et al. 2017). The Mahalanobis Distance is a standard distance metric for multivariate continuous observations accommodating covariates of different scales as well as pairwise correlations between the covariates. Propensity score matching is an alternative to covariate matching, but the small number of CoFMA wards in the present sample made fitting a logistic model, which is typically part of the propensity score matching procedure, undesirable.

Furthermore, a bootstrapping method of Otsu and Rai (2017) based on covariate matching is applicable and readily available to our data structure.

For the categorical covariate soil type, the matching procedure required an exact match between CoFMA wards and control wards. Once wards were matched based on one of three soil categories, within each soil category, Mahalanobis distances were calculated for each continuous covariate (precipitation, distance to coast, distance to road, distance to Wete, elevation, slope, population density in 2002, population growth rate in 2012, area of ward, forest area in 2002, forest change 2002-2010). The closest five control wards to each CoFMA ward were then identified using a nearest neighbor method. Matching was performed with replacement, therefore a given control ward may be matched to more than one CoFMA ward (Table S1.4).

2.5 Average effect of CoFMA status

To examine whether CoFMA status had an effect on forest cover change, we used matched CoFMA and control wards to estimate the *average treatment effect on the treated* (ATET) (Jones and Lewis 2015). The ATET could be formed by contrasting the forest cover change (2010 – 2018) in the CoFMA wards with the average forest cover change of their matched controls, then subsequently averaging these contrasts over all CoFMA wards. However, this simple matching estimator has been shown to contain a conditional bias term (Abadie and Imbens 2006). Therefore, we corrected for this bias by fitting a predictive model trained on the controls, and by subsequent use of a *difference in differences* estimator (details below) (Abadie and Imbens 2011, Otsu and Rai 2017). By using a bias-corrected matching estimator, we produced an alternative outcome for forest cover change (2010 – 2018) in each CoFMA ward under the scenario of an absence of REDD+ management.

To make predictions based on the controls, we fit a robust spatial autoregressive model for the rate of forest cover change for 2010 - 2018 as a function of the socio-ecological covariates listed above using the *stsls* function in the *spdep* package (Bivand and Wong 2018). We then estimated the bias corrected ATET. We defined N as the total number of wards, N_t as the number of treated CoFMA wards, and M as the number of control wards matched to each CoFMA ward. For each ward $n = 1,\dots N$, we defined $D_n = 1$, if ward n was a CoFMA ward, $D_n = 0$ if ward n was a control ward. Finally, Y_n is the dependent variable (forest cover change, 2010-2018) for ward n and $\hat{Y}_n$ is the predicted value for ward n from the robust spatial model trained on the controls. The bias corrected estimator of ATET is then:

$$\hat{\tau} = \frac{1}{N_t}\sum_{n=1}^{N} D_n \left[Y_n - \hat{Y}_n - \frac{1}{M}\sum_{j \epsilon J_M(n)} \left(Y_j - \hat{Y}_j\right) \right],$$

where the internal sum is over the set of wards $J_M(n)$ matched to ward n. Multiplication by the indicator D_n implies that only CoFMA wards and their matched control wards contribute to the estimator. $\hat{\tau}$ is a difference in differences statistic: $Y_n - \hat{Y}_n$ is the difference between the observed and predicted forest cover change for CoFMA ward n, and $\frac{1}{M}\sum_{j \epsilon J_M(n)}\left(Y_j - \hat{Y}_j\right)$ is the average difference between the observed and predicted forest cover change for control wards matched to CoFMA ward n.

$\hat{\tau}$ quantifies the average effect of treatment on CoFMA wards, i.e., it contrasts average rates of forest cover change of CoFMAs with average rates that potentially would have occurred, had they remained untreated. The null value, $\tau = 0$, would imply that the treatment had no effect on CoFMA wards; although $\hat{\tau}$ alone is not enough to assess the statistical support for the null or alternative hypotheses. Abadie and Imbens (2012) provide an expression for the variance of $\hat{\tau}$, which can be used to test hypotheses about τ, but our small dataset of 18 CoFMA wards makes use of this expression unadvisable. Otsu and Rai (2017) describe a valid bootstrapping procedure which we adopted here to obtain upper and lower confidence limits for τ.

We defined the sample elements to be bootstrapped as follows: for each *n* = 1,…*N*, $e_n = Y_n - \hat{Y}_n$, and $K_M(n)$ is the number of times ward *n* is used as a match. Subsequently,

$$e_n^* = \begin{cases} e_n; \text{ if ward } n \text{ is treated} \\ \dfrac{-K_M(n)}{M} e_n; \text{ if ward } n \text{ is a control.} \end{cases}$$

The bias corrected estimator of ATET can be written as the average $\frac{1}{N_t} \sum_{n=1}^{N} e_n^*$. A valid bootstrap confidence interval for τ can then be obtained by resampling $e_1^*, \dots e_N^*$ (Otsu and Rai 2017).

3. Results

3.1 Forest cover change

Overall forest extent on Pemba (excluding the Forest Protected Areas) was 260 km^2 in 2001 (25% of the area analyzed), 190 km^2 in 2010 (18%), and 154 km^2 in 2018 (15%) (Figure 1.3). Median forest cover change was -3.1 %/yr for 2001 – 2010, and -3.4%/yr for 2010 – 2018. Ward-level rates of forest cover change were generally negative, with 89% of wards experiencing a reduction in forest area during 2001 - 2010 and 75% during 2010 – 2018. Table S1.2 provides the percent change for each ward.

3.2 Socio-ecological factors

We found no evidence that factors associated with remoteness (ward area; human density; human growth rate; distance to road; distance to coast; distance to Wete; proportion of area with prior intact forest) had an impact on forest cover change for 2010-2018 across all wards on Pemba. Likewise, we were unable to detect an effect of productivity potential (precipitation; elevation; slope; soil type) on forest cover change. The estimated effects of these covariates are reported in Table S1.5.

3.3 Evidence of non-random selection of CoFMA wards and matching analysis

Prior to matching, the standardized mean difference of CoFMA wards versus control wards was large for certain covariates: in particular, the ratio of forest to ward area (Figure 1.4). CoFMA wards had a larger proportion of ward containing forest than control wards, suggesting that CoFMA selection was biased towards wards containing a larger proportion of forest. Compared to the controls, areas chosen for CoFMAs had more forest relative to ward area in 2010, higher precipitation, and greater total ward area (Figure 1.4). In contrast, areas chosen for CoFMAs tended to be closer to the sea and have lower population density (Figure 1.4). The post-match differences showed that selection of matches brought the standardized mean difference closer to zero, and therefore brought the explanatory variables of the matched controls into greater concordance with those of the CoFMA wards.

3.4 Average effect of CoFMA status

Finally, our analysis suggests that CoFMA wards had a slight positive effect on average, but uncertainty about the estimated effect is large compared to its magnitude ($\hat{\tau}$ = 0.07 %/yr, bootstrap 95% CI = - 2.2, 2.6). Although the average difference in forest cover change between treated wards and their matched controls is 0.07 %/yr, the bootstrap interval contains the value zero, therefore we were unable to rule out the possibility that control and CoFMA wards were equivalent in their rates of forest change, or that CoFMAs were doing slightly worse than controls (Figure 1.5).

4. Discussion

Our results imply that Community Forest Management Agreements (CoFMAs) had no demonstrable effect on forest cover change in Pemba wards during the eight years after initiation (Figure 1.5). These findings add to the growing evidence that reducing deforestation through community forest management (CFM) is not certain, and efficacy varies within and between projects (Somanathan et al. 2009, Urech et al. 2013, Pollini et al. 2014, Oldekop et al. 2019).

4.1 Factors contributing to the average effect of CoFMAs

Spatiotemporal factors likely contribute to our finding that CoFMA status does not have an effect on forest cover change. The spatial extent of Pemba is small – the island is approximately the size of Manhattan, NY. The amount of forest on Pemba is also small - in

2001, 25% of Pemba was forested, which was reduced to 15% by 2018 (Figure 1.3). Furthermore, the island is divided into >100 wards, which we use as the unit of analysis in our study (Figure 1.1). This reduced spatial scale is important in two ways. First, the buffer zone for reducing the likelihood of leakage (the spatial shift in extraction to a location outside the boundary) is small; thus, it is relatively easy for people to travel across ward boundaries and extract unsanctioned resources from another ward's forest. Second, relatively small levels of unregulated take or land use change have a large influence on the percent of forest cover within that ward. Other studies have also reported on the high variability of forest cover change between communities (Blackman et al. 2017, Santika et al. 2017), and the ability for larger forests to withstand deforestation pressure more effectively (Chhatre and Agrawal 2009, Oldekop et al. 2019).

When considering temporal scale, we focused on change across time, creating a simple before-after CoFMA scenario, and accounting for years with few satellite images – a common issue given Pemba's particular geographic location and cloud cover (Van Den Hoek et al. 2014). However, the eight years that elapsed between CoFMA initiation and the completion of our study may not have been long enough to detect the positive benefits of replanting programs through our satellite imagery. Studies that have demonstrated reduced deforestation in CFMs have had the benefit of a longer time frame and show that CFMs that have been in place for more than a decade are more likely to have reduced deforestation (Rasolofoson et al. 2015, Oldekop et al. 2019). To that end, we contend that REDD+ on Pemba remains promising, and we encourage localized forest monitoring to continue on Pemba in addition to remote sensing analyses, to be able to capture the future extent of reforestation efforts.

We focused on factors that represented productivity potential and opportunity cost. However, processes not measured in our study may have influenced forest removal. We used ward-level human population growth following the 2002 and 2012 population census, but growth rates since 2012 may have influenced forest cover change patterns we witnessed for 2010 – 2018. For example, anecdotal evidence suggests that four wards that experienced the greatest reversal from a positive rate of forest change (2002-2010) to a negative rate of forest change (2010-2018) had rapid rates of human population increase in recent years (M. Borgerhoff Mulder, unpublished). Likewise, Euclidean distance measures may have underestimated the remoteness of some areas. For instance, the three CoFMAs that had the most improved rate of forest cover change in comparison to the predicted were comprised of small islands accessible only by boat (Mtambwe Kusini; Kisiwa Panza, Shumba Mjini). Leakage associated with forest protected areas is a commonly cited phenomenon in the literature (Ewers and Rodrigues 2008, Wunder 2008). The five wards in proximity to the Ngezi Vumawimbi Nature Reserve exhibited worse rates of forest cover change relative to that predicted. Linkages between forest protected areas and the CFM approach warrant further exploration (Porter-Bolland et al. 2012, Sims and Alix-Garcia 2017). Finally, incentive structures have altered over time; CoFMA wards on Pemba have benefitted from an initial community payment in return for REDD+ inclusion and from strong land tenure rights. Accordingly, several wards that were not initially included have vocalized a desire to become REDD+ certified (Andrews et al. 2020). Conversely, additional carbon-based payments to communities have not appeared, due to the unreliable voluntary cap and trade system (Norman and Nakhooda 2015, Sunderlin et al. 2015); as such one of the 18 CoFMA wards has indicated they intend to renounce their status. Understanding factors influencing forest cover change may require examining specific cases in more detail in addition to examining the average effect. Accordingly, other studies have discussed that reporting the average treatment effect alone can mask the idiosyncratic spatiotemporal variation in forest cover change (Chhatre and Agrawal 2009, Fernandes et al. 2016, Lund et al. 2018).

4.2 Techniques for assessing CFMs

As expected, our results indicated that wards on Pemba were non-randomly selected as CoFMAs (Figure 1.4). As such, we accounted for non-random selection of CoFMAs by using a spatiotemporal baseline of condition and a high number of appropriate socio-ecological covariates. We also implemented a bias-corrected matching procedure with bootstrapping; a particularly effective protocol for estimating the average effect of CoFMAs when the number of designated CoFMA areas is low (Abadie and Imbens 2006, 2011). Our method satisfies recent calls for more rigorous experimental designs when assessing outcomes of REDD+ and other CFM projects (Andam et al. 2008, Bowler et al. 2012, Borner et al. 2016, Hajjar et al. 2016, Hajjar and Oldekop 2018, Schleicher et al. 2019).

4.3 Forest cover change

Our results demonstrate that yearly rate of forest loss for all wards across Pemba was slightly higher in the time period after CoFMA implementation (2001-2010 = -3.1%/yr vs 2010 – 2018 = -3.4%/yr; Figure 1.3). This scale of deforestation is seen across other islands such as Madagascar and Hawaii (Harper et al. 2007, Asner et al. 2016) and is in keeping with the notion that oceanic islands are particularly vulnerable regions (Hansen et al. 2006, Gilman et al. 2008, Ward et al. 2016). Although we were unable to identify specific ward-level drivers of forest cover change, Pemba's forests remain vulnerable to human extraction, pollutants, and land conversion, and Pemba's mangroves face additional climate change related stressors such as salt inundation resulting from sea level rise (Ngoile and Shunula 1992, Punwong, Marchant, and Selby 2013, Hamad, Mchenga, and Hamisi 2014; Mchenga and Ali 2015). These stressors on Pemba's forests need to be considered when assessing the future designation of sites on Pemba and future potential outcomes of REDD+. In addition, other REDD+ projects should factor in a sites' capability as a refuge area from climate-related pressures (Santika et al. 2017, Maharaj et al. 2019).

4.4 The future of REDD+ and CFMs

Since REDD+ came into existence following the Kyoto Protocol in 2012, REDD+ projects have been under intense scrutiny. Although the debate surrounding the efficacy of the REDD+ global strategy continues (Redford and Padoch 2013, Fletcher et al. 2016, 2017), it is also recognized that due to the complexities and unique settings of REDD+ projects, each project can offer new insights and potential lessons to be learnt (Simonet et al. 2015, Andrews et al. 2020). Therefore, it is important to assess local projects systematically and individually.

Our study supports the concept that "decentralization is not a panacea" (Paulson Priebe et al. 2015); there was no overall effect on forest cover change of ward participation in REDD+, though CoFMA wards that did better than expected are highlighted and should be examined in closer detail. In addition, enough time needs to elapse for the benefits of replanting projects to manifest, and our results demonstrate the importance of considering spatiotemporal scale when examining forest cover change as an outcome of CFM. These lessons learnt from Pemba can be applied to REDD+ and CFM globally, and future work should continue to monitor forest cover change using high-quality data and appropriate methodology. Given our new understanding of forest cover change on Pemba, attention should also be directed to linking these rates to additional outcomes of REDD+ projects, in the form of biodiversity, poverty alleviation improved livelihoods (Ellis and Freeman 2006, Strassburg et al. 2010, Panfil and Harvey 2016, Rasolofoson et al. 2017, Sollmann et al. 2017).

5. Acknowledgements

We thank We thank the 2nd Vice President's Office and the Ministry of Agriculture and Natural Resources for permission to conduct research in Zanzibar, Kate Tiedeman and Jay Riggio for help with Google Earth Engine code, Miza Khamis for accessing Pemba shape files at the DFNRNR, Said Juma Ali, Bidawa Bakari Hamadi, Hassan Sellieman Khamis, Abdi Mzee and Assaa Sharif Ngwali for project implementation and field support in Pemba, and Jon Salerno for census and population growth data. Funding for this project was made possible by the Rafe Sagarin Fund for Innovative Ecology.

6. Literature Cited

Abadie, A., and G. W. Imbens. 2006. LARGE SAMPLE PROPERTIES OF MATCHING ESTIMATORS. Econometrica 74:235–267.

Abadie, A., and G. W. Imbens. 2011. Bias-Corrected Matching Estimators for Average Treatment Effects. Journal of Business and Economic Statistics 29:1–11.

Andam, K. S., P. J. Ferraro, A. Pfaff, G. A. Sanchez-Azofeifa, and J. A. Robalino. 2008. Measuring the effectiveness of protected area networks in reducing deforestation. Proceedings of the National Academy of Sciences 105:16089 LP – 16094.

Andrews, J. B., T. Caro, S. Juma Ali, A. C. Collins, B. Bakari Hamadi, H. Sellieman Khamis, A. Mzee, A. Sharif Ngwali, and M. Borgerhoff Mulder. 2020. Does REDD+ have a chance? Implications from Pemba, Tanzania. Oryx:1–7.

Andrews, J., and M. Borgerhoff Mulder. 2018. Cultural group selection and the design of

REDD+: insights from Pemba. Sustainability science 13:93–107.

Asner, G. P., S. Sousan, D. E. Knapp, P. C. Selmants, R. E. Martin, R. F. Hughes, and C. P. Giardina. 2016. Rapid forest carbon assessments of oceanic islands: a case study of the Hawaiian archipelago. Carbon balance and management 11:1.

Barraclough, S., and K. Ghimire. 1995. Forests and Livelihoods The Social Dynamics of Deforestation in Developing Countries. Palgrave Macmillan UK.

Bivand, R., and D. W. S. Wong. 2018. Comparing implementations of global and local indicators of spatial association. TEST 27:716–748.

Blackman, A., L. Corral, E. Santos, and G. P. Asner. 2017. Titling indigenous communities protects forests in the Peruvian Amazon. Pnas 114:4123–4128.

Blaikie, P. 2006. Is Small Really Beautiful? Community-based Natural Resource Management in Malawi and Botswana. World Development 34:1942–1957.

Borner, J., K. Baylis, E. Corbera, D. Ezzine-de-blas, P. J. Ferraro, R. Lapeyre, U. M. Persson, S. Wunder, and J. Honey-rose. 2016. Emerging Evidence on the Effectiveness of Tropical Forest Conservation. PLoS ONE 11:1–11.

Bowler, D. E., L. M. Buyung-ali, J. R. Healey, J. P. G. Jones, T. M. Knight, and A. S. Pullin. 2012. Does community forest management provide global environmental benefits and improve local welfare? Frontiers in Ecology and the Environment 10:29–36.

Capital, T. G. 2014. HIMA (Hifadhi ya Misitu ya Asili ya jamii) REDD+ Program PD v-0-19 DRAFT. vcsprojectdatabase.org/#/pipeline_details/PL1381.

CEPF. 2010. Conservation Outcomes Eastern Arc Mountains and Coastal Forests.

Chhatre, A., and A. Agrawal. 2009. Trade-offs and synergies between carbon storage and livelihood benefits from forest commons. Proceedings of the National Academy of Sciences 106:17667 LP – 17670.

Cohen B, Goward, S. N. 2004. Landsat's Role in Ecological Applications of Remote Sensing. BioScience 54:535–545.

Congalton, R. G. 1991. A Review of Assessing the Accuracy of Classifications of Remotely Sensed Data. Remote Sensing of Environment 37:35–46.

Curtis, P. G., C. M. Slay, N. L. Harris, A. Tyukavina, and M. C. Hansen. 2018. Classifying drivers of global forest loss. Science 361:1108–1111.

Eklund, J., F. G. Blanchet, J. Nyman, R. Rocha, T. Virtanen, and M. Cabeza. 2016. Contrasting spatial and temporal trends of protected area effectiveness in mitigating deforestation in Madagascar. Biological Conservation 203:290–297.

Ellis, F., and H. A. Freeman. 2006. Rural Livelihoods and Poverty Reduction Strategies in Four African Countries. Journal of Development Studies 40:1–30.

Ewers, R. M., and A. S. L. Rodrigues. 2008. Estimates of reserve effectiveness are confounded by leakage. Trends in Ecology & Evolution 23:113–116.

Fagerholm, N. 2012. Community inhabitants' values and benefits in dynamic tropical forest landscapes Participation and spatial analysis in landscape knowledge integration. University of Turku.

Farr, T. G., P. A. Rosen, E. Caro, R. Crippen, R. Duren, S. Hensley, M. Kobrick, M. Paller, E.

Rodriguez, L. Roth, D. Seal, S. Shaffer, J. Shimada, J. Umland, M. Werner, M. Oskin, D. Burbank, and D. Alsdorf. 2007. The Shuttle Radar Topography Mission. Reviews of Geophysics 45:1–33.

Fernandes, A., T. Avelino, K. Baylis, and J. Honey-rose. 2016. Goldilocks and the Raster Grid : Selecting Scale when Evaluating Conservation Programs. PLoS ONE 11:1–24.

Fick, S. E., and R. J. Hijmans. 2017. WorldClim 2: new 1-km spatial resolution climate surfaces for global land areas. International Journal of Climatology 37:4302–4315.

Fletcher, R., W. Dressler, B. Bram, and Z. R. Anderson. 2016. Questioning REDD + and the future of market-based conservation. Conservation biology 30:673–675.

Fletcher, R., W. Dressler, B. Bram, and Z. R. Anderson. 2017. Debating REDD + and its implications : reply to Angelsen et al . Conservation biology 31:721–723.

Foga, S., P. L. Scaramuzza, S. Guo, Z. Zhu, R. D. Dilley, T. Beckmann, G. L. Schmidt, J. L. Dwyer, M. J. Hughes, and B. Laue. 2017. Remote Sensing of Environment Cloud detection algorithm comparison and validation for operational Landsat data products. Remote Sensing of Environment 194:379–390.

Fuentes, I., J. Padarian, F. Van Ogtrop, and R. Willem Vervoort. 2019. Spatiotemporal evaluation of inundated areas using MODIS imagery at a catchment scale. Journal of Hydrology 573:952–963.

GADM. 2018. GADM database of Global Administrative Areas version 3.6. www.gadm.org.

Gilman, E. L., J. Ellison, N. C. Duke, and C. Field. 2008. Threats to mangroves from climate change and adaptation options : A review. Aquatic Botany 89:237–250.

Gorelick, N., M. Hancher, M. Dixon, S. Ilyushchenko, D. Thau, and R. Moore. 2017. Google Earth Engine: Planetary-scale geospatial analysis for everyone. Remote Sensing of Environment 202:18–27.

Hajjar, R., and J. A. Oldekop. 2018. Research frontiers in community forest management. Current Opinion in Environmental Sustainability 32:119–125.

Hajjar, R., J. A. Oldekop, P. Cronkleton, E. Etue, P. Newton, A. J. M. Russel, J. S. Tjajadi, W. Zhou, and A. Agrawal. 2016. The data not collected on community forestry. Conservation Biology 30:1357–1362.

Hamad, H. M., I. S. S. Mchenga, and M. I. Hamisi. 2014. STATUS OF EXPLOITATION AND REGENERATION OF MANGROVE FORESTS IN PEMBA ISLAND , TANZANIA. Global Journal of Bio-Science and Biotechnology 3:12–18.

Hansen, J., M. Sato, R. Ruedy, K. Lo, D. W. Lea, and M. Medina-elizade. 2006. Global temperature change. Pnas 103:14288–14293.

Harper, G. J., M. K. Steininger, C. J. Tucker, D. Juhn, and F. Hawkins. 2007. Fifty years of deforestation and forest fragmentation in Madagascar. Environmental Conservation 34:325–333.

Hayes, T. M. 2006. Parks, People, and Forest Protection: An Institutional Assessment of the Effectiveness of Protected Areas. World Development 34:2064–2075.

Hijmans, R. J., and J. van Etten. 2012. raster: Geographic analysis and modeling with raster data. R package version 2.0–12.

Ho, D., K. Imai, G. King, E. Stuart, and A. Whitworth. 2017. Nonparametric Preprocessing for Parametric Casual Interference.

Jones, K. W., and D. J. Lewis. 2015. Estimating the counterfactual impact of conservation programs on land cover outcomes: The role of matching and panel regression techniques. PLoS ONE 10:1–22.

Lund, J. F., R. L. Rutt, and J. Ribot. 2018. Trends in research on forestry decentralization policies. Current Opinion in Environmental Sustainability 32:17–22.

MacDicken, K., Ö. Jonsson, L. Piña, S. Maulo, V. Contessa, Y. Adikari, M. Garzuglia, E. Lindquist, G. Reams, and R. D'Annunzio. 2016. Global Forest Resources Assessment 2015: how are the world's forests changing? FAO.

Maharaj, S. S., H. Asmath, S. Ali, J. Agard, S. A. Harris, and M. New. 2019. Land Use Policy Assessing protected area effectiveness within the Caribbean under changing climate conditions : A case study of the small island, Trinidad. Land Use Policy 81:185–193.

Margules, C. R., and R. L. Pressey. 2000. Systematic conservation planning. Nature 405:243–53.

Mchenga I. S. S., Ali, A. I. 2015. A Review of Status of Mangrove Forest in Zanzibar Island, Tanzania. International Journal of Research and Review 2:518–526.

Meng, Q., B. E. Borders, C. J. Cleszewskl, and M. Madden. 2009. Closest spectral fit for removing clouds and cloud shadows. Photogrammetric Engineering and Remote Sensing 75:569–576.

Ngoile, M. A. K., and J. P. Shunula. 1992. Status and exploitation of the mangrove and associated fishery resources in Zanzibar. Hydrobiologia 247:229–234.

Norman, M., and S. Nakhooda. 2015. The State of REDD + Finance.

Oldekop, J. A., K. R. E. Sims, B. K. Karna, M. J. Whittingham, and A. Agrawal. 2019. Reductions in deforestation and poverty from decentralized forest management in Nepal. Nature Sustainability 2:421–428.

Ostrom, E. 2015. Governing the commons. Cambridge university press.

Otsu, T., and Y. Rai. 2017. Bootstrap Inference of Matching Estimators for Average Treatment Effects. Journal of the American Statistical Association 112:1720–1732.

Panfil, S. N., and C. A. Harvey. 2016. REDD + and Biodiversity Conservation: A Review of the Biodiversity Goals, Monitoring Methods, and Impacts of 80 REDD + Projects. Conservation Letters 9:143–150.

Paulson Priebe, M. E., T. Evans, K. Andersson, and E. Castellanos. 2015. Decentralization, forest management, and forest conditions in Guatemala. Journal of Land Use Science 10:425–441.

Pollini, J., N. Hockley, F. Muttenzer, and B. Ramamonjisoa. 2014. The transfer of natural resource management rights to local communities. Page Conservation and Environmental Management in Madagascar.

Porter-Bolland, L., E. A. Ellis, M. R. Guariguata, R.-M. Isabel, S. Negrete-Yankelevich, and V. Reyes-garcía. 2012. Community managed forests and forest protected areas: An assessment of their conservation effectivness across the tropics. Forest Ecology and

Management 268:6–17.

Pressey, R. L., P. Visconti, and P. J. Ferraro. 2015. Making parks make a difference: poor alignment of policy, planning and management with protected-area impact, and ways forward. Philosophical transactions of the Royal Society of London. Series B, Biological sciences 370:20140280.

Punwong, P., R. Marchant, and K. Selby. 2013. Holocene mangrove dynamics and environmental change in the Rufiji Delta, Tanzania. Vegetation History and Archaeobotany 22:381–396.

Rasolofoson, R. A., P. J. Ferraro, C. N. Jenkins, and J. P. G. Jones. 2015. Effectiveness of Community Forest Management at reducing deforestation in Madagascar. Biological Conservation 184:271–277.

Rasolofoson, R. A., P. J. Ferraro, G. Ruta, M. S. Rasamoelina, P. L. Randriankolona, H. O. Larsen, and J. P. G. Jones. 2017. Impacts of Community Forest Management on Human Economic Well-Being across Madagascar. Conservation Letters 10:346–353.

Redford, K. H., and C. Padoch. 2013. Fads , Funding , and Forgetting in Three Decades of Conservation. Conservation biology 27:437–438.

Roe, D., F. Nelson, and C. Sandbrook. 2009. Community management of natural resources in Africa: Impacts , experiences and future directions.

RStudio Team. 2015. RStudio: Integrated Development for R. RStudio, Inc., Boston, MA.

Salerno, J. D., M. B. Mulder, and S. C. Kefauver. 2014. Human migration, protected areas, and conservation outreach in Tanzania. Conservation biology 28:841–850.

Santika, T., E. Meijaard, S. Budiharta, E. A. Law, A. Kusworo, J. A. Hutabarat, T. P. Indrawan, M. Struebig, S. Raharjo, I. Huda, A. D. Ekaputri, S. Trison, M. Stigner, and K. A. Wilson. 2017. Community forest management in Indonesia : Avoided deforestation in the context of anthropogenic and climate complexities. Global Environmental Change 46:60–71.

Schleicher, J., J. Eklund, M. D. Barnes, J. Geldmann, J. A. Oldekop, and J. P. G. Jones. 2019. Statistical matching for conservation science. Conservation Biology 00:1–12.

Siex, K. S. 2011. Protected Area Spatial Planning for Unguja and Pemba Islands, Zanzibar. Page A Consultancy to the UNDP-GEF-Extending the Coastal Forest Area Protected Area subsystem in Tanzania. Wildlife Conservation Society.

Simonet, G., A. Karsenty, P. Newton, C. De Perthuis, B. Schaap, and C. Seyller. 2015. REDD + projects in 2014 : an overview based on a new database and typology. Les Cahiers de la Chaire Economie du Climat Information and debates Series.

Sims, K. R. E., and J. Alix-Garcia. 2017. Parks versus PES: Evaluating direct and incentive-based land conservation in Mexico. Journal of Environmental Economics and Management 86:8–28.

Sollmann, R., A. Mohamed, L. Ambu, P. Lagan, S. Mannan, R. C. Ong, A. Langner, B. Gardner, and A. Wilting. 2017. Quantifying mammal biodiversity co-benefits in certified tropical forests. Diversity and Distributions 23:317–328.

Somanathan, E., R. Prabhakar, and B. Singh. 2009. Decentralization for cost-effective conservation. Pnas 106:4143–4147.

Stehman, S. V. 1997. Selecting and interpreting measures of thematic classification accuracy. Remote sensing of Environment 62:77–89.

Strassburg, B. B. N., A. Kelly, A. Balmford, R. G. Davies, H. K. Gibbs, A. Lovett, L. Miles, C. D. L. Orme, J. Price, R. K. Turner, and A. S. L. Rodrigues. 2010. Global congruence of carbon storage and biodiversity in terrestrial ecosystems. Conservation Letters 3:98–105.

Sunderlin, W. D., E. O. Sills, A. E. Duchelle, A. D. Ekaputri, D. Kweka, M. A. Toniolo, S. Ball, N. Doggart, C. D. Pratama, J. T. Padilla, A. Enright, and R. M. Otsyina. 2015. REDD+ at a critical juncture: assessing the limits of polycentric governance for achieving climate change mitigation. International Forestry Review 17:400–413.

Team, Q. D. 2018. QGIS Geographic information System. Open Source Geospatial Foundation Project.

Thompson, I. D., J. Ferreira, T. Gardner, M. Guariguata, L. P. Koh, K. Okabe, Y. Pan, C. B. Schmitt, J. M. Tylianakis, J. Barlow, V. Kapos, W. A. Kurz, J. A. Parrotta, M. D. Spalding, and N. van Vliet. 2012. Forest biodiversity, carbon and other ecosystem services : relationships and impacts of deforestation and forest degradation. Pages 22–41 IUFRO World Series. 31st edition. International Union of Forest Research Organisations, Vienna, Austria.

Urech, Z. L., J.-P. Sorg, and H. R. Felber. 2013. Challenges for Community-Based Forest Management in the KoloAla Site Manompana. Environmental Management 51:602–615.

Ward, R. D., D. A. Friess, R. H. Day, and R. A. Mackenzie. 2016. Impacts of climate change on mangrove ecosystems : a region by region overview. Ecosystem Health and Sustainability 2.

Wunder, S. 2008. Chapter 7 How do we deal with leakage ? Pages 65–75 Moving ahead with REDD: Issues, options and implications.

Figures

Figure 1.1. Location of Pemba Island, Tanzania, and the 18 wards that signed Community Forest Management Agreements (green).

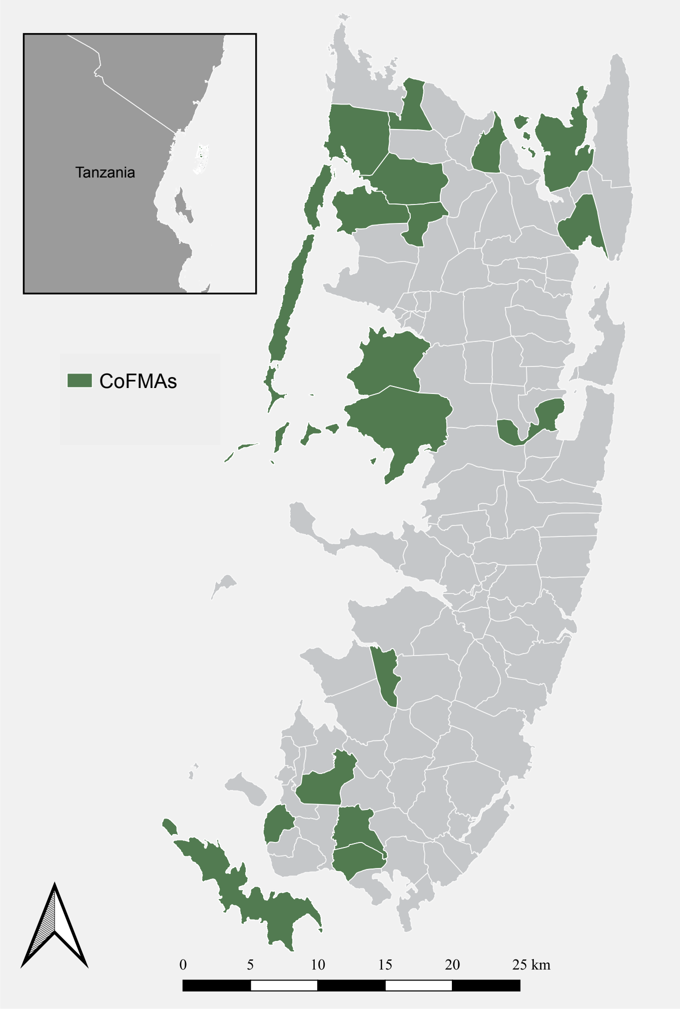

Figure 1.2. Heat map of covariates used for matching analysis on Pemba Island, Tanzania: (a) median April precipitation mm (1970-2000) (b) elevation (mm) (c) slope (d) soil type; Hypoluvic Arenosols, Eutri-humic Regosols, and Ferralic Cambisols (e) human density per km^2 per ward in 2002 (f) human population growth rate for 2002-2012 (g) distance to road (h) distance to coast (i) distance to Wete.

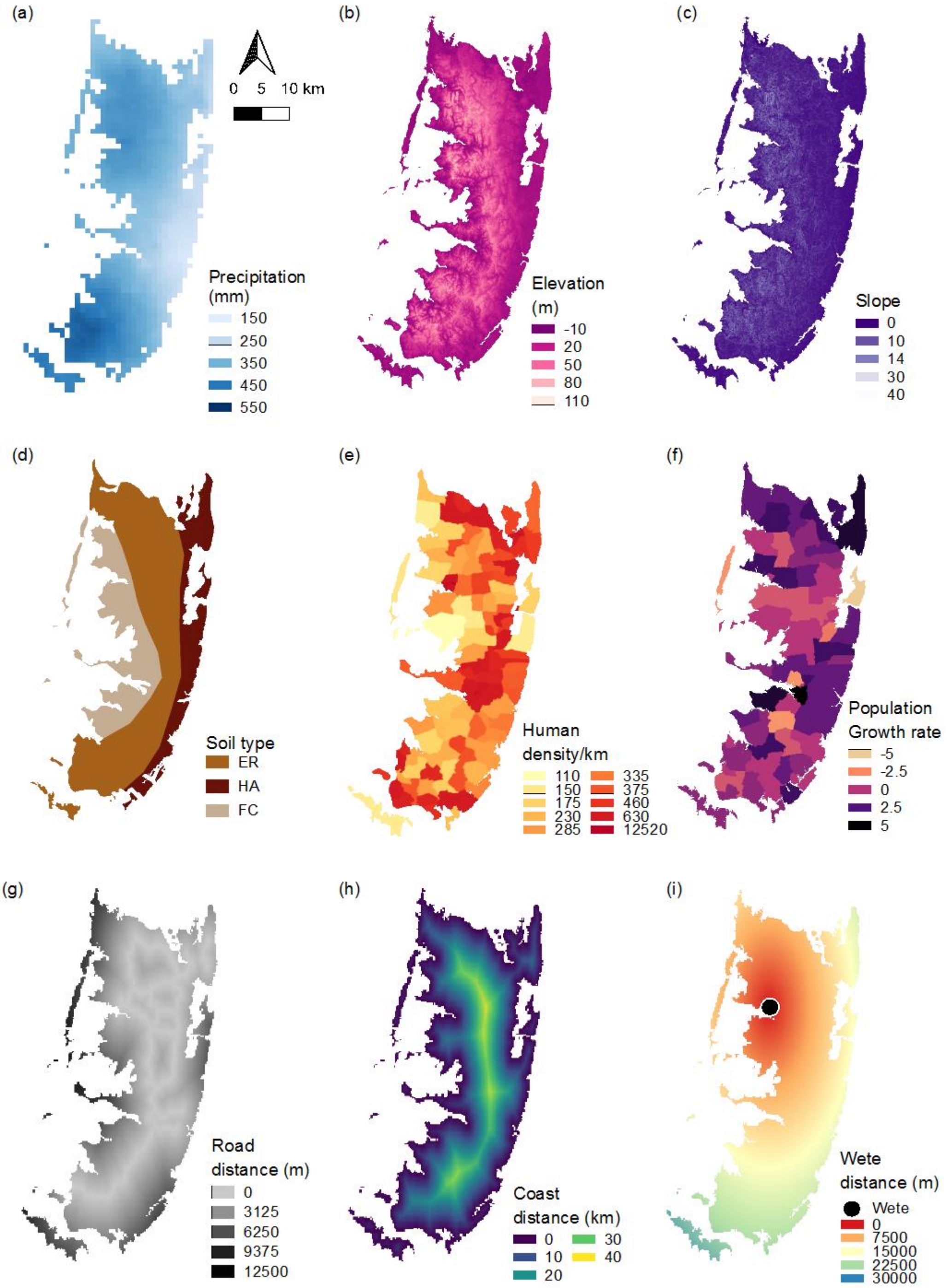

Figure 1.3. Forest cover on Pemba Island, Tanzania, for (a) 2001 (b) 2010 and (c) 2018.

Forest protected areas in the North were excluded from analysis (grey shading).

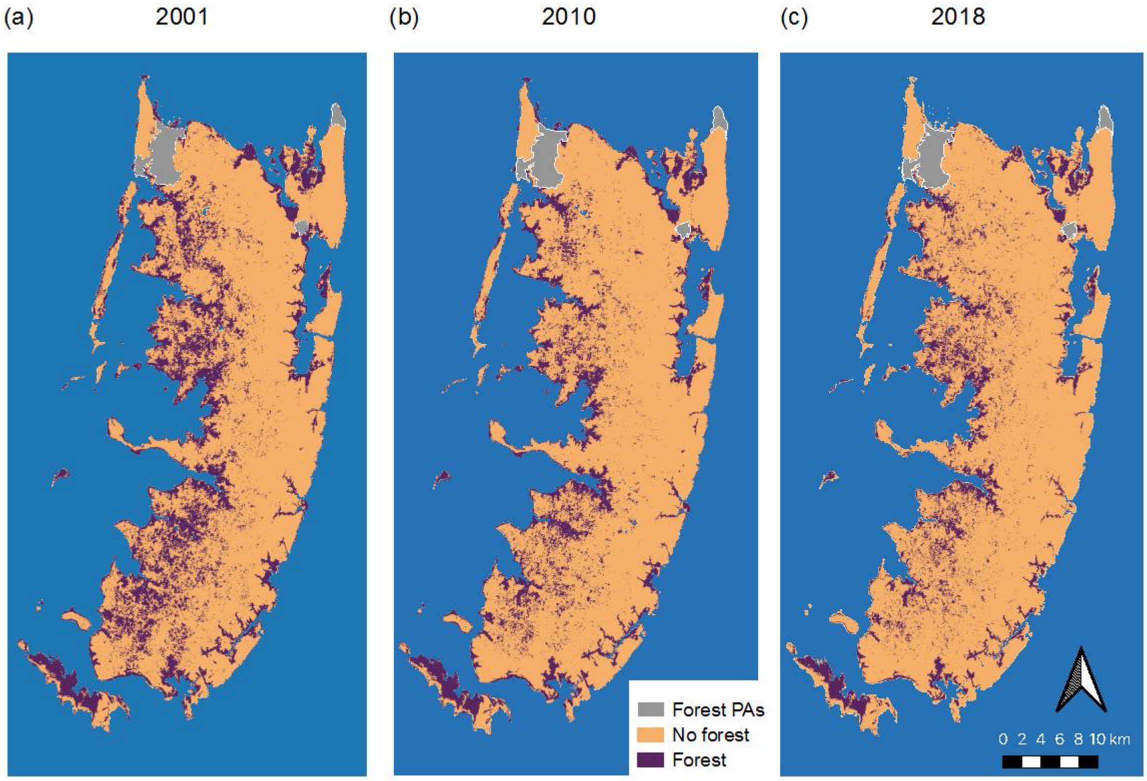

Figure 1.4. Love plot demonstrating the standardized mean difference between CoFMA treated wards and control wards on Pemba Island, Tanzania. Control wards prior to matching include all 98 controls, post-matching include the 48 selected. Negative standardized mean difference indicates treated CoFMAs had a lower mean covariate value than the controls, and positive values indicate a higher mean.

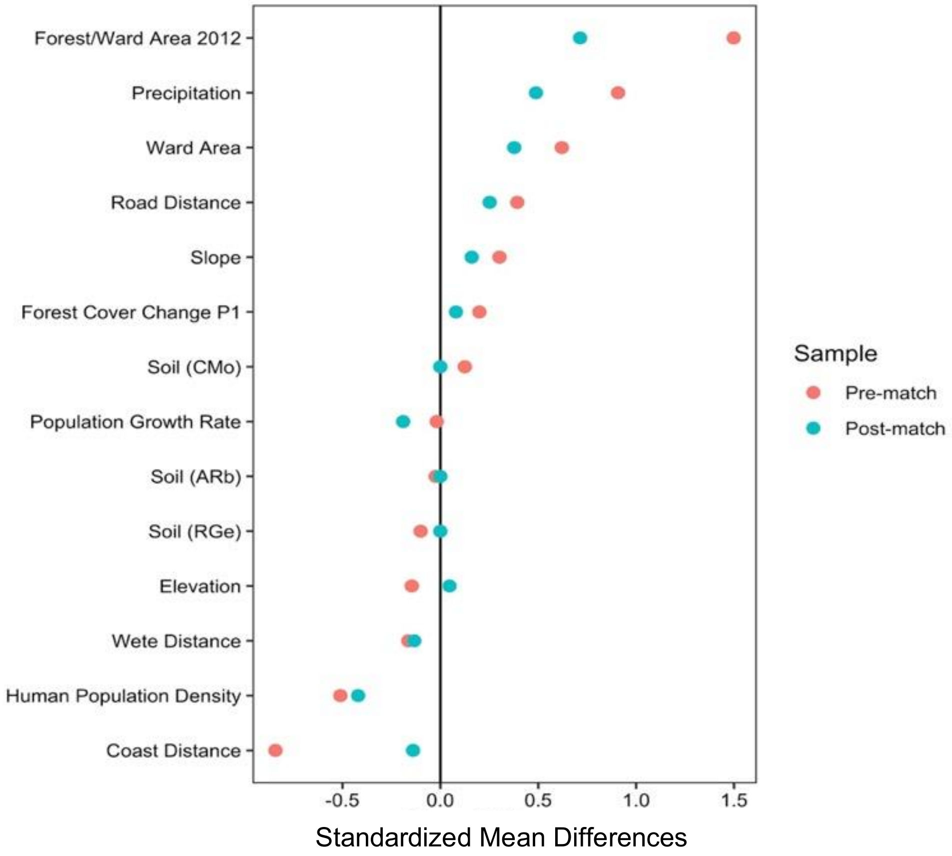

Figure 1.5. A comparison of predicted and observed forest change from 2010 - 2018 for treated CoFMA wards (red circles) and matched control wards (grey circles) on Pemba Island, Tanzania. Predicted forest change is based on the spatial autoregressive model derived from control wards. The line of equality (grey line) depicts wards that would have an equal predicted to observed value.

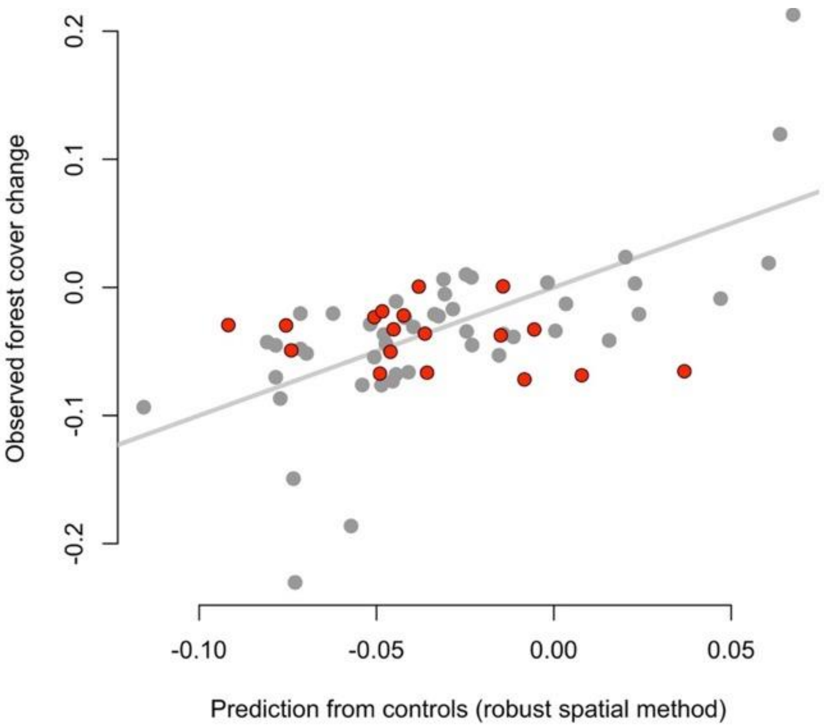

Supplement

Table S1.1. Confusion matrices of the classification map resulting from the Landsat 5 composite image for 2001, Landsat 7 composite for 2010, and Landsat 8 composite for 2018. User and producer accuracy was calculated as per Congalton (Congalton 1991).

2001	**Non-forest**	**Forest**	**Row Total**	**User Accuracy**
Non-forest	86	5	91	94.51%
Forest	3	46	49	93.88%
Column Total	89	51	140	
Producer Accuracy	96.63%	90.20%		
Kappa Coefficient	0.88			

2010	**Non-forest**	**Forest**	**Row Total**	**User Accuracy**
Non-forest	79	3	82	96.34%
Forest	2	41	43	95.35%
Column Total	81	44	125	
Producer Accuracy	97.53%	93.18%		
Kappa Coefficient	0.91			

2018	**Non-forest**	**Forest**	**Row Total**	**User Accuracy**
Non-forest	82	0	82	100.00%
Forest	5	38	43	88.37%
Column Total	87	38	125	
Producer Accuracy	94.25%	100.00%		
Kappa Coefficient	0.91			

Table S1.2. Ward-level forest cover (%) for the three years of analysis, and the annual rate of forest cover change for 2001-2010 (time period 1) and 2010-2018 (time period 2). Treated CoFMA wards are printed in red italicized bold font. Foot notes indicate wards that were removed from analysis due to zero forest. Wards classed as urban were removed from the matching procedure.

Ward	**2001 forest cover (%)**	**2010 forest cover (%)**	**2018 forest cover (%)**	**Annual rate of change period 1**	**Annual rate of change period 2**	**Urban status**
Bopwe	2.77	3.06	4.62	1	5.8	Urban
Chachani[1]	0.00	0.00	0.00	-	-	Urban
Chambani	17.33	12.42	8.96	-3.4	-4.4	Rural
Changaweni	51.92	31.14	21.43	-5.2	-5	Mixed
Chanjaani	23.67	17.49	15.55	-3.1	-1.6	Mixed
Chimba	3.18	1.15	4.67	-10.1	21.3	Rural
Chokocho	20.02	12.20	9.17	-5.1	-3.9	Rural
Chonga	34.65	20.33	14.12	-5.5	-4.9	Rural
Chumbageni	47.21	28.67	20.72	-5.1	-4.4	Rural
Chwale	13.32	10.11	5.22	-2.9	-8.7	Rural
Dodo	13.77	10.34	8.23	-3	-3.1	Rural
Finya	9.43	3.55	3.36	-9.8	-0.8	Rural
Fundo	31.72	22.27	13.44	-3.7	-6.7	Rural
Gando	40.37	33.17	28.92	-2	-1.9	Rural
Jadida	26.23	27.77	27.92	0.6	0.1	Urban
Jombwe	12.46	11.40	8.13	-0.9	-4.6	Rural
Junguni	42.11	29.28	19.73	-3.8	-5.3	Rural
Kambini	10.64	9.78	5.93	-0.9	-6.7	Rural
Kangagani	15.24	12.18	9.26	-2.3	-3.7	Rural
Kangani	24.46	18.23	15.53	-3	-2.2	Rural
Kendwa	12.32	8.40	9.10	-4	1.1	Rural
Kengeja	31.13	22.87	18.51	-3.2	-2.9	Mixed
Kibokoni	9.91	8.01	7.08	-2.2	-1.7	Rural
Kichungwani	54.12	69.54	50.11	2.7	-4.4	Urban
Kifundi	27.27	22.72	17.83	-1.9	-3.3	Rural
Kilindi	45.86	42.43	36.55	-0.8	-2	Rural
Kinowe	24.77	21.21	18.73	-1.6	-1.7	Rural

---

[1] Removed from analysis for having zero forest cover

Kinyasini	29.81	9.52	10.72	-11.3	1.6	Rural
Kinyikani	2.08	1.31	2.21	-4.7	7.5	Rural
Kipangani	34.65	30.42	25.35	-1.4	-2.5	Urban
Kisiwa Panza	60.89	59.45	47.88	-0.3	-2.9	Rural
Kisiwani	22.85	15.81	16.73	-3.8	0.8	Rural
Kiungoni	5.59	5.52	3.18	-0.1	-7.3	Rural
Kiuyu Kigongoni	0.75	0.32	0.56	-8.5	8	Rural
Kiuyu Mbuyuni	9.21	8.58	5.06	-0.7	-7	Rural
Kiuyu Minungwini	19.00	13.56	14.58	-3.5	1	Rural
Kiwani	29.48	24.17	17.45	-2.1	-4.4	Rural
Kizimbani	1.27	0.88	7.34	-3.8	33.9	Urban
Kojani	24.01	21.83	14.98	-1	-5.1	Rural
Konde	2.00	0.87	0.99	-8.5	1.9	Mixed
Kuukuu	48.34	47.10	34.31	-0.3	-4.3	Rural
Kwale	13.39	9.58	10.14	-3.5	0.8	Rural
Limbani	33.38	17.36	22.52	-6.7	3.7	Urban
Madungu	7.98	10.53	4.23	3	-11.8	Urban
Majenzi	38.11	36.29	31.94	-0.5	-1.7	Urban
Makangale	25.48	25.98	5.83	0.2	-18.6	Rural
Makombeni	39.71	33.37	22.72	-1.8	-5.2	Rural
Makoongwe	33.84	33.44	10.36	-0.1	-14.9	Rural
Matale	5.27	2.75	2.51	-6.6	-1.3	Rural
Maziwa Ng'ombe	2.91	2.70	0.40	-0.8	-23	Rural
Maziwani	3.39	2.89	2.49	-1.7	-2	Rural
Mbuguani	54.83	39.12	27.36	-3.5	-4.8	Mixed
Mbuyuni	42.53	38.65	23.80	-1	-6.5	Urban
Mbuzini	3.82	2.17	2.03	-5.8	-0.9	Rural
Mchanga Mdogo	6.35	6.67	4.06	0.5	-6.6	Rural
Mfikiwa	6.58	3.25	3.12	-7.2	-0.5	Rural
Mgagadu	23.52	18.35	13.84	-2.6	-3.8	Rural
Mgelema	57.43	36.52	30.80	-4.7	-2.3	Rural
Mgogoni	26.73	11.63	7.12	-8.4	-6.5	Rural
Mgogoni South	5.12	10.56	2.80	7.9	-16.7	Rural
Michenzani	23.34	20.34	15.98	-1.4	-3.3	Rural
Micheweni	9.05	7.06	9.77	-2.6	4.6	Mixed
Michungwani	18.20	9.75	9.96	-6.4	0.3	Rural
Mihogoni	3.45	1.41	3.19	-9	12	Rural

Minazini	18.40	11.06	8.41	-5.2	-3.7	Rural
Mizingani	48.53	23.02	24.08	-7.6	0.6	Rural
Mjimbini	30.32	16.37	9.53	-6.3	-7.2	Rural
Mjini Ole	5.60	3.05	2.33	-6.2	-3.6	Rural
Mjini Wingwi	26.09	21.42	14.86	-2.1	-4.9	Rural
Mkanyageni	33.63	11.74	10.07	-10.5	-2.1	Rural
Mkoroshoni	5.84	0.89	2.22	-18	13.5	Urban
Mkungu	25.54	9.82	10.09	-9.6	0.4	Rural
Mlindo	2.14	4.27	1.06	7.6	-17.5	Rural
Mpambani	39.29	39.09	20.88	-0.1	-8.3	Rural
Msingini	2.09	3.95	1.16	6.9	-15.5	Urban
Msuka Magharibi	7.89	5.27	3.14	-4.2	-6.9	Rural
Msuka Mashariki	12.74	8.29	6.45	-4.4	-3.4	Rural
Mtambile	29.74	8.82	6.80	-12	-3.5	Mixed
Mtambwe Kaskazini	44.07	29.80	29.98	-4	0.1	Rural
Mtambwe Kusini	55.01	39.34	39.51	-3.5	0.1	Rural
Mtangani	16.88	13.14	11.32	-2.6	-2	Rural
Mtemani	15.54	13.24	6.86	-1.7	-8.7	Rural
Muambe	10.56	9.28	6.83	-1.4	-4.1	Rural
Mvumoni	18.73	15.67	7.69	-1.9	-9.4	Rural
Mzambarauni Takao	25.17	7.96	13.33	-11.4	7.4	Rural
Ndagoni	30.33	27.67	18.44	-1	-5.4	Rural
Ng'ambwa	3.91	0.54	1.11	-18.8	10.4	Mixed
Ng'ombeni	12.87	10.87	6.73	-1.8	-6.4	Urban
Ngwachani	26.33	9.87	7.26	-9.8	-4.1	Rural
Ole	5.24	2.38	1.66	-8	-4.9	Rural
Pandani	6.29	2.94	6.52	-7.7	11.6	Rural
Pembeni	8.89	8.26	7.14	-0.8	-2	Rural
Piki	33.22	12.94	15.33	-9.4	2.4	Rural
Pujini	5.48	3.20	1.80	-5.5	-7.6	Rural
Selem	23.78	15.99	27.36	-4.1	7.7	Urban
Shamiani	35.02	27.91	15.09	-2.4	-8.1	Rural
Shengejuu	16.79	14.43	11.57	-1.6	-3	Rural
Shidi	46.55	29.06	22.16	-4.8	-3.7	Rural
Shumba Mjini	52.48	44.60	35.84	-1.7	-3	Rural
Shumba Viamboni	5.58	1.35	5.17	-13.8	20.3	Rural

Shungi	39.20	28.97	16.29	-3.1	-7.6	Rural
Sizini	16.57	15.55	13.07	-0.7	-2.4	Rural
Stahabu	16.18	11.13	8.63	-3.9	-3.4	Rural
Tibirinzi	38.50	26.52	26.95	-3.8	0.2	Urban
Tondooni	24.76	20.99	16.08	-1.7	-3.6	Rural
Tumbe Magharibi	18.47	12.64	9.58	-3.9	-3.7	Rural
Tumbe Mashariki	30.76	29.74	17.86	-0.4	-6.8	Rural
Ukunjwi	42.85	31.63	27.12	-3.1	-2.1	Rural
Ukutini	10.85	7.01	5.09	-4.5	-4.3	Rural
Utaani[2]	0.00	0.00	2.37	-	-	Urban
Uwandani	2.79	2.35	0.64	-1.8	-16.3	Rural
Uweleni	47.05	23.86	16.79	-6.9	-4.7	Urban
Vitongoji	2.22	2.49	0.38	1.2	-22.8	Rural
Wambaa	37.53	24.81	17.76	-4.3	-4.5	Rural
Wara	1.34	3.43	0.51	10.5	-23.2	Urban
Wawi	0.61	1.97	3.25	13.1	7.1	Rural
Wesha	32.94	21.90	21.07	-4.2	-0.5	Rural
Wingwi Mapofu	9.01	8.00	7.38	-1.2	-1.1	Rural
Wingwi Mjananza	31.93	28.73	20.54	-1.1	-4.5	Rural
Wingwi Njuguni	0.45	0.91	0.36	7.6	-11.9	Rural
Ziwani	23.77	20.40	17.30	-1.6	-2.2	Rural

---

[2] Removed from analysis for having zero forest cover

Table S1.3. All wards on Pemba and their associated neighboring wards.

Mtangani	Ukutini							
Muambe	Shamiani							
Ng'ombeni	Uweleni							
Ngwachani	Ukutini							
Shamiani								
Shidi	Uweleni							
Stahabu								
Ukutini								
Uweleni								
Wambaa								

Mbuyuni	Mgagadu	Michenzani	Minazini	Mizingani	Mjimbini	Mkanyageni	Mkungu	Mtambile
Ng'ombeni	Minazini	Mkanyageni	Mizingani	Mtambile	Mkanyageni	Mtambile	Mtambile	
Shidi	Mizingani	Shidi	Mkungu		Mkungu	Shidi	Muambe	
Uweleni	Ngwachani	Stahabu	Mtambile		Mtambile	Stahabu		
	Ukutini		Ukutini					

Jombwe	Kangani	Kendwa	Kengeja	Kisiwa Panza	Kiwani	Kuukuu	Makombeni	Makoongwe	Mbuguani
Kendwa	Kengeja	Kiwani	Kuukuu		Mtangani		Mbuguani		Mizingani
Kiwani	Kuukuu	Minazini	Mjimbini				Ng'ombeni		Uweleni
Mkungu	Mjimbini	Mkungu	Mkungu				Uweleni		
Muambe	Mkanyageni	Mtangani	Muambe						
		Ukutini	Shamiani						

Uwandani	Vitongoji	Wara	Wawi	Wesha	Ziwani	Chambani	Changaweni	Chokocho	Chumbageni
Vitongoji	Wawi	Wawi				Mtangani	Mbuguani	Mkanyageni	Mbuguani
						Ngwachani	Mizingani	Stahabu	Mgagadu
						Ukutini	Mkanyageni		Mizingani
							Mtambile		Wambaa
							Shidi		
							Uweleni		

Mgogoni South	Michungwani	Mkoroshoni	Msingini	Mvumoni	Ndagoni	Ng'ambwa	Pujini	Shungi	Tibirinzi
Mvumoni	Ng'ambwa	Msingini	Tibirinzi	Pujini	Wesha	Tibirinzi			Wara
Wawi	Tibirinzi	Ng'ambwa	Wara	Wawi		Uwandani			Wesha
	Wesha	Tibirinzi				Vitongoji			
	Ziwani	Wara				Wara			
						Wawi			

Dodo	Kibokoni	Kichungwani	Kilindi	Kwale	Madungu	Matale	Mbuzini	Mfikiwa	Mgelema
Matale	Mvumoni	Madungu	Mgelema	Mbuzini	Mgogoni South	Shungi	Ng'ambwa	Mgogoni South	Chumbageni
Mfikiwa	Vitongoji	Msingini	Shungi	Michungwani	Msingini	Chambani	Ziwani	Mvumoni	Mgagadu
Pujini	Wawi	Shungi	Wambaa	Ng'ambwa	Wara			Pujini	Wambaa
Shungi		Tibirinzi		Ziwani	Wawi				
Chamba									

Ole	Pandani	Pembeni	Piki	Selem	Shengejuu	Ukunjwi	Utaani	Chachani	Chanjaani	Chonga
Mbuzini	Pembeni	Shengejuu		Ukunjwi				Kichung wani	Dodo	Kilindi
Ng'ambwa	Shengejuu							Msingini	Kichungwani	Matale
Uwandani								Tibirinzi	Madungu	Mgelema
Ziwani									Matale	Shungi
									Mfikiwa	Chambani
									Mgogoni South	Chumbag.
									Shungi	Mgagadu
										Ngwachan.

Kizimbani	Kojani	Limbani	Maziwani	Mchanga Mdogo	Mjini Ole	Mpambani	Mtambwe Kaskazini	Mtambwe Kusini	Mzamba rauni Takao
Limbani	Mpambani	Mtambwe Kaskazini	Mzambara uni Takao		Ole		Mtambwe Kusini	Piki	Pandani
Utaani		Mzambara uni Takao	Pandani				Piki		Piki
		Pandani	Pembeni						
		Piki	Piki						
		Utaani	Shengejuu						

Jadida	Junguni	Kambini	Kangagani	Kinyikani	Kipangani	Kisiwani	Kiungoni	Kiuyu Kigongoni	Kiuyu Minungwini
Kipangani	Ukunjwi	Kinyikani	Kiuyu Kigongoni	Maziwani	Selem	Kiuyu Kigongoni	Pandani	Kiuyu Minungwini	
Limbani		Kisiwani	Kiuyu Minungwini	Mchanga Mdogo		Kiuyu Minungwini	Pembeni	Mjini Ole	
Utaani		Kiuyu Minungwini	Mjini Ole	Mzambara uni Takao		Mtambwe Kusini		Ole	
		Mchanga Mdogo		Piki		Ole			
		Piki				Piki			
						Ziwani			

Sizini	Tondooni	Tumbe Magharibi	Tumbe Mashariki	Wingwi Mapofu	Wingwi Mjananza	Wingwi Njuguni	Bopwe	Chwale	Fundo	Gando
Tumbe Mashariki		Tumbe Mashariki		Wingwi Njuguni	Kiungoni		Jadida	Kinyikani		Junguni
Wingwi Mapofu							Kipangani	Maziwani		
							Kizimbani	Mchanga Mdogo		
							Selem	Shengejuu		
							Ukunjwi			
							Utaani			

Maziwa Ng'ombe	Mgogoni	Micheweni	Mihogoni	Mjini Wingwi	Mlindo	Msuka Magharibi	Msuka Mashariki	Mtemani	Shumba Mjini	Shumba Viamboni
Micheweni	Gando	Mjini Wingwi	Shumba Viamboni	Sizini	Mtemani	Msuka Mashariki		Wingwi Mapofu		
Mjini Wingwi	Junguni	Shumba Mjini	Sizini	Wingwi Mapofu	Wingwi Mapofu	Tondooni		Wingwi Mjananza		
Shumba Mjini			Tumbe Magharibi		Wingwi Mjananza			Wingwi Njuguni		
			Tumbe Mashariki		Wingwi Njuguni					
			Wingwi Mapofu		Kiungoni					
					Pandani					

Ward name	Chimba	Finya	Kifundi	Kinowe	Kinyasini	Kiuyu Mbuyuni	Konde	Majenzi	Makangale
neighbor 1	Kifundi	Kinyasini	Konde	Konde	Mgogoni	Maziwa Ng'ombe	Msuka Magharibi	Micheweni	Msuka Magharibi
neighbor 2	Kinowe	Mihogoni	Mgogoni	Msuka Mashariki	Shumba Viamboni	Shumba Mjini	Msuka Mashariki	Mjini Wingwi	Tondooni
neighbor 3	Kinyasini	Mlindo	Tondooni	Tumbe Magharibi	Bopwe		Tondooni	Shumba Mjini	
neighbor 4	Konde	Shumba Viamboni	Gando		Junguni			Sizini	
neighbor 5	Mgogoni	Wingwi Mapofu			Kizimbani				
neighbor 6	Mihogoni	Limbani			Limbani				
neighbor 7	Shumba Viamboni	Pandani			Ukunjwi				
neighbor 8	Tumbe Magharibi								

Table S1.4. The CoFMA treated wards and their respective five matched control wards.

Michenzani	**Mjimbini**	**Mjini Wingwi**	**Msuka Magharibi**	**Mtambwe Kaskazini**	**Mtambwe Kusini**	**Shumba Mjini**	**Tondooni**	**Tumbe Magharibi**
Stahabu	Mbuguani	Mtemani	Msuka Mashariki	Ziwani	Wesha	Kiuyu Mbuyuni	Makangale	Sizini
Chokocho	Mkanyageni	Kiuyu Mbuyuni	Chimba	Junguni	Ukunjwi	Mtemani	Mtangani	Msuka Mashariki
Makombeni	Chokocho	Wingwi Mjananz	Konde	Wesha	Kilindi	Maziwa Ng'ombe	Dodo	Kinowe
Kengeja	Stahabu	Maziwa Ng'ombe	Mihogoni	Shungi	Junguni	Mvumoni	Msuka Mashariki	Tumbe Mashariki
Makoongwe	Mtangani	Mjini Ole	Sizini	Wambaa	Shungi	Pujini	Matale	Wingwi Mapofu

CoFMA Ward	**Changaweni**	**Fundo**	**Gando**	**Kambini**	**Kangani**	**Kifundi**	**Kisiwa Panza**	**Mgelema**	**Mgogoni**
Match 1	Mbuguani	Ndagoni	Ukunjwi	Mchanga Mdogo	Chokocho	Kisiwani	Mtangani	Michungwani	Piki
Match 2	Shidi	Wesha	Wesha	Kiungoni	Stahabu	Wingwi Mapofu	Chambani	Shungi	Ngwachani
Match 3	Mizingani	Wambaa	Junguni	Wingwi Mapofu	Kuukuu	Sizini	Kuukuu	Junguni	Mbuzini
Match 4	Makombeni	Ukunjwi	Michungwani	Kiuyu Minungwini	Kengeja	Kiungoni	Kengeja	Wesha	Kisiwani
Match 5	Mkungu	Michungwani	Kilindi	Sizini	Makoongwe	Piki	Makangale	Wambaa	Kinowe

Table S1.5. The mean of each covariate used for the matching procedure for treated and control wards before and after matching.

Ward-level covariates	**Means Treated**	**Means control Pre-match**	**Means control post-match**
Annual deforestation rate (2010-2018)	-0.033	-0.037	-0.034
Growth rate (2002-2012)	0.933	0.962	1.2
Median elevation	20.6	22.4	20
Median slope	4.7	4	4.3
Ward area	16.2	15.9	16
Population density	5.7	6	5.9
Forest relative to total area 2010	-1.5	-2.4	-1.9
Median April precipitation	6	5.8	5.9
Median distance to coast	1	1.7	1.2
Median distance to nearest major road	2.6	1.8	2
Median distance to Wete	11.6	12.8	12.6

Table S1.6. The coefficients and SE in parentheses of the two spatial autoregressive (SAR) models; Ordinary lagged SAR and two-stage robust lagged SAR, performed to make predictions for treated wards based on the controls (average effect of CoFMA status), along with models fitted by the same methods for the combined dataset of treated and controls (socioecological factors). A covariate for which | estimate/SE | ≥ 2.91 can be considered a significant predictor of forest cover change under the Bonferroni multiple-testing rule.

	Lagged SAR		2-stage Robust SAR	
Variable	**Controls only Bias-corrected ATET**	**All Observations Treated & controls**	**Controls only Bias-corrected ATET**	**All Observations Treated & controls**
Annual deforestation rate in time period 1	-0.756 (0.163)	-0.704 (0.419)	-0.656 (0.364)	-0.661 (0.332)
Growth rate	0.002 (0.004)	0.002 (0.004)	0.003 (0.003)	0.003 (0.003)
Median elevation	0.001 (0.001)	0.00 (0.001)	0.001 (0.002)	0.001 (0.001)
Median slope	-0.008 (0.009)	-0.01 (0.008)	-0.004 (0.009)	-0.008 (0.007)
Ward area	-0.008 (0.017)	0.004 (0.015)	0.001 (0.021)	0.008 (0.017)
Population density	0.006 (0.015)	0.01 (0.014)	0.013 (0.017)	0.015 (0.014)
Area of forest in 2012	-0.01 (0.009)	-0.007 (0.008)	-0.01 (0.012)	-0.009 (0.012)
Median April precipitation	0.028 (0.045)	0.038 (0.041)	0.014 (0.052)	0.032 (0.046)
Median distance to coast	-0.003 (0.012)	-0.003 (0.011)	-0.005 (0.012)	-0.005 (0.01)
Median distance to nearest major road	0.003 (0.006)	0.0002 (0.005)	0.002 (0.008)	0.00009 (0.005)
Soil (CMo)	0.003 (0.025)	0.013 (0.021)	-0.003 (0.023)	0.01 (0.018)
Soil (RGe)	-0.034 (0.022)	-0.025 (0.019)	-0.021 (0.025)	-0.021 (0.02)
Median distance to Wete	-0.003 (0.002)	-0.002 (0.001)	-0.002 (0.002)	-0.001 (0.001)
CoFMA status	-	-0.003 (0.015)	-	-0.006 (0.011)

Chapter 2: Evidence that the landscape of fear and human shield are mutually inclusive: Differential spatiotemporal responses of wildlife to sensory pollution on roads

Amy C. Collins, Travis Longcore, T. Winston Vickers, Fraser M. Shilling

1. Introduction

Roads are ubiquitous features of the modern landscape, with a network of 6.2 million km in the United States (Forman and Alexander 1998, Forman 2000). Though road networks increase connectivity and mobility of humans, roads can and do have detrimental effects on both humans and wildlife. Collisions between wildlife and vehicles on roads are a common source of human-wildlife conflict, and often result in high financial losses, injury, and mortality; in the United States, over 59,000 human injuries and 440 human fatalities occur annually (Nyhus 2016, Conover 2019). Roads also cause habitat loss and fragmentation for wildlife by creating barriers across the landscape that can be impervious to wildlife movement (Ree et al. 2015).

Crossing structures (CS) provide a safe route for wildlife to navigate across roads, simultaneously reconnecting habitat and promoting human-wildlife coexistence by lowering collision rates (Clevenger and Waltho 2000, Rytwinski et al. 2016, Claireau et al. 2019). Many studies have demonstrated wildlife use of a diverse set of CS such as underpasses, overpasses, bridges, and culverts (Ree et al. 2007), but documentation of use is distinct from an assessment of CS efficacy (van der Grift et al. 2013, Rytwinski et al. 2015). CS efficacy can be influenced by factors such as structural design and pedestrian activity by humans

(Clevenger and Waltho 2000, Brunen et al. 2020). Further, the efficacy of CS might be affected by the exposure of animals to increased noise and artificial light at night produced by vehicles and the surrounding environment (Clevenger and Waltho 2005, Kintsch and Cramer 2011, Gaston and Holt 2018).

The effects of anthropogenic noise and light at night on wildlife, collectively referred to as sensory pollution, are widespread and now at the forefront of conservation biology (Madliger 2012, Dominoni et al. 2020, Owens et al. 2020). Noise and light pollution can impact wildlife near roads in multiple ways. For instance, noise pollution from vehicles has caused declines in population density and species richness of birds, and experimental additions of noise to undisturbed areas, known as 'phantom roads', has negatively impacted bird distributions, and foraging-vigilance behavioral trade-offs (Goodwin and Shriver 2011, Blickley et al. 2012, McClure et al. 2013, Ware et al. 2015, Konstantopoulos, Moustakas, and Vogiatzakis 2020). Static sources of light pollution such as streetlights at or within CS can reduce use by herpetofauna and some mammals (Woltz et al. 2008, Bliss-ketchum et al. 2016). At night, vehicles are a source of noise and light pollution simultaneously, with exposure being irregular and unpredictable during periods of lower traffic volume (Halfwerk and Slabbekoorn 2015).

Few studies have examined the effect of the two pollutants together. Those that have revealed mixed results; either negative synergistic effects on host-parasite interactions, bird activity and reproductive success (McMahon, Rohr, and Bernal 2017, Dominoni et al. 2020, Ferraro, Le, and Francis 2020), or a singular negative effect of noise pollution on bird physiology (Raap et al. 2017). Consequently, there is an urgent need to understand the effects of both noise and light pollution on mammals. Furthermore, species-level responses to sensory pollution are differential, and are determined by species' sensory systems, behavioral plasticity, and community assemblage (Swaddle et al. 2015, Da Silva, Valcu, and Kempenaers 2016, Dominoni et al. 2020). Therefore, responses to combined sensory pollutants need to be considered at the species and community level.

Decisions made by wildlife when moving across the landscape are thought to be influenced by the risk of predation. Alterations in behavior or distribution of wildlife in response to perceived predation risk can be classified as consequences of the 'Landscape of Fear' (Laundré et al. 2001, Laundre et al. 2010), and this concept is now being applied to anthropogenic disturbances (Darimont et al. 2015). Sensory pollution, as a type of anthropogenic disturbance, may be considered a predation risk by wildlife and could induce behavioral changes associated with minimizing predation risk (Francis and Barber 2013). Two common behavioral responses to heightened risk in a LOF are temporal and spatial avoidance (Oriol-cotterill et al. 2015). 'Road avoidance zones' have been documented for a number of mammal species (Forman 2000, 2003), and such spatial avoidance likely is costly for wildlife. Individuals consistently avoiding CS will lose access to, and benefits of, otherwise-viable habitat and associated resources, and because CS are expensive and consequently rare within the landscape, alternative passages for wildlife usually are unavailable (Gill et al. 2001). Temporal avoidance may be an alternate or additional response by wildlife to noise and light pollution at CS; some mammal species have altered their diurnal activity patterns to avoid human interactions (Gaynor et al. 2018). Increased nocturnality can have costs, such as altered trophic interactions and decreased physiological health from sleep deprivation and stress (Patten, Burger, and Mitrovich 2019, Dominoni et al. 2020).

In contrast to avoiding CS because of increased risk, some wildlife species may perceive CS as having relatively low predation risk. CS with high levels of light pollution may facilitate detection of predators by prey species. Further, avoidance of noise or light pollution by predators may create a predator-free space near CS, thus offering a ‘Human Shield’ against predators for the potential prey (Shultz and Noe 2002, Berger 2007, Francis et al. 2009). For example, some prey species have been observed spatially redistributing to human-frequented features such as roads and railroads in order to seek refuge from predators (Berger 2007). Under this scenario, whether actively utilized for this reason or not, it would be beneficial for prey species to increase their association with CS.

Our objective was to evaluate the impact of vehicular noise and light pollution from vehicles and streetlights on the mammal community at 26 wildlife CS across northern, central, and southern California. We tested two alternative hypotheses regarding how noise and light conditions impacts spatiotemporal distributions of mammals at CS; the Landscape of Fear, which predicts mammals will spatiotemporally avoid the CS, and the Human Shield, which predicts prey species will be attracted to the CS. Using camera trap methods, we determined spatial avoidance by quantifying effects on species richness of mammals and by examining changes in the number of visitations to the CS in a subset of species from two trophic levels: two mesopredators, bobcat (*Lynx rufus*) and coyote (*Canis latrans*), and one prey species, mule deer (*Odocoileus hemionus*). In addition, we determined whether noise and light pollution affect the time of day (i.e. temporal response) at which these focal species are present at CS by investigating diel activity patterns.

2. Methods

2.1 Study Area

The study was conducted July 2017 through October 2019 and included five regions of California: Shasta Cascades, San Francisco Bay Area, Central Valley, Eastern Sierras, and Southern California (Figure 2.1). Across the five regions, we selected 26 CS that were underpasses and box culverts built with the intention of facilitating wildlife crossings, or were underpasses, bridges, and culverts primarily constructed for road conveyance over watercourses. To encompass a broad spectrum of levels of exposure to noise and light, we selected CS that crossed state or federal highways ranging from one to five lanes of traffic, and that represented a range of traffic volume (910 – 253,000 Average Annual Daily Traffic; California Department of Transportation 2015a, 2015b). CS in southern California and the Bay Area were predominantly located in urban habitats, with some CS located in coastal sage scrub or riparian habitats. CS in the Shasta Cascades, Central Valley, and Eastern Sierras were surrounded by a mix of urban habitats, conifer forest, oak woodland, riparian woodland, or annual grassland.

2.2 Camera trapping

To detect wildlife presence and diel activity at CS, we deployed four camera trap stations at each CS for an average of 44 days (range = 21 – 117 days). One camera was placed near each side of both entrances of the CS, facing toward the inside of the structure, at a 45-degree angle to the entrance. We positioned cameras (Bushnell Trophy Cam HD Aggressor) approximately 0.5 m above the ground (Meek et al. 2014) using available mounting surfaces such as trees or boulders. Cameras were set to a minimum of 3 seconds between trigger events, with one trigger event at a time.

To establish a baseline for species richness and diel activity in the vicinity of the CS, we identified a reference region 0.7 – 3.0 km (mean = 1.8 km) from the CS, in a direction perpendicular to the highway. Each reference region was chosen based on the following criteria: 1) undeveloped habitat, i.e. conifer forest, oak woodland, or coastal sage scrub ; 2) accessibility, i.e. public forest land, public recreational areas, or private ranch land with granted access; 3) exposure to only ambient noise levels, identified as ~ 1 km from the highway (Francis and Barber 2013); and 4) close enough to be within the home range of resident wildlife, to ensure observations of individuals that also have access to the CS. We deployed an eight-camera array in the reference region for the same duration as was used at the CS. Camera stations were >100 m apart, positioned along wildlife trails, disused access roads, and openings in vegetation. Four of the eight reference stations were left as non-baited and were used to inform us of species richness and diel activity patterns. We collected additional information on species richness using two reference stations that were baited for herbivores (corn, peanut butter, and dried fruit), and two reference stations that were baited for carnivores (raw chicken meat, cat food, and commercial Lynx© spray, a carnivore lure) to ensure we captured as diverse an array of species as possible. Cameras were set to have a 10-second delay between trigger events due to the high occurrence of false triggers caused by wind-induced vegetation movement.

Wildlife images were uploaded to an online database “Wildlife Observer Net” developed by the UC Davis Road Ecology Center. A trained observer identified species present in each image, and each identification was then verified by a second trained observer. We classed a unique detection event of the same species as two images ≥ 1 hour apart, as per Sollmann (2018). One hour was chosen to accommodate long feeding bouts observed at the baited camera trap stations. All domestic animals were eliminated from the dataset.

2.3 Measurements of noise and light pollution

To quantify vehicular noise, we sampled sound pressure levels after the camera trapping period was complete for each CS, beginning early 2019. Two digital sound level meters (TENMA 72-947 and PCE-322; 30-130 range, slow setting) were placed at the entrance of the CS closest to the reference region, on a tripod 0.5 m in height. Sound pressure levels were measured in 59-second increments over a 7-day period. We chose the maximum length of incremental measurements (59 seconds) to allow for a week-long period of data collection without exceeding the data storage capacity of the sound meter. Sound meters measured noise in decibels, one meter used a C-weighting filter (dBC) and the other an A-weighting filter (dBA). After data collection, we extracted the median noise (L_{50}) for each CS. Due to an equipment failure on the A-weighted meter at one site, we focus on dBC data hereafter, and provide site-level data for L_{50} dBC and dBA in the supplemental (Table S2.1). We also identified 24-hour profiles of traffic noise at sites at which each species was recorded.

To measure night-time illuminance emitted by vehicle headlights, skyglow, and streetlight sources at the CS, we followed methods outlined in Simons, Yin and Longcore (2020). We recorded a still, 180° image of the night sky at the same CS entrance where sound measurements were taken, using a digital camera (Canon Rebel T6; ISO 1600, aperture f/2.8) with a circular fisheye lens (Sigma 4.5 mm F^{-2}.8 EX DC). For each location, the camera was adjusted to face 0 degrees N, levelled horizontally to 0 degrees inclination, with the fisheye lens oriented upwards. Camera exposure time was manually chosen to reduce the level of image saturation. Exposure time varied between 0.5 – 127.6 seconds. To avoid capturing moonlight, images were taken during the new moon phase. Scalar illuminance (SI) was then extracted from the raw images using image processing software (Sky Quality Camera, Euromix Ltd, V1.9) and the following equation (Duriscoe 2016, Jechow et al. 2017, Simons et al. 2020):

$$SI = \int_{2\pi 0} \int_{\pi 20} L(\theta,\phi)\sin(\theta)d\theta d\phi \qquad (1)$$

Where θ represents the zenith angle, ϕ the azimuthal angle, and L(θ,ϕ) the function for night sky luminosity.

2.4 Measurements of covariates

In addition to noise and light pollution, we quantified attributes of CS architecture and environmental characteristics surrounding the CS that may influence spatiotemporal patterns. We determined elevation using a handheld GPS device (Garmin eTrex 20x) at the point of the CS entrance. We measured CS width and length with a handheld digital laser rangefinder (Suaoki PRO 600m). CS that were too long to measure manually were measured using Google Earth Pro and its ruler function. We recorded whether flowing water or fencing was present at the CS. Water was classified as present or absent, and fencing was classified as: 1) fencing absent; 2) fencing present but partial (not extended all the way to the entrance, and < 2 m height); or 3) fencing present and complete (extending all the way to the CS entrance, > 2 m height).

Because surrounding habitat might influence occurrence of wildlife at CS, we used the 2016 National Land Cover Database (NLCD; Dewitz 2016), a raster dataset based on Landsat satellite imagery, to determine the percentage of the various types of habitats and ground coverages at each CS. Each 30-m cell is categorized into 20 different land cover classifications, based on relative density and type. The locations of each of the CS, initially represented as points, were buffered by 100 m to make associated polygons. We used the tool Quantum GIS (Version 2.18; Team 2018) to load and analyze the data, using the raster library functions Zonal Histogram and Zonal Statistics. Within the buffer region of each CS, the associated raster cells were counted (by type) and summary statistics performed to get the dominant (majority) land cover type for each CS. Sites that had the dominant land cover type 'Developed – open space', 'Developed – low intensity', and 'Developed – medium intensity' were aggregated into one group defined as 'Developed' for analysis.

We obtained records of daily minimum temperature from the National Oceanic and Atmosphere Administration online climate data (Version V01r00; Young et al. 2018) for every camera station at each CS and reference region using measurements from the closest weather station. We then calculated the mean daily minimum temperature for the duration of each camera station's sampling period.

Finally, the frequency of daily visitations by human pedestrians to each CS was quantified using images that had been tagged as humans present in the "Wildlife Observer Net" database. All images that contained humans within the online database were rendered publicly inaccessible. All analyses described below were performed in RStudio (R v. 3.6.1; RStudio Team 2015).

2.5 Statistical analyses

2.5.1 Spatial displacement

Species richness

We evaluated whether traffic noise (dBC L_{50}) and scalar illuminance (mlx) of the night sky would negatively impact species richness of mammals by employing a Poisson regression with a logit link (*glmmADMB* package; Bolker et al. 2012) We included covariates in the model representative of CS architecture and environmental characteristics: CS length, CS width, elevation, dominant NLCD category within 100 m buffer region of CS (developed; shrub/scrub; evergreen forest), water presence/absence, fencing type, daily minimum temperature, frequency of human daily visitation, and sampling year (2017; 2018; 2019). To account for variation in the sampling period between sites, sampling period was declared an offset. Site and individual camera were introduced as nested random effects. We fit three separate models: 1) a base model that included random effects, camera location (CS or reference region), baited or non-baited condition, sample year, and the offset; 2) the base model plus covariates, with traffic noise and light excluded; 3) the full model with all covariates, plus noise and light metrics. The model with the lowest AIC value was selected as the best model. We performed regression diagnostics on the best model using Pearson's residuals.

To visualize the relationship of the response variable, species richness, with noise and light pollution, we simulated data using the ‘predict.glmmadmb’ function and the link scale for the full model (*glmmadmb* package; Bolker et al. 2012). We fixed each continuous covariate at the median value, and each categorical covariate as the level that had the best fit to the observed data. Because we were interested in the effect on species richness specifically at the crossing structure as opposed to the reference region, we set the covariates to non-baited, CS cameras. Random effects were set to zero. Using the range of observed values for noise and light, we generated values of equal increments for each in turn (Table S2.1).

Frequency of daily visitations

To test for the effect of traffic noise and light on a second measure of spatial displacement, we examined daily visitation rates of three focal species that had an adequate number of observations: mule deer, bobcats, and coyotes. Due to differences in the distribution of count data for mule deer, a negative binomial model resulted in a better fit than the Poisson model. Subsequently, we employed a negative binomial with a logit link for mule deer observations. We employed a Poisson model with a logit link for bobcat and coyote observations. Covariates and methods for model selection and data simulation that were applied to species richness models were also applied to this analysis.

2.5.2 Temporal displacement

To test for effects of noise or light pollution on temporal displacement, we examined diel activity patterns of mule deer, bobcats, and coyotes in turn across three groups: the reference region; at CS exposed to low levels of noise or light pollution; at CS exposed to high levels of noise or light pollution. We defined the threshold for low/high noise pollution to be -/+ the median l_{50}, > 59.7 dBC, and we defined the threshold for low/high light as 10 mlx. Due to activity potentially being altered at baited cameras in the reference region, we used only non-baited cameras for analysis of temporal displacement.

To account for variation in the time of year of sampling (Nouvellet et al. 2012), we converted the clock time of each detection into sun time using the 'sunTime' function, *overlap* package (Ridout and Linkie 2009, Meredith and Ridout 2017). For each species, we then generated activity curves by kernel density estimation (*overlap* package). For noise and light pollution in turn, we calculated the coefficients of overlap Δ (0 – 1, with 1 representing complete overlap) for activity curves in the reference region vs low-pollution CS, reference region vs high-pollution CS, and low-pollution vs high-pollution CS. The overlap coefficient estimator was $\hat{\Delta}_4$, unless number of observations was < 75, in which case $\hat{\Delta}_1$ was used (Ridout and Linkie 2009).

We examined whether there was a difference in diel activity pattern between two groups in turn: reference vs low-pollution; reference vs high-pollution; low-pollution vs high-pollution, using the Mardia-Watson-Wheeler test for homogeneity in the *circular* package (Lund et al. 2017). This test considers differences in the mean and variance of the two samples, while taking into consideration the circular nature of the data.

For noise and light pollution in turn, we also summed the percent of diel activity that occurred during night-time hours (18:00 – 06:00 h), referred to as nocturnality, for the activity curves in the reference region vs CS classed as low pollution, reference region vs CS classed as high pollution, and low- pollution vs high- pollution. Light pollution from vehicle headlights can peak at specific times, generating short-term responses that single illuminance values overlook. Hence, for activity curves associated with light pollution, we additionally calculated the mean density estimation of activity for the two periods associated with peak headlight exposure, 04:00 – 06:00 h and - 18:00 – 20:00 h. Peak headlight exposure was estimated based off of peak traffic-noise measures during the hours of darkness (18:00 – 06:00 h).

3. Results

3.1 Spatial displacement

Cameras were operational for 8,226 trap nights across the 26 sites, each with four cameras (218 camera stations). We identified 15 native and one non-native mammal species of medium or large body size: American badger (*Taxidea taxus*); American marten (*Martes americana*); black bear (*Ursus americanus*); bobcat; coyote; gray fox (*Urocyon cinereoargenteus*); long-tailed weasel (*Mustela frenata*); mountain lion (*Puma concolor*); mule deer and Columbian black-tailed deer (*O. h. columbianus*); North American river otter (*Lontra canadensis*); raccoon (*Procyon lotor*); striped skunk (*Mephitis mephitis);* Virginia opossum (*Didelphis virginiana*); western spotted skunk (*Spilogale gracilis*); and yellow-bellied marmot (*Marmota flaviventer*) (See Table S2 for a list of species observed at each camera station). Mammals that were detected at the reference regions but absent from all CS were the American marten and the western spotted skunk. Species detected only at CS were the long-tailed weasel and the North American river otter. Levels of both noise and light varied considerably among CS, although three CS (SR 79 Arroyo Seco, SR 89 Indian Creek, US 97 PM6) did not have vehicle headlights present in the night-time illuminance image due to low levels of night-time vehicular traffic.

The best-fit model for assessment of species richness and frequency of visitations was the full model, which included light and noise metrics (AIC; Table 2.1). Fewer species were documented at CS that had higher levels of noise ($p < 0.002$; Figure 2.2A). However, contrary to predictions, fewer species were present at CS with lower levels of light pollution ($p = 0.012$; Figure 2.2B). Examining the three focal species' responses to the impact of noise and light, mule deer showed the same direction of response as did species richness: fewer visitations at CS with higher levels of noise, but lower levels of light pollution (noise $p < 0.001$; light $p < 0.001$; Figure 2.3A, 2.3B). Mesopredators demonstrated a differential response to noise pollution; bobcat visits were highest at intermediate levels ($p = 0.019$; Figure 2.3C), and coyote visits remained unaffected ($p = 0.065$; Figure 2.3E). Yet both bobcat and coyote visitations were highest at intermediate levels of light (bobcat: $p < 0.001$; coyote: $p < 0.001$; Figure 2.3D, 2.3F).

Species richness was higher at longer CS, CS with no fencing, lower average annual daily traffic, higher temperatures, and for the sampling years 2017 and 2019 (no vs full fencing: $p = 0.005$; length $p = 0.003$; no water vs water, daily traffic, minimum temperature, 2018 sampling $p = < 0.001$; Table 2.1). Species richness was not influenced by human presence, the NLCD landcover category, and CS width (human $p = 0.224$; developed vs evergreen forest NLCD $p = 0.281$ and developed vs shrub/scrub NLCD $p = 0.169$; width $p = 0.725$; Table 2.1). Examining the effect of additional covariates on all three focal species, two factors had effects on mule deer visits that opposed those on coyotes and bobcats. Visitation rates increased with temperature for mule deer but decreased for bobcats and coyotes (mule deer: $p = 0.029$; bobcat $p = 0.049$; coyote $p = 0.042$; Table 2.1), and visitation rates were lower for mule deer during the sample year 2018, but higher for bobcats and coyotes that year (mule deer: $p < 0.001$; bobcat $p = 0.012$; coyote $p = 0.009$; Table 2.1). Additionally, mule deer visits were greater at CS with no fencing, CS with no water, and CS in evergreen forest (no vs partial fencing $p = 0.007$; no vs complete fencing $p = 0.051$; no water vs water $p = 0.002$; forest $p = 0.002$; Table 2.1). Bobcats had fewer visits to CS that had partial fencing ($p = 0.013$; Table 2.1). Coyotes had fewer visits to CS that were wider and that had lower human activity (width $p = 0.019$; human activity $p = 0.042$; Table 2.1).

3.2 Temporal displacement

Peaks in traffic noise occurred during the daytime at 08:20 and 16:10 h (Figure 2.4A-C). Mule deer, bobcats and coyotes responded differentially to noise pollution. Activity patterns of mule deer differed between CS with high and low noise levels ($p < 0.001$, $w = 23.62$; Figure 2.4D), and between CS with high noise levels and the reference region ($p = 0.007$, $w = 9.97$; Figure 2.4G). A comparison of percent nocturnality suggests this difference is due to a 44% increase in nocturnality from low to high-noise CS, and a 19% increase in nocturnality from reference region to high-noise CS (Figure 2.5A). On the other hand, activity patterns for bobcats did not alter (Figure 2.4E, 2.4H, 2.5B). Interestingly, coyote activity at the high-noise CS was no different than activity at the reference region ($p = 0.226$, $w = 2.98$; Figure 2.4I). However, coyote activity differed at the low-noise CS when compared to activity in the reference region ($p < 0.001$, $w = 32.46$; Figure 2.4F, 2.4I) and the high-noise CS ($p < 0.001$, $w = 29.52$; Figure 2.4F), with the greatest percent nocturnality at the low-noise CS (Figure 2.5C).

All species demonstrated a shift in activity at high-light CS in comparison to the reference region (deer $p < 0.001$, $w = 23.78$; bobcat $p = 0.002$, $w = 12.63$; coyote $p = 0.018$, $w = 8.02$; Figure 2.6B, 2.6D, 2.6F); mule deer and bobcats increased nocturnality by 21% and 24% respectively at high-light CS, whereas coyote nocturnal activity doubled at high-light CS (Figure 2.5A-C). Mule deer and bobcat activity also differed between low-light CS and high-light CS (deer $p < 0.001$, $w = 30.34$; bobcat $p < 0.001$, $w = 18.94$; Figure 2.6A, 2.6C). Similar to coyote activity at high-light CS, coyote activity at low-light CS altered and percent nocturnality doubled when compared to the reference region ($p = 0.003$, $w = 11.09$; Figure 2.5C, 2.6D, 2.6F), demonstrating that coyotes had the highest sensitivity to light of the three species.

All focal species responded to estimated peaks in vehicular light pollution, but responses differed. For mule deer, mean density estimation of activity during the morning peak (04:00 – 06:00 h) was greater at high-light CS relative to activity at low-light CS and reference region activity (Figure 2.6A-B). However, for bobcats and coyotes the reverse was true, with greater activity in the evening peak (18:00 – 20:00 h) at high-light CS (Figure 2.6C-F).

4. Discussion

4.1 Sensory pollution and the Landscape of Fear

Our results indicate that spatiotemporal displacement of wildlife arises from noise and light pollution. At the community level, the response to noise was largely one of avoidance, with fewer species being detected at noisier CS (Figure 2.2A). At the species-level, mule deer were the most responsive to traffic noise, by reducing visitation rates and shifting to a higher degree of nocturnality (Figure 2.3A; Figure 2.4A; 2.4D). Bobcats too demonstrated spatial avoidance to intermediate levels of traffic noise (Figure 2.3C), and coyotes demonstrated temporal shifts to intermediate levels of noise (Figure 2.4F; 2.4I; 2.5C). In response to light pollution, bobcats and coyotes reduced daily visitations to CS (Figure 2.3D; 2.3F), and all three species displayed greater levels of nocturnality (Figure 2.5-6). This aversion to noise and light at CS is likely attributable to the Landscape of Fear, whereby species alter spatial and temporal patterns due to the risk affects associated from vehicular noise (Laundré et al. 2001, Bleicher 2017).

4.2 Light pollution and the Human Shield

An unexpected and important finding from our study is a preference toward brighter CS at the community level (species detections), which was exemplified at the species level by visitation rates of mule deer (Figure 2.2B; 2.3B). CS that are brightly lit may facilitate the detection of predators and/or may result in predator avoidance of the area, and thus provide a safer condition for movement of prey species through the CS (Haikonen and Summala 2001). Accordingly, we found the reverse pattern for mesopredators (bobcats and coyotes) in our study, whose visitation rates decreased at brighter CS (Figure 2.3D; 2.3F). This differential response of prey and predators suggests that light exposure at the CS is acting as a Human Shield rather than contributing to a Landscape of Fear for prey species and potentially altering predator-prey dynamics (Longcore and Rich 2004). A similar increase in prey and decrease in predator presence from exposure to street lighting has been documented using mammal roadkill data (Kreling et al. 2019).

4.3 Implications of spatial & temporal avoidance

Species richness declined at noisier CS. This avoidance is likely detrimental, as failure to use these wildlife CS could result in otherwise-available habitat no longer being accessible. Habitat inaccessibility could be exacerbated if the highway has infrequent CS or is part of an expansive network of roads. Further, for CS built with the intentional purpose of facilitating wildlife movement, species absence at the CS is an undesirable conservation outcome, particularly if the species absent from CS are the target species, and/or species of conservation concern. Louder and brighter CS that were visited by the three focal species demonstrated lower visitation rates; deer and bobcats reduced visits at louder CS and bobcats and coyotes at brighter CS. This form of spatial avoidance indicates a lower likelihood of the species crossing and suggests a barrier effect of noise and light pollution.

Species that use CS exposed to sensory pollution might still avoid high levels of exposure through a shift in activity. At louder CS we observed greater percent nocturnality in mule deer, and at brighter CS we observed an increase in percent nocturnality for all focal species. Although altered activity patterns imply potential costs such as increased predation (Gaynor et al. 2018), it enables use of the CS, hence access to potential habitat. For CS, temporal avoidance can offer additional benefits, such as reducing the risk of collision if wildlife arrive at the roadside as opposed to the CS entrance, or avoidance of human-wildlife conflict with pedestrians. Other studies have shown that temporal shifts to nocturnality can provide benefits through reducing human-wildlife conflict in the daytime or increasing food and water intake (Gaynor et al. 2018, Levy et al. 2019, Dominoni et al. 2020).

4.4 Differential responses among species

Species richness at CS was reduced, but not eliminated, by sensory pollution, and accordingly our three focal species showed differential responses to sensory pollution. Differential responses have been reported for other taxa; for example Da Silva *et al.* (2016) detected differences between bird species' ability to adjust the onset of dawn singing in response to artificial light at night. Species-level differences in response to noise and light are likely driven by differences among species in the sensory system (Swaddle et al. 2015). For example, coyotes avoided light pollution more than noise pollution, whereas mule deer showed the reverse pattern (Figure 2.3A, 2.3B, 2.3E, 2.3F; 2.5). Coyotes use visual cues when hunting (Wells 1978, Darrow and Shivik 2009, Kreling et al. 2019), whereas mule deer are better able to hear than see; thus mule deer primarily draw on auditory or olfactory cues for predator detection (Ditchkoff 2011, Lashley et al. 2014).

Species-level differences in response to sensory pollution could also be linked to other factors that were explored in this study. For instance, deer visitations were lower at CS with water present. Natural noise produced by flowing streams or creeks might inhibit predator detection for deer, which rely on auditory cues (Siemers and Schaub 2011a). We also found the highest rate of visitations during intermediate levels of light and noise pollution for bobcats and light pollution for coyotes (Figure 2.3C; 2.3D; 2.3F). This quadratic response could be a result of traffic at the low-pollution CS being so infrequent that individuals preferentially cross the road instead of navigating through the CS. Roadkill data have exhibited a similar pattern, with peak mortality at intermediate levels of traffic volume (Clarke, White, and Harris 1998, Seiler 2005, Farmer and Brooks 2012, Jacobson et al. 2016). In contrast, we observed a linear as opposed to quadratic response in mule deer, potentially due to deer-proof fencing funneling mule deer to the CS and blocking highway access;

bobcat and coyote visitations were less impacted by fencing (Table 2.1). We also observed a positive relationship between coyote activity and human visitation. This may be due to the ability of coyotes to tolerate human presence, as indicated by the prevalence of coyotes in urban environments (Crooks 2002, Bateman and Fleming 2012). Finally, coyote visits at CS decreased at wider CS. Differential preferences by species toward CS structural design have been documented (Ree et al. 2015), and these responses make planning for CS design problematic.

4.5 Avoidance among trophic levels

Our study suggests that trophic interactions may also feature in decisions about navigating CS. In addition to trophic-level differences that indicate a Landscape of Fear and Human Shield acting simultaneously, bobcats and coyotes decreased activity during the morning period of vehicular light pollution (04:00 – 06:00; Figure 2.6C-F), whereas mule deer decreased activity during the evening period (18:00 – 20:00 h; Figure 2.6A-B). This differential activity suggests a short-term avoidance of the unpredictable timing of headlights (Landscape of Fear, or risky places hypothesis), while simultaneously avoiding species of higher trophic levels that are moving through the landscape – a phenomenon known as the risky times hypothesis (Brown et al. 1999, Creel et al. 2008). For example, prior research has shown female white-tailed deer with fawns temporally avoid coyotes, while coyotes and bobcats co-occur temporally (Thornton et al. 2004, Higdon et al. 2019). Studies are emerging that show species-level differential responses to anthropogenic disturbance, and that increased nocturnal activity in apex predators may result in a 'behavioral release' of mesocarnivores on the landscape (Frey et al. 2020). Further research should be directed towards disentangling how responses to noise and light affect temporal niche partitioning and predator-prey interactions (Gaston and Holt 2018).

5. Management recommendations

We recommend both noise and light pollution be considered when planning, constructing, or retrofitting CS. Structural modifications to consider include noise and light barriers, vegetation, or ‘furniture’ (rock boulders) that provides material for sound and light to be absorbed (Ree et al. 2007). Temporal zoning is a tool already implemented at certain CS; temporary road closures or reduced speed limits during critical periods of the day or year (e.g. annual mass migration) can alleviate exposure to noise and light pollution during particularly high periods of wildlife activity (e.g. 23:00 – 01:00 h for mule deer; Figure 2.4D; 2.4G). We also recommend consideration of the impacts of vehicle design on wildlife use of CS. Halogen bulbs are now being replaced by light-emitting diode, xenon, and high intensity discharge bulbs, which create higher levels of light pollution (Schubert and Kim 2005, Gaston and Holt 2018). Simultaneously, research is being directed toward understanding how much light exposure is safe for wildlife, and which light colors are less intrusive (van Grunsven et al. 2014, Contín et al. 2016, Spoelstra et al. 2017). This research could be applied to vehicle headlights, to identify light bulbs that both improve driver visibility and lower impact on wildlife vision. Finally, future research should further ascertain whether noise and light pollutants combined are additive, antagonistic, or synergistic for mammals, and identify tolerance thresholds for individual species.

6. Acknowledgements

Funding for this project was made possible by a Dissertation grant from the National Center for Sustainable Transportation (NCST), University of California, Davis, and a research grant from the NCST, supported by U.S. Department of Transportation through the University Transportation Centers program, University of California, Davis. We thank Dr. David Waetjen, Rich Codington, Jamie Bourdon, Ben Banet, Harrison Knapp, Collin Raff, Catherine Le, Annabelle Louderback-Valenzuela, Mia Guarnieri, Parisa Farman, Tricia Nguyen, Mia Macneill, Jeffrey Scott, Rachel Alsheikh, Pao Perez, Vivian Lei for assistance with data collection and processing.

7. Literature Cited

Bateman, P. W., and P. A. Fleming. 2012. Big city life: Carnivores in urban environments. Journal of Zoology 287:1–23.

Berger, J. 2007. Fear, human shields and the redistribution of prey and predators in protected areas. Biology Letters 3:620–623.

Bleicher, S. S. 2017. The landscape of fear conceptual framework: definition and review of current applications and misuses. PeerJ 5:e3772.

Bliss-ketchum, L. L., C. De Rivera, B. C. Turner, and D. M. Weisbaum. 2016. The effect of artificial light on wildlife use of a passage structure. Biological Conservation 199:25–28.

Bolker, B., H. Skaug, A. Magnusson, and A. Nielsen. 2012. Getting started with the glmmADMB package.

Brown, J. S., J. W. Laundré, and M. Gurung. 1999. The Ecology of Fear: Optimal Foraging, Game Theory, and Trophic Interactions. Journal of Mammalogy 80:385–399.

Brunen, B., C. Daguet, and J. A. G. Jaeger. 2020. What attributes are relevant for drainage culverts to serve as efficient road crossing structures for mammals? Journal of Environmental Management 268:110423.

California Department of Transportation. 2015a. Bridges, California State Highway System, 2015. http://purl.stanford.edu/td948by1459.

California Department of Transportation. 2015b. Local Agency Owned Bridges, California, 2015. http://purl.stanford.edu/cx668kz9577.

Claireau, F., Y. Bas, J. F. Julien, N. Machon, B. Allegrini, S. J. Puechmaille, and C. Kerbiriou. 2019. Bat overpasses as an alternative solution to restore habitat connectivity in the context of road requalification. Ecological Engineering 131:34–38.

Clarke, G. P., P. C. L. White, and S. Harris. 1998. Effects of roads on badger Meles meles populations in south-west England. Biological Conservation 86:117–124.

Clevenger, A. P., and N. Waltho. 2000. Factors Influencing the Effectiveness of Wildlife Underpasses in Banff National Park , Alberta , Canada 14:47–56.

Clevenger, A. P., and N. Waltho. 2005. Performance indices to identify attributes of highway crossing structures facilitating movement of large mammals. Biological conservation 121:453–464.

Conover, M. R. 2019. Numbers of human fatalities, injuries, and illnesses in the United States due to wildlife. Human-Wildlife Interactions 13:264–276.

Contín, M. A., M. M. Benedetto, M. L. Quinteros-Quintana, and M. E. Guido. 2016. Light pollution: The possible consequences of excessive illumination on retina. Eye 30:255–263.

Creel, S., J. A. Winnie, D. Christianson, and S. Liley. 2008. Time and space in general models of antipredator response: tests with wolves and elk. Animal Behaviour 76:1139–1146.

Crooks, K. R. 2002. Relative Sensitivities of Mammalian Carnivores to Habitat Fragmentation. Society for Conservation Biology 16:488–502.

Darimont, C. T., C. H. Fox, H. M. Bryan, and T. E. Reimchen. 2015. The unique ecology of human predators. Science 349:858–860.

Darrow, P. A., and J. A. Shivik. 2009. Bold, shy, and persistent: Variable coyote response to light and sound stimuli. Applied Animal Behaviour Science 116:82–87.

Dewitz, J. 2016. National Land Cover Database (NLCD) 2016 Products: U.S. Geological Survey data release.

Ditchkoff SS. 2011. Anatomy and physiology. Pages 43–73 *in* Hewitt DG, editor. Biology and management of white-tailed deer. CRC Press, Taylor and Francis Group, Boca Raton, Florda USA.

Dominoni, D. M., W. Halfwerk, E. Baird, R. T. Buxton, E. Fernández-Juricic, K. M. Fristrup, M. F. McKenna, D. J. Mennitt, E. K. Perkin, B. M. Seymoure, D. C. Stoner, J. B. Tennessen, C. A. Toth, L. P. Tyrrell, A. Wilson, C. D. Francis, N. H. Carter, and J. R. Barber. 2020a. Why conservation biology can benefit from sensory ecology. Nature Ecology and Evolution 4:502–511.

Dominoni, D., J. A. H. Smit, M. E. Visser, and W. Halfwerk. 2020b. Multisensory pollution: Artificial light at night and anthropogenic noise have interactive effects on activity patterns of great tits (Parus major). Environmental Pollution 256.

Duriscoe, D. M. 2016. Photometric indicators of visual night sky quality derived from all-sky brightness maps. Journal of Quantitative Spectroscopy and Radiative Transfer 181:33–45.

Farmer, R., and R. Brooks. 2012. Integrated Risk Factors for Vertebrate Roadkill in Southern Ontario. The Journal of Wildlife Management 76:1215–1224.

Ferraro, D. M., M.-L. T. Le, and C. D. Francis. 2020. Combined effect of anthropogenic noise and artificial night lighting negatively affect Western Bluebird chick development. The Condor.

Forman, R. T. T. 2000. Estimate of the area affected ecologically by the road system in the

United States. Conservation biology 14:31–35.

Forman, R. T. T. 2003. Road ecology: science and solutions. Island Press.

Forman, R. T. T., and L. E. Alexander. 1998. ROADS AND THEIR MAJOR ECOLOGICAL EFFECTS. Annual Review of Ecology and Systematics 29:207–231.

Francis, C. D., and J. R. Barber. 2013. A framework for understanding noise impacts on wildlife : an urgent conservation priority.

Francis, C. D., C. P. Ortega, and A. Cruz. 2009. Noise Pollution Changes Avian Communities and Species Interactions. Current Biology 19:1415–1419.

Frey, S., J. P. Volpe, N. A. Heim, J. Paczkowski, and J. T. Fisher. 2020. Move to nocturnality not a universal trend in carnivore species on disturbed landscapes. Oikos:1128–1140.

Gaston, K. J., and L. A. Holt. 2018. Nature, extent and ecological implications of night-time light from road vehicles. Journal of Applied Ecology 55:2296–2307.

Gaynor, K. M., C. E. Hojnowski, N. H. Carter, and J. S. Brashares. 2018. The influence of human disturbance on wildlife nocturnality 1235:1232–1235.

Gill, J. A., K. Norris, and W. J. Sutherland. 2001. Why behavioural responses may not reflect the population consequences of human disturbance. Biological Conservation 97:265–268.

van der Grift, E. A., R. van der Ree, L. Fahrig, S. Findlay, J. Houlahan, J. A. G. Jaeger, N. Klar, L. F. Madriñan, and L. Olson. 2013. Evaluating the effectiveness of road mitigation measures. Biodiversity and Conservation 22:425–448.

van Grunsven, R. H. A., M. Donners, K. Boekee, I. Tichelaar, K. G. van Geffen, D. Groenendijk, F. Berendse, and E. M. Veenendaal. 2014. Spectral composition of light sources and insect phototaxis, with an evaluation of existing spectral response models. Journal of Insect Conservation 18:225–231.

Haikonen, H., and H. Summala. 2001. Deer-vehicle crashes—extensive peak at 1 hour after sunset. American journal of preventive medicine 21:209–213.

Halfwerk, W., and H. Slabbekoorn. 2015. Pollution going multimodal: The complex impact of the human-altered sensory environment on animal perception and performance. Biology Letters 11.

Higdon, S. D., C. A. Diggins, M. J. Cherry, and W. M. Ford. 2019. Activity patterns and temporal predator avoidance of white-tailed deer (Odocoileus virginianus) during the fawning season. Journal of Ethology 37:283–290.

Jacobson, S. L., L. L. Bliss-Ketchum, C. E. De Rivera, and W. P. Smith. 2016. A behavior-based framework for assessing barrier effects to wildlife from vehicle traffic volume. Ecosphere 7:1–15.

Jechow, A., Z. Kolláth, S. J. Ribas, H. Spoelstra, F. Hölker, and C. C. M. Kyba. 2017. Imaging and mapping the impact of clouds on skyglow with all-sky photometry. Scientific Reports 7:1–10.

Kintsch, J., and P. C. Cramer. 2011. Permeability of existing structures for terrestrial wildlife: a passage assessment system.

Konstantopoulos, K., A. Moustakas, and I. N. Vogiatzakis. 2020. A spatially explicit impact assessment of road characteristics, road-induced fragmentation and noise on birds species in Cyprus. Biodiversity 00:1–11.

Kreling, S. E. S., K. M. Gaynor, and C. A. C. Coon. 2019. Roadkill distribution at the wildland-urban interface. Journal of Wildlife Management 83:1427–1436.

Lashley, M. A., M. C. Chitwood, M. T. Biggerstaff, D. L. Morina, C. E. Moorman, and C. S. DePerno. 2014. White-tailed deer vigilance: The influence of social and environmental factors. PLoS ONE 9:1–6.

Laundré, J. W., L. Hernández, and K. B. Altendorf. 2001. Wolves, elk, and bison: reestablishing the "landscape of fear" in Yellowstone National Park, U.S.A. Canadian Journal of Zoology 79:1401–1409.

Laundre, J. W., L. Hernandez, and W. J. Ripple. 2010. The Landscape of Fear: Ecological Implications of Being Afraid. The Open Ecology Journal 3:1–7.

Levy, O., T. Dayan, W. P. Porter, and N. Kronfeld-Schor. 2019. Time and ecological resilience: can diurnal animals compensate for climate change by shifting to nocturnal activity? Ecological Monographs 89:1–21.

Longcore, T., and C. Rich. 2004. Ecological light pollution. Frontiers in Ecology and the Environment 2:191–198.

Lund, U., C. Agostinelli, H. Arai, A. Gagliardi, E. Garcia Portuges, D. Giunchi, J.-O. Irisson, M. Pocermnich, and F. Rotolo. 2017. R package "circular": Circular Statistics (version 0.4-93). R package.

Madliger, C. L. 2012. Toward improved conservation management: A consideration of sensory ecology. Biodiversity and Conservation 21:3277–3286.

McMahon, T. A., J. R. Rohr, and X. E. Bernal. 2017. Light and noise pollution interact to disrupt interspecific interactions. Ecology 98:1290–1299.

Meek, P. D., G. Ballard, A. Claridge, R. Kays, K. Moseby, T. O'Brien, A. O'Connell, J. Sanderson, D. E. Swann, M. Tobler, and S. Townsend. 2014. Recommended guiding principles for reporting on camera trapping research. Biodiversity and Conservation 23:2321–2343.

Meredith, A. M., and M. Ridout. 2017. Package ' overlap .'

Nouvellet, P., G. S. A. Rasmussen, D. W. Macdonald, and F. Courchamp. 2012. Noisy clocks and silent sunrises : measurement methods of daily activity pattern 286:179–184.

Nyhus, P. J. 2016. Human–Wildlife Conflict and Coexistence. Page Annual Review of Environment and Resources.

Oriol-cotterill, A., M. Valeix, L. G. Frank, C. Riginos, and D. W. Macdonald. 2015. Landscapes of Coexistence for terrestrial carnivores : the ecological consequences of being downgraded from ultimate to penultimate predator by humans. Oikos 124:1263–1273.

Owens, A. C. S., P. Cochard, J. Durrant, B. Farnworth, E. K. Perkin, and B. Seymoure. 2020. Light pollution is a driver of insect declines. Biological Conservation 241.

Patten, M. A., J. C. Burger, and M. Mitrovich. 2019. The intersection of human disturbance and diel activity, with potential consequences on trophic interactions. PLoS ONE 14:1–13.

Raap, T., R. Pinxten, G. Casasole, N. Dehnhard, and M. Eens. 2017. Ambient anthropogenic noise but not light is associated with the ecophysiology of free-living songbird nestlings. Scientific Reports 7:1–8.

Ree, R. Van Der, E. Van Der Grift, N. Gulle, K. Holland, C. Mata, and F. Suarez. 2007. Overcoming the barrier effect of roads - how effective are mitigation strategies? An international review of the use and effectiveness of underpasses and overpasses designed to increase the pereability of roads for wildlife. Pages 423–431 Proceedings of the 2007 International Conference on Ecology and Transportation.

Ree, R. Van Der, D. Smith, and C. Grilo, editors. 2015. Handbook of Road Ecology. John Wiley & Sons, Oxford.

Ridout, M. S., and M. Linkie. 2009. Estimating Overlap of Daily Activity Patterns From Camera Trap Data. Springer 14:322–337.

RStudio Team. 2015. RStudio: Integrated Development for R. RStudio, Inc., Boston, MA.

Rytwinski, T., R. Van Der Ree, G. M. Cunnington, L. Fahrig, C. S. Findlay, J. Houlahan, J. A. G. Jaeger, K. Soanes, and E. A. Van Der Grift. 2015. Experimental study designs to improve the evaluation of road mitigation measures for wildlife. Journal of Environmental Management 154:48–64.

Rytwinski, T., K. Soanes, J. A. G. Jaeger, L. Fahrig, S. Findlay, J. Houlahan, R. Van Der Ree, and E. A. Van Der Grift. 2016. How Effective Is Road Mitigation at Reducing Road-Kill ? A Meta-Analysis:1–25.

Schubert, E. F., and J. K. Kim. 2005. Solid-state light sources getting smart. Science 308:1274–1278.

Seiler, A. 2005. Predicting locations of moose-vehicle collisions in Sweden. Journal of Applied Ecology 42:371–382.

Shultz, S., and R. Noe. 2002. The consequences of crowned eagle central-place foraging on predation risk in monkeys. Proceedings of the Royal Society B: Biological Sciences 269:1797–1802.

Siemers, B. M., and A. Schaub. 2011. Hunting at the highway: traffic noise reduces foraging efficiency in acoustic predators. Proceedings of the Royal Society B: Biological Sciences 278:1646–1652.

Da Silva, A., M. Valcu, and B. Kempenaers. 2016. Behavioural plasticity in the onset of dawn song under intermittent experimental night lighting. Animal Behaviour 117:155–165.

Simons, A. L., X. Yin, and T. Longcore. 2020. High correlation but high scale-dependent variance between satellite measured night lights and terrestrial exposure. Environmental Research Communications 2.

Sollmann, R. 2018. A gentle introduction to camera-trap data analysis. African Journal of Ecology 56:740–749.

Spoelstra, K., R. H. A. van Grunsven, J. J. C. Ramakers, K. B. Ferguson, T. Raap, M. Donners, E. M. Veenendaal, and M. E. Visser. 2017. Response of bats to light with different spectra: Light-shy and agile bat presence is affected by white and green, but not red light. Proceedings of the Royal Society B: Biological Sciences 284:11–15.

Swaddle, J. P., C. D. Francis, J. R. Barber, C. B. Cooper, C. C. M. Kyba, D. M. Dominoni, G. Shannon, E. Aschehoug, S. E. Goodwin, A. Y. Kawahara, D. Luther, K. Spoelstra, M. Voss, and T. Longcore. 2015. A framework to assess evolutionary responses to anthropogenic light and sound. Trends in Ecology and Evolution 30:550–560.

Team, Q. D. 2018. QGIS Geographic information System. Open Source Geospatial Foundation Project.

Thornton, D. H., M. E. Sunquist, and M. B. Main. 2004. Ecological separation within newly sympatric populations of coyotes and bobcats in south-central Florida. Journal of Mammalogy 85:973–982.

Wells, M. C. 1978. Coyote senses in predation: Environmental influences on their relative use. Behavioural Processes 3:149–158.

Woltz, H. W., J. P. Gibbs, and P. K. Ducey. 2008. Road crossing structures for amphibians and reptiles: informing design through behavioral analysis. Biological Conservation 141:2745–2750.

Young, A. H., K. R. Knapp, A. Inamdar, W. Hankins, and W. B. Rossow. 2018. The International Satellite Cloud Climatology Project H-Series climate data record product. Earth System Science Data 10:583–593.

Tables

Table 2.1. Relationships among attributes included in the full model and response variables.

Attribute examined	Species richness	Deer visitation	Bobcat visitation	Coyote visitation
AIC of full model	792.1	964	630.1	614.5
ΔAIC from base model	-13.9	-11	-34.8	-54.8
ΔAIC from partial model	-10.5	-15.6	-169.9	-42.6
NLCD	N/S	Evergreen forest = 0.002	N/S	N/S
Water present	< 0.001	0.002	N/S	N/S
Fencing present	0.005	Complete 0.051 Partial 0.007	Partial 0.013	N/S
CS width	N/S	N/S	N/S	0.019
CS length	0.003	N/S	N/S	N/S
Minimum daily temperature	< 0.001	0.029	0.049	0.042
Sampling year (2018)	< 0.001	< 0.001	0.012	0.009
Human activity	N/S	N/S	N/S	0.042
Daily vehicle traffic	< 0.001	N/S	N/S	N/S
Background or underpass camera	N/S	N/S	0.009	N/S
Baited cameras	N/S	N/S	0.019	N/S

Figures

Figure 2.1. Locations of the 26 crossing structures across California, USA (pink circles).

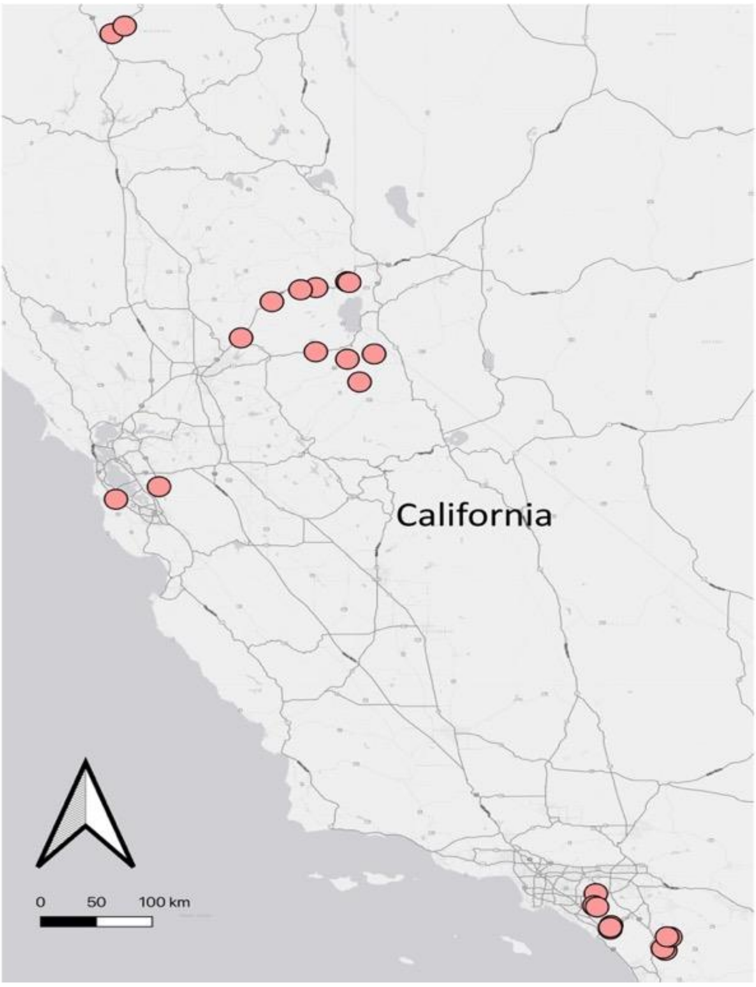

Figure 2.2. Results from the ‘predict’ function executed for the model testing species richness in response to A) noise pollution and B) light pollution at crossing structures. Black circles represent observations, with the line of best fit (noise = purple, light = orange) and confidence intervals derived from the predicted data.

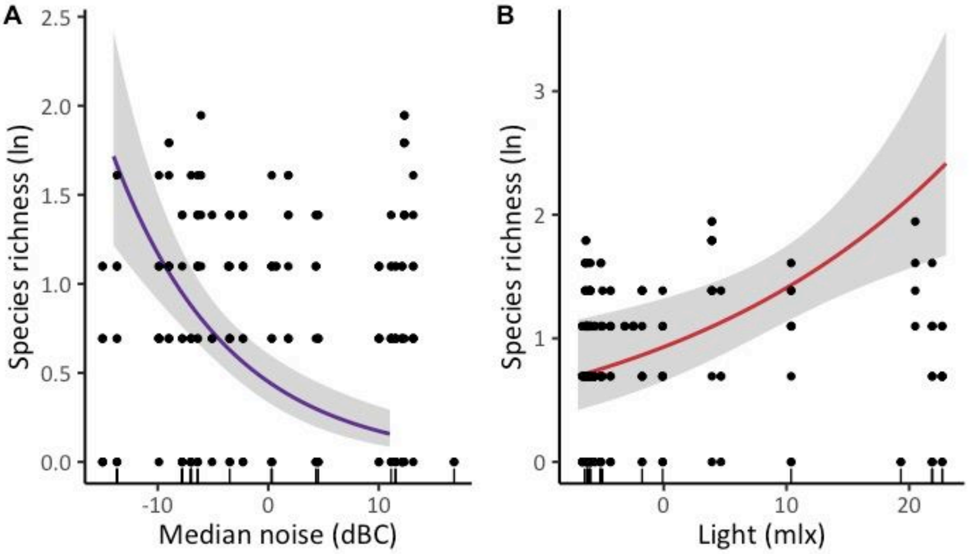

Figure 2.3. Results from the ‘predict’ function executed for the model testing visitations of A-B) mule deer, C-D) bobcat and E-F) coyote in response to noise pollution and light pollution at crossing structures. Black circles represent observations, with the line of best fit (noise = purple, light = orange) and confidence intervals derived from the model predicted values.

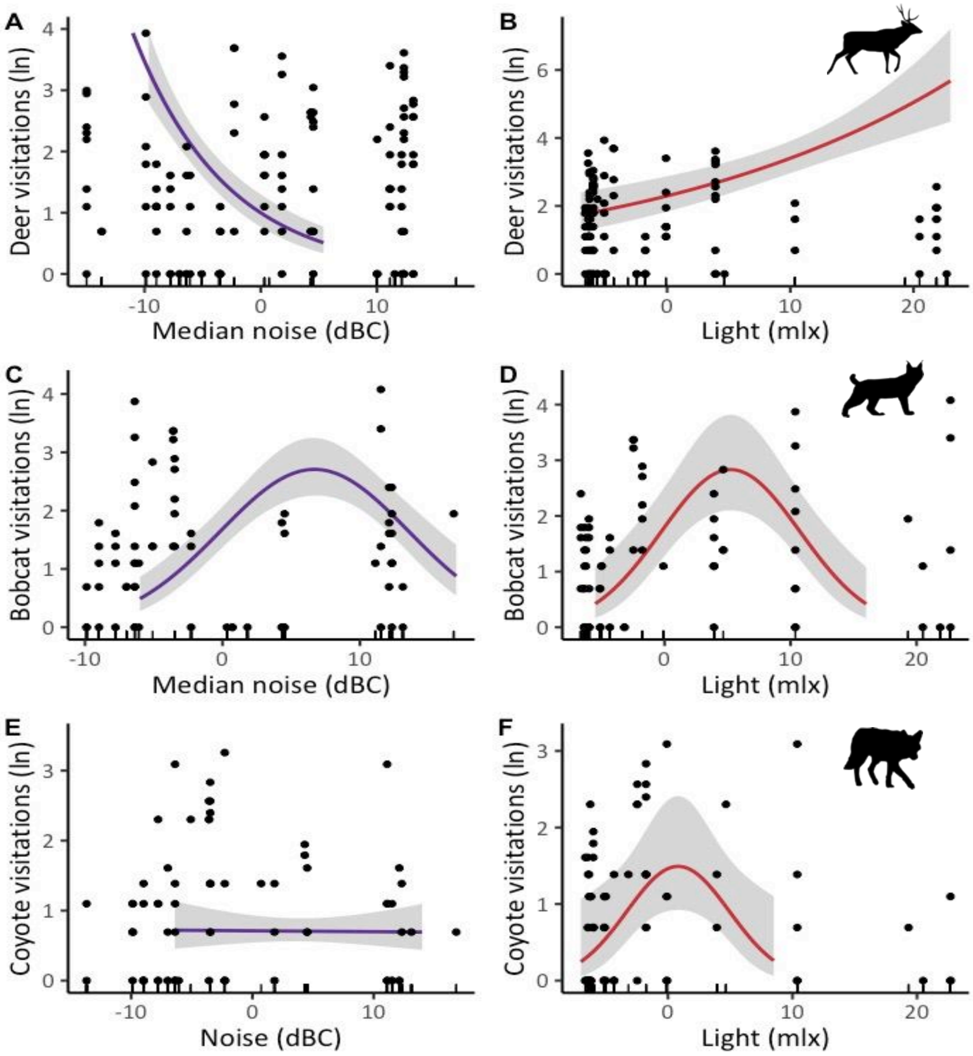

Figure 2.4. Daily profile of week-long traffic recordings (A-C) for all sites at which each species was detected. Below the traffic profiles, diel activity curves and temporal overlap between loud (purple line) versus quiet (green dashed line) CS for D) mule deer (N_{loud} = 324, N_{quiet} = 80), E) bobcat (N_{loud} = 152, N_{quiet} = 192) and F) coyote (N_{loud} = 66, N_{quiet} = 109), and activity curves and temporal overlap between loud CS versus reference regions (black dashed line) for G) mule deer ($N_{background}$ = 239), H) bobcat ($N_{background}$ = 80) and I) coyote ($N_{background}$ = 84). Activity overlap is represented by the coefficient of overlap, $\hat{\Delta}$ (grey shaded area); 1 denotes complete overlap.

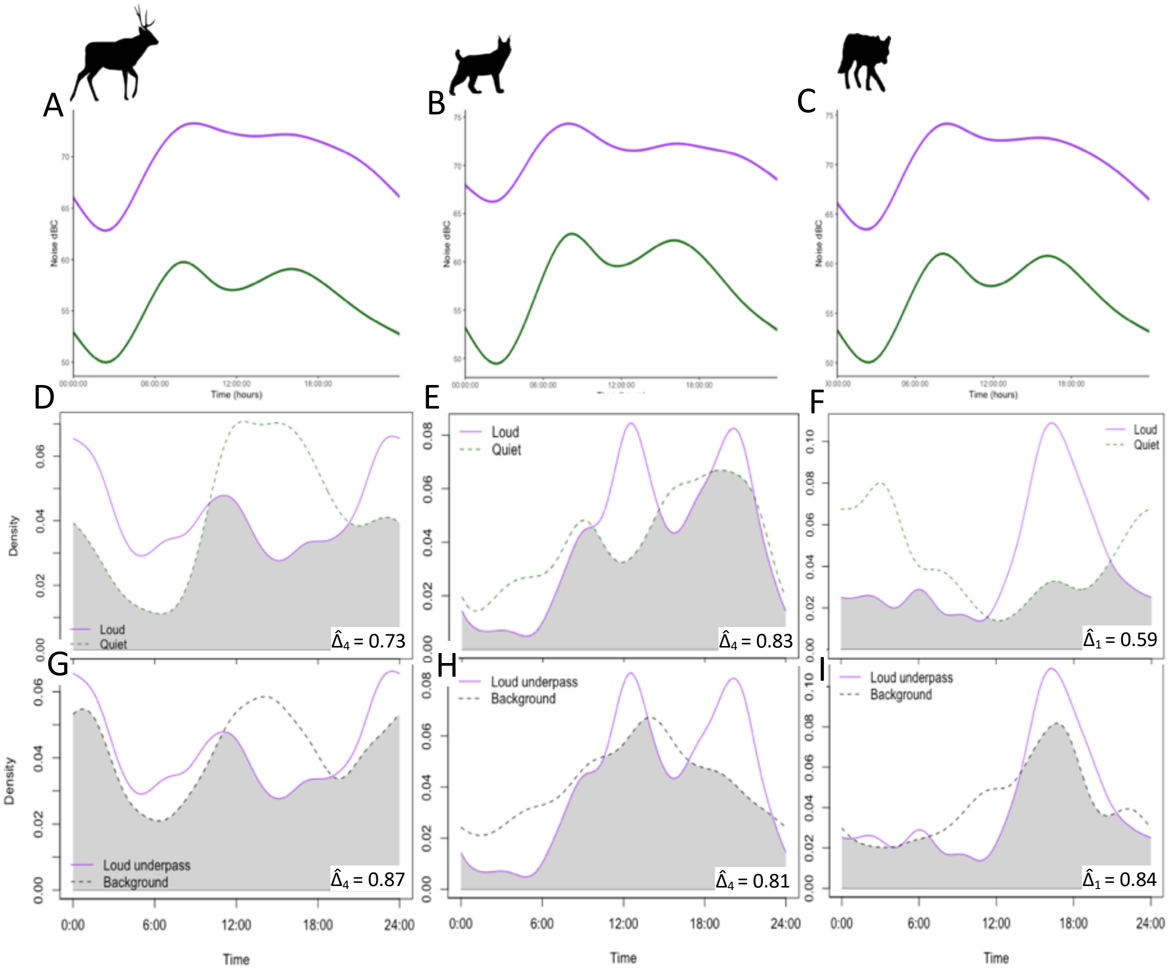

Figure 2.5. Percent of nocturnal activity (18:00 – 06:00 h) under different exposure levels of noise and light disturbance for A) mule deer, B) bobcat and C) coyote. The three exposure levels are RR = reference region (orange), CS low = low levels of pollution (yellow) and CS high = high levels of pollution (blue). We include a 50% threshold (dashed black line) to represent the point at which diurnal (< 50%) or nocturnal (> 50%) activity is dominant.

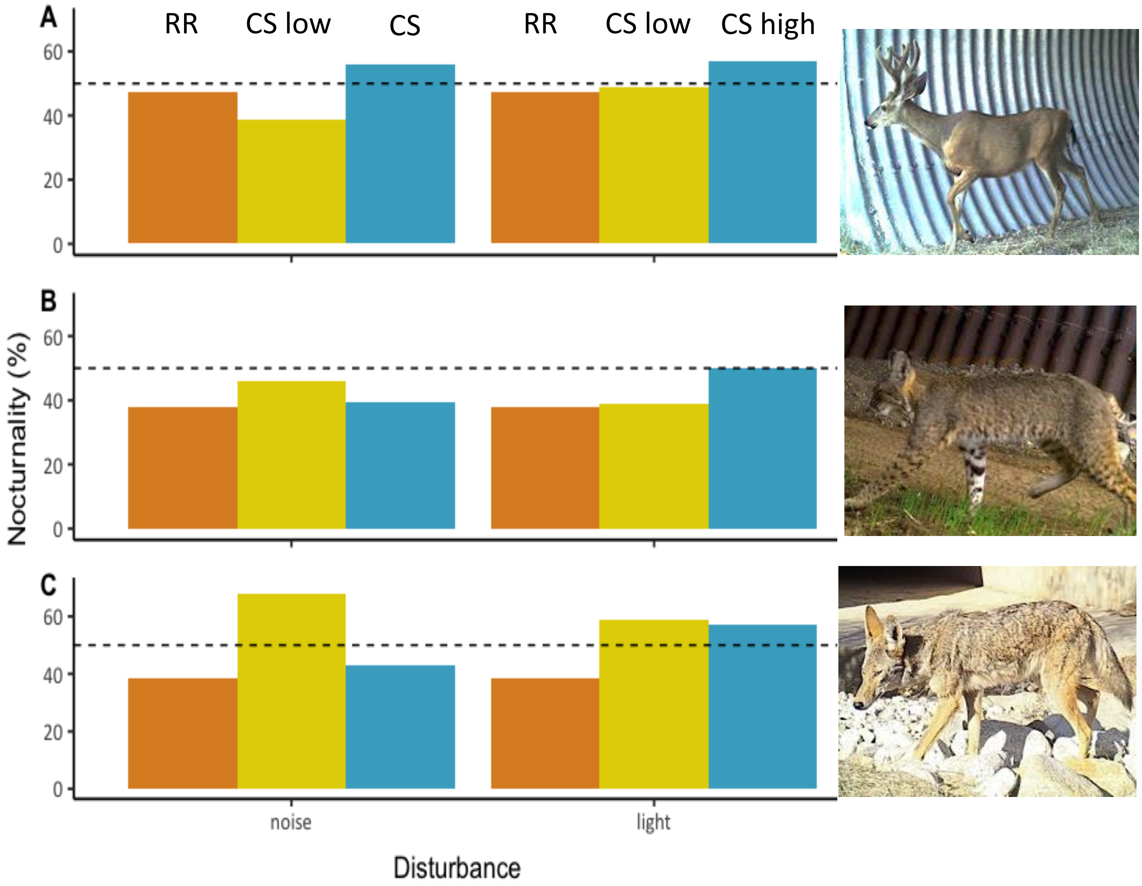

Figure 2.6. Diel activity curves and temporal overlap for mule deer (A-B; N_{light} = 125, N_{dark} = 297, $N_{background}$ = 239), bobcat (C-D; N_{light} = 144, N_{dark} = 200, $N_{background}$ = 80) and coyote (E-F; N_{light} = 40, N_{dark} = 135, $N_{background}$ = 84) between low (blue dashed line) versus high (black solid line) levels of light pollution at CS (A, C, E), and high levels of light pollution at CS versus unbaited cameras in the reference region (blue dashed line) (B, D, F). Sunrise and sunset (yellow vertical lines) occur at 06:00 & 18:00. Activity overlap is represented by the coefficient of overlap, $\hat{\Delta}$ (grey shaded area); 1 denotes complete overlap.

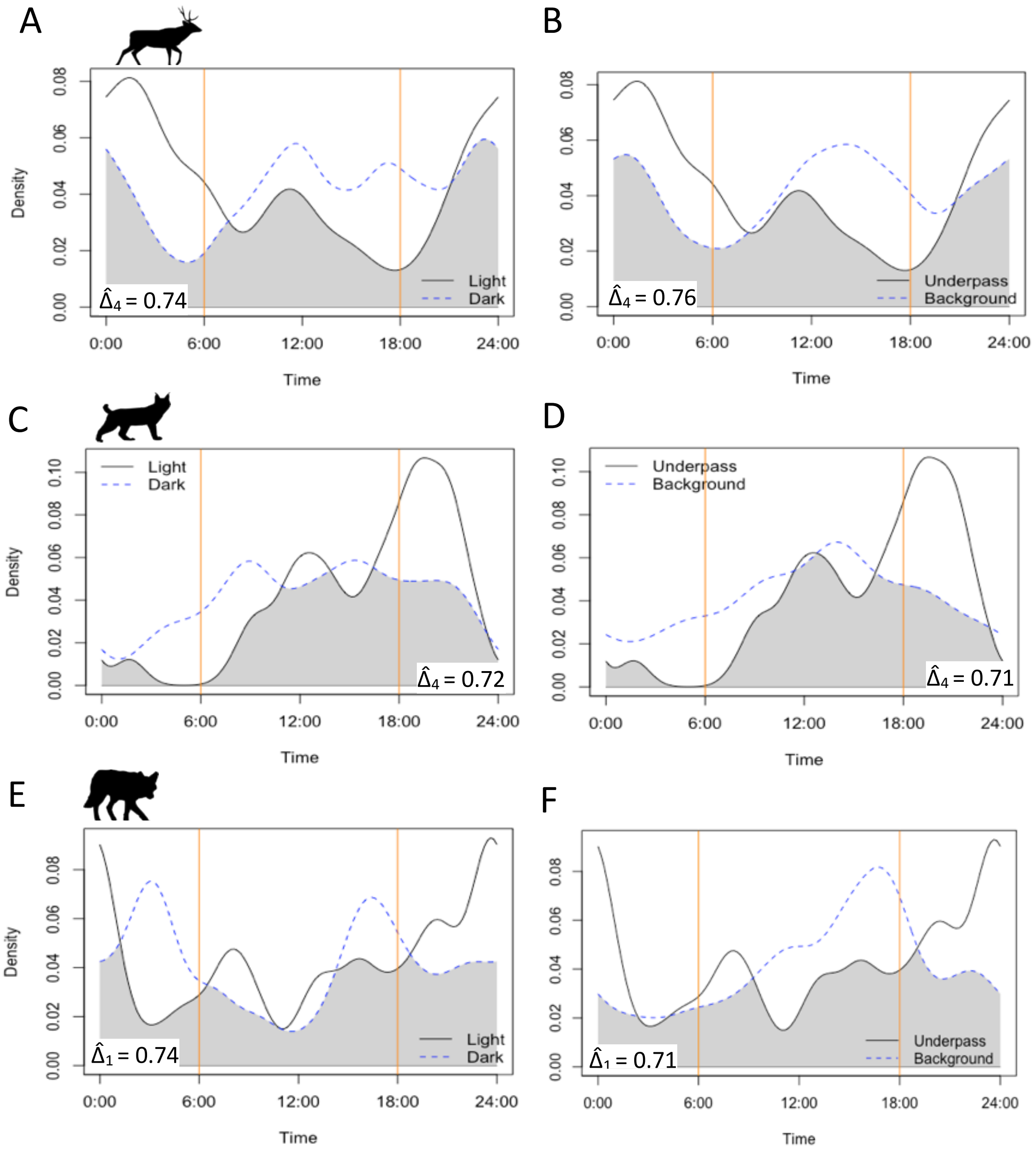

Supplement

Table S2.1. Noise and light metrics measured at each crossing structure. Noise measurements for C-weighting (dBC) were used for analysis.

Site	Highway	Noise (median dBC)	Noise (Median dBA)	Light (Illuminance mlx)
Agua Tibia	SR 76	56.2	46	1.92
Andrade	I-680	75.5	52.8	10.98
Arroyo Seco	SR 79	60.9	51.5	2.72
Auburn	I-80	65	51.9	0.65
Casa Loma Alta	I-80	73.2	61.9	1.41
Coal Canyon	SR 91	80	65.4	26.38
Coal Canyon Culvert	SR 91	74.7	61.2	29.75
Edgewood	I-280	74.3	56.2	6.97
Frey	SR 76	56.8	46.1	2.07
Hirschdale	I-80	67.5	56.5	1.07
Hwy 79 Round	SR 79	63.9	54.4	3.88
Indian Creek	SR 89	49.5	39.9	0.88
Jackass Gulch	SR 4	48.2	39	0.77
Kirkwood	SR 88	53.3	43.3	1.96
Marion Creek	SR 76	56.2	43.3	0.62
Mesa 1	SR 74	59.7	48.7	5.30
Mesa 2	SR 74	59.6	49.1	4.59
PM24	I-80	67.7	59.5	1.06
PM6	US 97	54.2	43	0.72
SAFR	US 50	63.5	53.6	28.93
Santiago Canyon Box Culvert	Santiago	57.1	49.5	27.55
Santiago Canyon Underpass	Santiago	56.8	47.8	17.44
Sheep Rock	US 97	55.4	-	0.82
Soda Springs	I-80	75.3	61.8	0.42
Unknown Bridge	I-80	76.3	64.3	1.08
White Bridge	SR 74	58.1	50.5	11.72

Table S2.2. Species detected at each camera station during the sampling period of camera trapping for each site location. Treatment distinguished between reference region (R) and crossing structure (U).

Site	Treat-ment	Bait type	ID	N	Species Common Name
Agua Tibia	R	Bait	114	1	Mule (or Black tailed) Deer
Agua Tibia	R	Bait	605	1	Virginia Opossum
Agua Tibia	R	Bait	702	2	Mountain Lion, Mule (or Black tailed) Deer
Agua Tibia	R	No_bait	604	5	Mountain Lion, Gray Fox, Raccoon, Coyote, Virginia Opossum
Agua Tibia	R	No_bait	703	2	Bobcat, Mountain Lion
Agua Tibia	U	NA	119	1	Gray Fox
Agua Tibia	U	NA	601	1	Coyote
Andrade	R	Bait	13	6	Virginia Opossum, Raccoon, Striped Skunk, Mule (or Black tailed) Deer, Bobcat, American Badger
Andrade	R	Bait	14	4	Raccoon, Mule (or Black tailed) Deer, Virginia Opossum, Striped Skunk
Andrade	R	Bait	16	2	Virginia Opossum, Mule (or Black tailed) Deer
Andrade	R	Bait	20	6	Virginia Opossum, Bobcat, Gray Fox, Mule (or Black tailed) Deer, Striped Skunk, Raccoon
Andrade	R	No_bait	17	4	Mule (or Black tailed) Deer, Raccoon, Striped Skunk, Virginia Opossum
Andrade	R	No_bait	18	6	Bobcat, Mule (or Black tailed) Deer, Striped Skunk, Coyote, Virginia Opossum, Gray Fox
Andrade	R	No_bait	23	4	Virginia Opossum, Mule (or Black tailed) Deer, Striped Skunk, Bobcat
Andrade	R	No_bait	24	4	Raccoon, Mule (or Black tailed) Deer, Coyote, Gray Fox
Andrade	U	NA	15	1	Mule (or Black tailed) Deer

Andrade	U	NA	19	7	Mule (or Black tailed) Deer, Gray Fox, Striped Skunk, Raccoon, Bobcat, Virginia Opossum, Mountain Lion
Andrade	U	NA	21	6	Mule (or Black tailed) Deer, Striped Skunk, Raccoon, Bobcat, Gray Fox, Virginia Opossum
Andrade	U	NA	22	7	Mule (or Black tailed) Deer, Striped Skunk, Bobcat, Virginia Opossum, Raccoon, Gray Fox, American Badger
Arroyo Seco	U	NA	701	3	Mule (or Black tailed) Deer, Raccoon, Coyote
Arroyo Seco	U	NA	702	2	Mule (or Black tailed) Deer, Coyote
Arroyo Seco	U	NA	804	1	Mule (or Black tailed) Deer
Auburn	R	Bait	1	4	Mule (or Black tailed) Deer, Striped Skunk, Raccoon, Gray Fox
Auburn	R	Bait	3	5	Raccoon, Mule (or Black tailed) Deer, Coyote, Virginia Opossum, Gray Fox
Auburn	R	Bait	5	2	Mule (or Black tailed) Deer, Raccoon
Auburn	R	No_bait	2	3	Mule (or Black tailed) Deer, Raccoon, Coyote
Auburn	R	No_bait	4	2	Mule (or Black tailed) Deer, Raccoon
Auburn	R	No_bait	6	2	Mule (or Black tailed) Deer, Coyote
Auburn	U	NA	100	4	Mule (or Black tailed) Deer, Raccoon, Striped Skunk, Bobcat
Auburn	U	NA	NA	5	Mule (or Black tailed) Deer, Gray Fox, Raccoon, Striped Skunk, Virginia Opossum
Caspers (Mesa 1; Mesa 2; White Bridge)	R	Bait	101	1	Virginia Opossum
Caspers (Mesa 1; Mesa 2; White Bridge)	R	Bait	131	2	Mule (or Black tailed) Deer, Coyote
Caspers (Mesa 1; Mesa 2; White Bridge)	R	Bait	602	2	Coyote, Mule (or Black tailed) Deer

Caspers (Mesa 1; Mesa 2; White Bridge)	R	Bait	605	3	Striped Skunk, Coyote, Mountain Lion
Caspers (Mesa 1; Mesa 2; White Bridge)	R	No_bait	4	4	Mule (or Black tailed) Deer, Gray Fox, Coyote, Bobcat
Caspers (Mesa 1; Mesa 2; White Bridge)	R	No_bait	124	4	Coyote, Bobcat, Mule (or Black tailed) Deer, Mountain Lion
Caspers (Mesa 1; Mesa 2; White Bridge)	R	No_bait	130	1	Mule (or Black tailed) Deer
Casa Loma Alta	R	Bait	1	3	Black Bear, Striped Skunk, Gray Fox
Casa Loma Alta	R	Bait	5	1	Black Bear
Casa Loma Alta	R	Bait	7	2	Gray Fox, Black Bear
Casa Loma Alta	R	No_bait	2	3	Virginia Opossum, Striped Skunk, Mule (or Black tailed) Deer
Casa Loma Alta	R	No_bait	4	3	Black Bear, Striped Skunk, Mule (or Black tailed) Deer
Casa Loma Alta	R	No_bait	6	2	Black Bear, Gray Fox
Casa Loma Alta	R	No_bait	8	2	Black Bear, Gray Fox
Casa Loma Alta	U	No_bait	NA	1	Mule (or Black tailed) Deer
Casa Loma Alta	U	No_bait	NA	2	Black Bear, Mule (or Black tailed) Deer
Coal Canyon	R	Bait	4	1	Gray Fox
Coal Canyon	R	Bait	131	2	Mountain Lion, Gray Fox
Coal Canyon	R	Bait	600	1	Gray Fox
Coal Canyon	R	Bait	602	2	Gray Fox, Striped Skunk
Coal Canyon	R	No_bait	125	2	Bobcat, Gray Fox
Coal Canyon	R	No_bait	609	2	Mule (or Black tailed) Deer, Gray Fox
Coal Canyon	U	NA	100	1	Bobcat
Coal Canyon	U	NA	202	1	Coyote
Coal Canyon Culvert	U	NA	117	2	Coyote, Bobcat
Coal Canyon Culvert	U	NA	651	3	Bobcat, Coyote, Long-Tailed Weasel
Coal Canyon Culvert	U	NA	652	3	Bobcat, Coyote, Virginia Opossum
Edgewood	R	Bait	4	1	Mule (or Black tailed) Deer
Edgewood	R	Bait	5	3	Mule (or Black tailed) Deer, Coyote, Virginia Opossum

Edgewood	R	Bait	7	3	Mule (or Black tailed) Deer, Virginia Opossum, Mountain Lion
Edgewood	R	No_bait	1	1	Bobcat
Edgewood	R	No_bait	6	2	Mule (or Black tailed) Deer, Virginia Opossum
Edgewood	R	No_bait	8	2	Mule (or Black tailed) Deer, Mountain Lion
Edgewood	U	NA	9	2	Mule (or Black tailed) Deer, Coyote
Edgewood	U	NA	10	4	Mule (or Black tailed) Deer, Coyote, Mountain Lion, Raccoon
Edgewood	U	NA	11	2	Mule (or Black tailed) Deer, Coyote
Edgewood	U	NA	12	2	Mule (or Black tailed) Deer, Coyote
Frey	U	NA	10	2	Coyote, Virginia Opossum
Frey	U	NA	110	3	Bobcat, Mule (or Black tailed) Deer, Mountain Lion
Frey	U	NA	603	4	Mountain Lion, Bobcat, Coyote, Mule (or Black tailed) Deer
Hirschdale	R	Bait	1	3	Mule (or Black tailed) Deer, Mountain Lion, Black Bear
Hirschdale	R	Bait	3	1	Black Bear
Hirschdale	R	Bait	6	4	Black Bear, Mule (or Black tailed) Deer, Western Spotted Skunk, Bobcat
Hirschdale	R	Bait	8	3	Mule (or Black tailed) Deer, Western Spotted Skunk, Striped Skunk
Hirschdale	R	No_bait	2	1	Black Bear
Hirschdale	R	No_bait	4	1	Bobcat
Hirschdale	U	NA	1	4	Coyote, Mule (or Black tailed) Deer, Bobcat, Black Bear
Hirschdale	U	NA	2	2	Mule (or Black tailed) Deer, Coyote
Hwy 79 (Arroyo Seco; Hwy79 round)	R	Bait	800	2	Gray Fox, Western Spotted Skunk
Hwy 79 (Arroyo Seco; Hwy79 round)	R	Bait	801	3	Gray Fox, Bobcat, Coyote

Hwy 79 (Arroyo Seco; Hwy79 round)	R	Bait	802	4	Gray Fox, Striped Skunk, Mule (or Black tailed) Deer, Coyote
Hwy 79 (Arroyo Seco; Hwy79 round)	R	No_bait	803	4	Gray Fox, Bobcat, Mule (or Black tailed) Deer, Coyote
Hwy 79 (Arroyo Seco; Hwy79 round)	R	No_bait	805	3	Gray Fox, Mountain Lion, Bobcat
Hwy 79 (Arroyo Seco; Hwy79 round)	R	No_bait	806	1	Gray Fox
hwy79 round	U	NA	604	3	Raccoon, Bobcat, Gray Fox
hwy79 round	U	NA	710	3	Raccoon, Coyote, Bobcat
Indian Creek	R	Bait	4	1	Black Bear
Indian Creek	R	Bait	103	3	Gray Fox, Black Bear, Western Spotted Skunk
Indian Creek	R	Bait	105	1	Black Bear
Indian Creek	R	Bait	116	2	Black Bear, Western Spotted Skunk
Indian Creek	R	No_bait	121	3	Gray Fox, Mule (or Black tailed) Deer, Black Bear
Indian Creek	R	No_bait	125	2	Black Bear, Gray Fox
Indian Creek	U	NA	126	3	Black Bear, Coyote, Mountain Lion
Indian Creek	U	NA	129	5	Black Bear, Striped Skunk, Mule (or Black tailed) Deer, Coyote, Mountain Lion
Jackass Gulch	R	Bait	602	2	Mule (or Black tailed) Deer, American Marten
Jackass Gulch	R	Bait	603	2	American Marten, Black Bear
Jackass Gulch	R	Bait	605	3	American Marten, Black Bear, Mule (or Black tailed) Deer
Jackass Gulch	R	Bait	609	3	American Marten, Mule (or Black tailed) Deer, Black Bear
Jackass Gulch	R	No_bait	127	2	Mule (or Black tailed) Deer, Black Bear
Jackass Gulch	U	NA	301	1	Mule (or Black tailed) Deer
Jackass Gulch	U	NA	303	1	Mule (or Black tailed) Deer
Jackass Gulch	U	NA	601	1	Mule (or Black tailed) Deer
Jackass Gulch	U	NA	604	1	Mule (or Black tailed) Deer
Kirkwood	R	Bait	101	3	Yellow-Bellied Marmot, Coyote, Mule (or Black tailed) Deer

Kirkwood	R	Bait	110	2	Mule (or Black tailed) Deer, Coyote
Kirkwood	R	Bait	120	2	Mule (or Black tailed) Deer, Coyote
Kirkwood	R	No_bait	111	5	Mule (or Black tailed) Deer, Yellow-Bellied Marmot, Coyote, Black Bear, Bobcat
Kirkwood	R	No_bait	112	2	Mule (or Black tailed) Deer, Coyote
Kirkwood	R	No_bait	124	2	Mule (or Black tailed) Deer, Coyote
Kirkwood	U	NA	106	2	Raccoon, Yellow-Bellied Marmot
Kirkwood	U	NA	108	3	Raccoon, Bobcat, Northern River Otter
Kirkwood	U	NA	201	1	Raccoon
Kirkwood	U	NA	202	2	Raccoon, Bobcat
Marion Creek	U	NA	103	1	Coyote
Marion Creek	U	NA	121	2	Bobcat, Coyote
Mesa 1	U	NA	103	2	Bobcat, Coyote
Mesa 1	U	NA	127	4	Bobcat, Coyote, Mountain Lion, Mule (or Black tailed) Deer
Mesa 1	U	NA	701	4	Coyote, Bobcat, Mountain Lion, Mule (or Black tailed) Deer
Mesa 2	U	NA	26	3	Bobcat, Coyote, Mule (or Black tailed) Deer
Mesa 2	U	NA	107	3	Coyote, Bobcat, Gray Fox
Mesa 2	U	NA	700	3	Bobcat, Coyote, Mule (or Black tailed) Deer
Mesa 2	U	NA	710	3	Gray Fox, Bobcat, Coyote
PM24	R	Bait	13	1	Mule (or Black tailed) Deer
PM24	R	Bait	16	2	Mule (or Black tailed) Deer, Coyote
PM24	R	Bait	24	2	Black Bear, Bobcat
PM24	R	No_bait	14	1	Mule (or Black tailed) Deer
PM24	R	No_bait	17	1	Mule (or Black tailed) Deer
PM24	R	No_bait	20	1	Mule (or Black tailed) Deer
PM24	R	No_bait	23	2	Striped Skunk, Mule (or Black tailed) Deer
PM24	U	NA	11	4	Bobcat, Mule (or Black tailed) Deer, Coyote, Black Bear
PM24	U	NA	12	4	Mule (or Black tailed) Deer, Bobcat, Black Bear, Coyote

PM6	R	Bait	602	3	Gray Fox, Coyote, Western Spotted Skunk
PM6	R	Bait	603	3	Mule (or Black tailed) Deer, Black Bear, Coyote
PM6	R	Bait	604	3	Black Bear, Mule (or Black tailed) Deer, Coyote
PM6	R	Bait	609	3	Mule (or Black tailed) Deer, Black Bear, Gray Fox
PM6	R	No_bait	601	6	Gray Fox, Mule (or Black tailed) Deer, Coyote, Bobcat, Striped Skunk, Black Bear
PM6	R	No_bait	605	5	Gray Fox, Coyote, Black Bear, Mule (or Black tailed) Deer, Striped Skunk
PM6	R	No_bait	608	6	Mule (or Black tailed) Deer, Striped Skunk, Coyote, Bobcat, Gray Fox, Black Bear
PM6	U	NA	116	2	Mule (or Black tailed) Deer, Bobcat
PM6	U	NA	121	2	Mule (or Black tailed) Deer, Bobcat
PM6	U	NA	129	2	Mule (or Black tailed) Deer, Bobcat
SAFR	R	Bait	110	2	Mule (or Black tailed) Deer, Gray Fox
SAFR	R	Bait	115	3	Gray Fox, Mule (or Black tailed) Deer, Striped Skunk
SAFR	R	Bait	121	3	Black Bear, Mule (or Black tailed) Deer, Gray Fox
SAFR	R	No_bait	105	5	Mule (or Black tailed) Deer, Gray Fox, Bobcat, Black Bear, Striped Skunk
SAFR	R	No_bait	125	2	Black Bear, Gray Fox
SAFR	R	NA	112	3	Mule (or Black tailed) Deer, Gray Fox, Striped Skunk
SAFR	U	NA	100	1	Mule (or Black tailed) Deer
SAFR	U	NA	111	1	Mule (or Black tailed) Deer
SAFR	U	NA	131	1	Mule (or Black tailed) Deer
Santiago Canyon	R	Bait	118	5	Bobcat, Gray Fox, Coyote, Mule (or Black tailed) Deer, Striped Skunk
Santiago Canyon	R	Bait	126	4	Bobcat, Coyote, Gray Fox, Striped Skunk
Santiago Canyon	R	Bait	250	1	Bobcat

Santiago Canyon	R	Bait	603	3	Bobcat, Gray Fox, Striped Skunk
Santiago Canyon	R	No_bait	116	3	Coyote, Bobcat, Gray Fox
Santiago Canyon	R	No_bait	251	2	Bobcat, Coyote
Santiago Canyon	R	No_bait	252	3	Gray Fox, Bobcat, Mule (or Black tailed) Deer
Santiago Canyon	R	No_bait	607	1	Bobcat
Santiago Canyon Box Culvert	U	NA	110	4	Gray Fox, Mule (or Black tailed) Deer, Raccoon, Virginia Opossum
Santiago Canyon Box Culvert	U	NA	111	7	Bobcat, Virginia Opossum, Gray Fox, Raccoon, Mule (or Black tailed) Deer, Mountain Lion, Coyote
Santiago Canyon Box Culvert	U	NA	115	3	Raccoon, Virginia Opossum, Mountain Lion
Santiago Canyon Box Culvert	U	NA	601	5	Virginia Opossum, Gray Fox, Mule (or Black tailed) Deer, Bobcat, Mountain Lion
Santiago Canyon Underpass	U	NA	125	4	Bobcat, Coyote, Mule (or Black tailed) Deer, Gray Fox
Sheep Rock	R	Bait	103	2	Coyote, Mule (or Black tailed) Deer
Sheep Rock	R	Bait	121	1	Coyote
Sheep Rock	R	No_bait	107	3	Mule (or Black tailed) Deer, Coyote, Bobcat
Sheep Rock	R	No_bait	113	2	Coyote, Bobcat
Sheep Rock	R	No_bait	128	1	Coyote
Sheep Rock	U	NA	0	1	Mule (or Black tailed) Deer
Sheep Rock	U	NA	4	4	Mule (or Black tailed) Deer, Bobcat, Mountain Lion, Black Bear
Sheep Rock	U	NA	301	4	Mule (or Black tailed) Deer, Bobcat, Black Bear, Mountain Lion
Soda Springs	R	Bait	40	1	Mule (or Black tailed) Deer
Soda Springs	R	Bait	44	2	Black Bear, Mule (or Black tailed) Deer
Soda Springs	R	No_bait	2	1	Mule (or Black tailed) Deer
Soda Springs	R	No_bait	4	2	Mule (or Black tailed) Deer, Black Bear

Soda Springs	R	No_bait	8	1	Mule (or Black tailed) Deer
Soda Springs	U	NA	35	3	Raccoon, Bobcat, Coyote
Soda Springs	U	NA	37	3	Bobcat, Coyote, Mule (or Black tailed) Deer
Soda Springs	U	NA	38	2	Bobcat, Coyote
Soda Springs	U	NA	39	1	Bobcat
Unknown Bridge	R	Bait	28	2	Black Bear, Mule (or Black tailed) Deer
Unknown Bridge	R	Bait	29	3	Gray Fox, Mule (or Black tailed) Deer, Black Bear
Unknown Bridge	R	Bait	30	5	Black Bear, Mule (or Black tailed) Deer, Coyote, Striped Skunk, Bobcat
Unknown Bridge	R	Bait	32	3	Mule (or Black tailed) Deer, Gray Fox, Black Bear
Unknown Bridge	R	No_bait	25	2	Black Bear, Mule (or Black tailed) Deer
Unknown Bridge	R	No_bait	26	4	Gray Fox, Mule (or Black tailed) Deer, Bobcat, Black Bear
Unknown Bridge	R	No_bait	27	2	Black Bear, Mule (or Black tailed) Deer
Unknown Bridge	U	NA	34	1	Mule (or Black tailed) Deer
Unknown Bridge	U	NA	43	2	Mule (or Black tailed) Deer, Gray Fox
White Bridge	U	NA	10	2	Bobcat, Gray Fox
White Bridge	U	NA	120	1	Gray Fox
White Bridge	U	NA	604	2	Bobcat, Gray Fox
White Bridge	U	NA	702	4	Gray Fox, Coyote, Mule (or Black tailed) Deer, Bobcat

Chapter 3: Fear responses to anthropogenic noise vary across temporal scales

Amy C. Collins, T. Winston Vickers, Fraser M. Shilling

1. Introduction

Humans have modified the majority of the Earth's ecosystems, and occupy approximately 50% of the global surface (Strano et al. 2020). Within human dominated ecosystems, humans have adopted the trophic position of 'super predator', being the dominant cause of wildlife mortality (Darimont et al. 2015). Given the threat that humans pose to wildlife, non-lethal human activity can elicit fear responses from organisms on the landscape by altering stress physiology, spatiotemporal habitat use, and behavior (Støen et al. 2015, Hammond et al. 2020). These anthropogenic stressors may result in modification to predator-prey interactions, and lead to trophic cascading effects, ultimately altering ecosystem structure and function (Kuijper et al. 2016, Schmitz et al. 2018, Zanette and Clinchy 2019).

Anthropogenic stressors that influence fear responses exist across multiple scales, for example heterogenous space use by humans, which leads to alterations in the movement decisions and distribution of predators at a fine-scale and across a landscape (Suraci et al. 2019, 2020). As such, the spatiotemporal scale that anthropogenic stressors occupy likely is related to fear responses (Dröge et al. 2017, Moll et al. 2017). Moll et al. (2017) and Prugh *et al.* (2019) recently noted the urgent need for multi-scale frameworks to disentangle the behavioral impacts of fear across scales, demonstrating that prior work examining fear responses has largely focused at a single scale, and inconsistent use of metrics preclude cross-study comparisons.

One anthropogenic stressor that varies across temporal scales is noise pollution. Anthropogenic noise pollution is pervasive across urban and wildland areas, and has been linked to behavioral shifts in migration, communication, prey detection, and predator avoidance among wildlife species (Francis et al. 2012, Buxton et al. 2017, Dominoni et al. 2020a). Fear is a commonly reported response to noise pollution, as wildlife perceive noise pollution as a predation threat (risk disturbance hypothesis: Frid and Dill 2002). However, fear-inducing responses appear to vary, with some species demonstrating habituation over time from repeated exposure (Nedelec et al. 2016, Neo et al. 2018, Walthers and Barber 2020). Under certain conditions, the response can be positive. Carnivores can be highly sensitive to anthropogenic noise (Smith et al. 2017), hence some ungulate and small mammal species use anthropogenic noise as a 'Human Shield' to seek shelter from predators (Berger 2007, Shannon et al. 2014b, Suraci et al. 2019).

To examine whether a fear response, habituation, or Human Shields occur when exposed to anthropogenic noise pollution, we need to consider the temporal scale and characteristics of the noise pollutant. *Instantaneous* noise (milliseconds) could startle the animal (acoustic startle response: Koch and Schnitzler 1997, Francis and Barber 2013) and induce a flight response. Longer timeframes, such as *acute* (seconds, minutes) and *chronic* (weeks, years) could alter anti-predator behavior such as vigilance (predator surveillance) and alterations to group size (many-eyes effect: Bednekoff and Lima 1998, Creel and Winnie 2005). It is important to parse out which type or types of noise pollution, instantaneous, acute, or chronic, is driving fear responses among wildlife.

Understanding fear responses can have beneficial implications for the management of applied conservation projects (Prugh et al. 2019, Gaynor et al. 2020). Crossing structures that are built under or over highways aim to mitigate habitat fragmentation, by reducing the barrier effect and road-related mortality (Clevenger and Waltho 2005, Rytwinski et al. 2016). However, the success of crossing structures depends on specific aspects of animal behavior, especially the likelihood of approaching the structure and entering the structure. Traffic-induced noise pollution that is persistent at a crossing structure could increase the perception of risk, thereby increasing anti-predator behavior and leading to suboptimal decision-making regarding entry into the crossing structure (Quinn et al. 2006, Shannon et al. 2014a, Owen et al. 2017). Avoiding fear responses at crossing structures will be particularly critical if there is no alternative route available to connect the habitat (Gill et al. 2001).

Many studies in birds have tested acoustic impacts of road noise on behavioral responses, such as predator avoidance behavior in house sparrows (*Passer domesticus*) (Meillère et al. 2015) and avoidance of 'phantom roads' (the experimental introduction of traffic noise to roadless areas) by migrating birds (McClure et al. 2013, Ware et al. 2015). Among mammals, activity patterns of white-tailed deer (*Odocoileus virginianus*), mule deer, and coyotes have been shown to shift during exposure to vehicular noise, and mule deer and bobcat visitation rates are lower at noisier crossing structures (Buxton et al. 2020, Chapter 2). Predation efficiency by bats and vigilance in prairie dogs (*Cynomys ludovicianus*) are known to be altered in response to noise, as is vigilance in impalas (*Aepyceros melampus*) alongside roads (Siemers and Schaub 2011, Mtui 2014, Shannon et al. 2014). However, little is yet known regarding the impact of traffic-related noise pollution on anti-predator behavior within mammals. Understanding these impacts is of particular importance given that large, mobile species are vulnerable to road mortality (Rytwinski and Fahrig 2015).

Using a multi-scale approach, we tested whether *fear, habituation,* or *Human Shields* exist at crossing structures exposed to traffic noise. We first tested the hypothesis that instantaneous noise levels affect the utilization of crossing structures, predicting that as noise levels rise, focal species will be more likely to flee rather than use the crossing structure. Secondly, we tested the hypothesis that acute noise will affect anti-predator behaviors, predicting that increased noise will be associated with increases in vigilance, running, and group size, and decreases in foraging. Finally, we examined whether differences in use of crossing structure or anti-predator behavior exist across crossing structures of varying chronic noise. We focused on two species, coyotes (*Canis latrans*) and mule deer (*Odocoileus hemionus*) which allowed us to examine the response of a predator and prey species to noise.

2. Methods

2.1 Study area

Our study was conducted from November 2018 through November 2019 at 10 crossing structures in California, USA: eight culverts and two bridges (Figure 3.1). Crossing structures were located along Interstate 80, Interstate 680, and U.S. Route 50 in central California, Interstate 5 and U.S. Route 97 in northern California, and State Route 74 in Southern California. Crossing structures were located under highways consisting of one to three lanes of traffic in each direction, in areas classed as low- or medium-intensity development, evergreen forest, or shrub/scrub.

2.2 Camera trapping

Behavior of coyotes and mule deer was assessed using camera traps. We placed six camera traps (Brownings Dark Ops Pro) at each crossing structure set to record high-quality video and audio, triggered by motion and infrared (no-glow). Once triggered, cameras recorded videos for 20 seconds, with a 5-second delay between triggers. Cameras were equipped with the 'smart IR setting'; videos during the daytime were recorded past 20 seconds if the camera continued to detect wildlife movement. We placed one camera at each of the two entrances of the crossing structure, ca. 5 m (range: 0 – 10 m) from the entrance. We also placed two cameras at each of the two 'approach zones', the area ca. 50 m from the crossing structure entry from which wildlife approach the crossing structure (range: 11 - 84 m). Cameras remained operational at each site for an average of 45 days (range: 1 – 106). We captured the location of each camera station and the crossing structure entrance via a handheld GPS device (Garmin eTrex 20x) and calculated the Euclidean distance of each camera station to the entrance of the crossing structure via Google Maps.

2.3 Flight and entry response, anti-predator behavior

We extracted activity from each camera trap video that included mule deer and coyotes using the Behavioral Observation Research Interactive Software (BORIS; Friard and Gamba 2016). To analyze flight and entry responses, videos from cameras positioned at the crossing structure entrance (ca. 5 m from entrance) were checked for observations in which animals were facing the direction of the crossing structure entryway or walking toward the crossing structure entryway. Within these observations, we scored each time a decision-making event occurred: 1. Entry, defined as stepping across the concrete edge of the crossing structure entrance; and 2. Flight, defined as an alteration in body direction and movement away from the crossing structure.

To analyze anti-predator behavior, we also scored activity of individual mule deer and coyotes for all videos. We focused on three categories of behavior associated with fear responses: 1. vigilance, defined as an individual standing or sitting upright, 2. foraging, defined as feeding or drinking, and 3. Running, defined as any movement faster than a walk. For each of these behaviors, we assigned a start and stop time within each video and calculated time as a proportion of total time the individual was present in the video. The BORIS software enabled analysis of multiple behaviors recorded simultaneously. To distinguish between individuals within one video, we assigned each conspecific a unique identification based on order of appearance or distance from the camera. For each video, we documented whether the video was taken in day (color) or night (black and white) mode, the temperature listed for each video collected by the camera's internal thermometer, and the maximum group size observed. We recorded the number of humans present in each video, and quantified the frequency of daily visitations by humans for each camera station. Research technicians who scored behaviors received extensive training in the recognition of behaviors across species and the BORIS software before classifying observations.

2.4 Noise indices

We considered noise pollution at multiple spatiotemporal scales; we quantified traffic-related noise pollution during each decision-making event, for the duration of wildlife presence in each video, and at each crossing structure site. Temporal scale varied across three levels: during the 2-second interval encompassing a decision-making event, during the ~20-second duration of the video, and over a 7-day period at the crossing structure. The 2-second interval represented “instantaneous”, the ~20-second represented “acute” and 7-day intervals represented “chronic” scales. Two spatial scales were represented: variation in behaviors among the six cameras at each crossing structure, and variation among the 10 crossing structures.

Instantaneous & acute noise

Audio waveform data recorded by the camera trap during each video were exported using BORIS software. Using the R function ‘cut_sels’ (*warbleR*; Araya-Salas and Smith-Vidaurre 2017) we cut selections of each audio file for 1) a 1-second period before and after each decision-making event (flight or entry) and 2) the start and stop time that we observed an individual animal in each video. For each cut audio file, we then produced an amplitude envelope of the waveform signal derived from the Hilbert transform using the ‘env’ function (*seewave*; Sueur et al. 2020). Using this envelope, we then extracted the relative maximum amplitude for each 2-second audio file, representing instantaneous noise, and the relative median amplitude for each ~20-second audio file, representing acute noise.

Chronic noise

To quantify the overall level of traffic-induced noise pollution associated with each crossing structure, during July – November 2019 we sampled sound pressure levels at each crossing structure for a 7-day period after removal of camera traps using TENMA 72-947 and PCE-322 sound pressure meters, which detect in the 30-130dB range and were set at the slow setting. We placed two sound meters at one entrance of the crossing structure facing inwards on a tripod 0.5 m above the ground. Sound pressure levels were measured in 59-second increments in decibels, set to a C-weighted filter (dBC), and an A-weighted filter (dBA). For each crossing structure, we then extracted L_{50} (median noise) measures. Owing to an equipment failure of the A-weighted sound meter at one crossing structure, we report findings on dBC hereafter, and provide comparative L_{50} dBA measure in the supplemental (Table S3.1).

2.5 Statistical analysis

We analyzed the effect of instantaneous, acute, and chronic noise on decision-making at the entrance of the crossing structure (entry or flight response), anti-predator behavior (proportion of time being vigilant, running, or foraging), and group size.

Decision-making events: flight and entry response

To examine the impact of instantaneous noise and chronic noise on whether coyote and mule deer entered or fled from the crossing structure entrance, we employed a hierarchical generalized linear (glm) model using the 'glm' function in R. Crossing structure and camera were specified as random effects, and a binomial distribution was selected based on the binary structure of the response variable. We included additional predictors for each observation that represented group size, time of day (binary; day/night), temperature recorded on each video for each camera, rate of human daily visitations, distance to crossing structure, and structure length. We performed step-wise removal of non-significant variables, and selected the best fit model based on the lowest AIC score.

Activity budgets: vigilance, running, and foraging

To test for the impact of acute and chronic noise on anti-predator behavior, we again employed hierarchical glms for proportion of time coyotes spent being vigilant and foraging, and time mule deer spent being vigilant, foraging and running, using crossing structure and camera as random effects. As we recorded no foraging by coyotes, a model for coyote foraging was not employed. Due to the response variable being proportional and to account for overdispersion in the data, we used a quasibinomial distribution.

Group size

To test for the impact of acute and chronic noise on group size, we employed negative binomial glms to deer and coyote observations separately. Site and camera were random effects, and temperature, time of day, crossing structure length, distance to crossing structure, and human visitation rate were used as additional predictors. We performed step-wise removal of non-significant variables, and selected the best fit model based on the lowest AIC score.

We checked for model robustness by comparing all models to the respective base model using ANOVA and plotting Pearson's residuals. All analyses were carried out in RStudio (R v. 3.6.1; RStudio Team 2015).

3. Results

3.1 Decision-making events: flight and entry response

We collected a total of 10 hours and 13 minutes of mule deer observations and 50 minutes of coyote observations throughout the study period. Within coyotes, we observed 50 decision-making events, nine that resulted in a flight response and 41 that resulted in an entry. Within mule deer, we observed 192 decision-making events, 35 that resulted in a flight response and 157 in an entry. For coyotes, flight responses were more likely to occur as levels of instantaneous noise increased; for mule deer, there was a trend in the same direction (Table 3.1; Figure 3.2A, coyote $p = 0.018$; Figure 3.2B, deer $p = 0.056$). We detected no effect of chronic noise on decision-making events (coyote $p = 0.829$; deer $p = 0.592$). The best fit model also demonstrated warmer temperatures increased the likelihood of coyotes entering the crossing structure ($p = 0.016$).

3.2 Activity budgets: vigilance, running and mule deer foraging

For mule deer, foraging rates increased during greater levels of acute noise (Figure 3.3), but decreased during greater levels of chronic noise (Table 3.2; acute and chronic noise $p < 0.001$). In response to greater levels of chronic noise, coyotes demonstrated a decrease in vigilance and an increase in running (vigilance and running $p < 0.001$; Figure 3.4). Acute and chronic noise had no effect on mule deer vigilance or running (vigilance acute noise $p = 0.316$, chronic noise $p = 0.484$; running acute noise $p = 0.235$, chronic noise $p = 0.969$).

Longer crossing structures caused a decrease in coyote vigilance and a decrease in vigilance and foraging for mule deer (coyote $p = 0.031$; deer foraging and vigilance $p < 0.001$). Coyotes increased their time spent vigilant during warmer periods, whereas for mule deer, vigilance decreased and foraging increased (coyote $p < 0.001$; deer vigilance $p = 0.003$; deer foraging $p < 0.001$). Additionally, mule deer demonstrated decreased levels of vigilance and greater levels of foraging in large groups (vigilance and group size of seven $p = 0.026$; foraging and group size of five $p = 0.007$), and decreased levels of vigilance during nighttime hours ($p < 0.001$). Proportion of time spent running for coyotes and mule deer increased during daylight hours (coyote $p = 0.004$; deer $p < 0.001$). The likelihood of coyotes running increased with distance from the crossing structure ($p < 0.001$), whereas mule deer ran less and foraged more with increasing distance from the crossing structure (vigilance $p = 0.004$; foraging $p < 0.001$). Additionally, mule deer ran more and foraged less at crossing structures with heavier human visitation (running and foraging $p < 0.001$).

3.3 Group size

For both mule deer and coyotes, neither acute nor chronic noise affected group size. Smaller group sizes were associated with longer crossing structures and higher human visitations and groups were smaller at the crossing structure entrance as opposed to the approach zone (length $p < 0.001$; humans $p = 0.047$; distance to crossing structure $p < 0.001$).

4. Discussion

We found that at crossing structures exposed to higher levels of instantaneous noise from vehicles, coyotes and mule deer were more likely to initiate a flight response than they were to use the crossing. Further, we detected greater levels of coyote running and mule deer foraging at crossing structures with more chronic noise. These behavioral changes are in accordance with the risk disturbance hypothesis, and suggest that both instantaneous and chronic noise induce a 'Landscape of Fear' in predator and prey species (Laundré et al. 2001). Though instantaneous and chronic noise elicited a fear response, noise examined at an intermediate level – acute noise – elicited a neutral or positive effect in anti-predator behavior, which suggest habituation and the Human Shield, respectively. Hence, wildlife response to noise pollution can vary according to temporal scale.

4.1 Instantaneous and chronic noise: fine-scale patch of fear and landscape of fear

We found support for our hypothesis that instantaneous noise from vehicles invokes a flight response (Figure 3.2) and provides additional support to prior findings that a fear response can be induced by fine-scale noise associated with land or sea transportation. For example, playbacks of ship noise under a lab setting prompted higher startle responses in two fish species (Voellmy et al. 2014), and playbacks of traffic noise prompted black-tailed prairie dogs (*Cynomys ludovicianus*) to flee more quickly (Shannon et al. 2016). Responses to instantaneous noise can add physiological stress and impact body condition, as demonstrated by an increase in heart rate and alarm behavior of mule deer and mountain sheep (*Ovis canadensis*) when exposed to aircraft noise (Weisenberger et al. 1996). Further, through invoking a flight response rather than an entry response, instantaneous noise pollution resulted in a suboptimal decision. Noise-altered decision-making has also been demonstrated in choice of optimal shell size by hermit crabs (*Pagurus bernhardus*) (Walsh et al. 2017, Tidau and Briffa 2019). Detrimental effects of noise pollution on decision-making could have consequences beyond the individual level. Failure to use the crossing structure could reduce habitat connectivity, and ultimately reduce gene flow, which could have long-term implications for the viability of populations (van der Ree et al. 2009). Reductions in habitat connectivity will be a particular issue in urban areas where the carrying capacity of subpopulations is already low. Similar types of population bottlenecks from artificial wildlife passages have been documented in fish ladders (Agostinho et al. 2007). Our work suggests that to ensure the viability of crossing, noise pollution should be considered during the design phase of crossing structures.

We also found that in response to crossing structures that were exposed to higher levels of chronic (one week) noise, coyotes decreased vigilance, but increased running (Figure 3.4), and mule deer decreased foraging rates. These alterations to anti-predator behavior expand upon findings that mule deer show spatiotemporal avoidance of louder crossing structures, and coyotes show temporal avoidance to intermediate noise levels (Chapter 2). Our findings also support other work that has identified alterations to anti-predator and feeding behavior upon exposure to noise pollution. Exposure to transportation noise has caused a decrease in foraging for terrestrial mammals (Shannon et al. 2014, Smith et al. 2017), marine mammals (Blair et al. 2016, Wisniewska et al. 2018) and other taxa (Wale et al. 2013, Castaneda et al. 2020). At the individual level, reduced foraging and/or increased levels of vigilance may lead to reduced body condition and fitness (Bachman 1993). At the landscape level, heterogeneous levels of noise pollution, and thus differences in fear responses, creates a Landscape of Fear, and could lead to altered natural predator-prey interactions, and ecosystem function (Gaynor et al. 2019, Zanette and Clinchy 2019).

4.2 Intermediate scale of acute noise: human shield and habituation

Our finding that high levels of acute noise coincided with increased mule deer foraging (Figure 3.3) suggests high traffic noise can provide a refuge from predation. Ungulates have displayed similar increases in foraging in response to anthropogenic stressors within U.S. National Parks (Berger 2007, Brown et al. 2012, Shannon et al. 2014). Carnivores display strong fear responses to noise pollution from the human ‘super predator’ (Smith et al. 2017). Large-bodied carnivores may also be particularly deterred from areas of high anthrophony (anthropogenic sounds) due to the low-frequency energy overlapping strongly with the frequencies in which carnivores communicate, or because of an inability to detect prey as a result of cue masking (Warren et al. 2006, Cardoso et al. 2018). Therefore, predation risk could be lower for ungulates during periods of higher noise pollution. Another explanation for increased foraging during acute periods of noise can be taken from the risk allocation hypothesis (Lima and Bednekoff 1999), which states that wildlife exposed to long-term, continuous pollutants are unable to sustain anti-predator behavior, and that anti-predator responses are used only when exposed to unpredictable stimuli. Though we did document a fear response in mule deer to instantaneous traffic noise, we also detected a fear response in mule deer from landscape-scale chronic noise, rendering the risk allocation hypothesis an unlikely explanation.

Acute noise showed no effect on coyote vigilance or running behavior. The most parsimonious explanation for this result is that coyotes are habituated to louder noise levels experienced within short timescales (Bejder et al. 2009). Habituation to motorboat noise has also been demonstrated in foraging fish, and fallow deer (*Dama dama*) were shown to habituate to playbacks of sound from road markings (strips of sound-producing material) after 10 nights (Ujvári et al. 2004, Magnhagen et al. 2017).

4.3 Consequences across spatial and temporal scale

Our results indicate a differential effect of noise pollution across spatial and temporal scales (Figure 3.5). Previous studies have recommended examining responses to fear across multiple spatiotemporal scales to capture variation in response (Creel and Christianson 2008, Moll et al. 2017, Prugh et al. 2019). Here, we sampled vehicular noise across different spatial and temporal dimensions. In doing so, we were able to identify that risk effects differ across temporal scales; fear responses occur at fine (instantaneous) and coarse (chronic) scales, while habituation and Human Shields occur at intermediate scales (acute) of noise pollution. Further, mechanisms driving fear responses differed spatially, at the fine scale of the camera and the coarse scale of the crossing structure. Our results further demonstrate that a Landscape of Fear and Human Shields are not mutually exclusive, and that prey and predators assess risk at various spatial and temporal scales concurrently. Much of our current knowledge surrounding the relation of risk to spatiotemporal scale is based upon herbivore-carnivore interactions. For example patch- and landscape-level fear occur in red deer (*Cervus elaphus*) when inhabiting wolf territories in Poland, and African ungulates increase vigilance during times of concurrent short-term and long-term risk (Kuijper et al. 2015, Dröge et al. 2017). Here we add to the ecology of fear and demonstrate anthropogenic stressors also mediate fear responses of wildlife across multiple scales.

Our primary goal was to assess the effect of noise pollution on anthropogenic, behaviorally-mediated effects; however, we also examined several covariates which could alter the fear response. Though we detected no alterations to group size at louder crossing structures in response to patch and landscape interference, we did detect an increase in foraging and a decrease in vigilance among mule deer when in large groups (five and seven). Similar findings for the effect of group size on foraging have been reported for white-tailed deer (Lashley et al. 2014). The well-documented trade-off between vigilance and group size is likely due to individuals requiring less time to scan for predators (many eyes hypothesis) in larger groups, and individuals benefiting from a lowered predation risk through dilution effects (Roberts 1996). Accordingly, vigilance of California ground squirrels (*Otospermophilus beecheyi*) only increased when small groups, but not large groups, were exposed to loud playbacks of natural sounds (e.g. rivers) (Le et al. 2019). As expected, the higher number of humans present at the crossing structure decreased foraging of deer, and vigilance was reduced for both species at night. This supports previous findings demonstrating that wildlife fear human presence, and wildlife shift to more nocturnal activity as a way to avoid humans (Stankowich 2008, Ciuti et al. 2012, Gaynor et al. 2018, Chapter 2).

Coyotes increased vigilance further from the crossing structure, a response similar to pronghorn (*Antilocapra americana*) at crossing structures (Seidler et al. 2018). Foraging behavior of mule deer increased at camera stations further away from the crossing structure, and during warmer periods, which could be a result of higher densities of vegetation during warmer seasons and in locations further from the concrete crossing structure. In contrast, coyote vigilance increased during warmer temperatures, potentially due to activity of their predators being greater. For example, black bears (*Ursus americanus*) are only a predation risk for coyotes during the spring and summer months when they are not hibernating (Rogers 1992). Longer crossing structures were associated with decreased mule deer and coyote vigilance behavior, which could mean longer crossing structures are perceived as less risky (Clevenger and Waltho 2005).

Our study detected a fear response to vehicular noise that led to alterations in anti-predator behavior, however vigilance and running responses in deer, and a running response in coyotes decreased during nighttime hours. During nighttime hours, wildlife experience additional exposure to artificial light from headlights. Previous work has shown that wildlife respond differently to vehicular light pollution than to noise pollution, with deer demonstrating an affinity to brightly lit crossing structures (Chapter 2). Future research needs to include experimental playbacks to disentangle the relationship between noise and visual disturbances. Finally, to determine the impact alterations in behavior can have on individual fitness and whether unsuccessful crossings have a population-level impact, future research should examine whether flight is the consistent response of certain individuals, or a proportion of decisions made by all individuals. Individuals could be monitored through GPS telemetry data or software that enables individual recognition from data collected by camera traps. Monitoring individual responses could also shed light on whether fear responses are characteristic of certain personalities. For instance, Eastcott et al. (2020) found among-individual behavioral differences in vigilance behavior to traffic noise playbacks.

4.4 Conclusions

Road networks are expanding globally, with the addition of 25 million km predicted by 2050 (Dulac 2013, Laurance et al. 2014). With this expansion comes increased interactions between wildlife and the human ‘super predator’. Our work demonstrates that a fear response of wildlife to anthropogenic noise stressors is likely to differ depending on spatiotemporal scale and characteristics of the stressor. This dynamic response to fear could alter natural predator-prey interactions and scale up to ecosystem-level consequences such as trophic cascades (Smith et al. 2017, Zanette and Clinchy 2019). To ensure a landscape of coexistence, additional research is needed to understand what anthropogenic stressors drive fear responses in wildlife and how spatiotemporal scale plays a role.

5. Acknowledgements

Funding for this project was made possible by a Dissertation grant from the National Center for Sustainable Transportation (NCST), University of California, Davis, and a research grant from the NCST, supported by U.S. Department of Transportation and the California Department of Transportation through the University Transportation Centers program. We thank Dr. David Waetjen, Rich Codington, Jamie Bourdon, Collin Raff, Catherine Le, Annabelle Louderback-Valenzuela, Mia Guarnieri, Parisa Farman, Mia Macneill, Jeffrey Scott, Pao Perez, Vivian Lei for assistance with data collection and Rachel Alsheikh, Tricia Nguyen and Mia Guarnieri for assistance with video tagging.

6. Literature Cited

Agostinho, C. S., A. A. Agostinho, F. Pelicice, D. A. De Almeida, and E. E. Marques. 2007. Selectivity of fish ladders: A bottleneck in Neotropical fish movement. Neotropical Ichthyology 5:205–213.

Araya-Salas, M., and G. Smith-Vidaurre. 2017. warbleR: an R package to streamline analysis of animal acoustic signals. Methods in Ecology and Evolution 8:184–191.

Bachman, G. C. 1993. The effect of body condition on the trade-off between vigilance and foraging in Belding's ground squirrels. Animal Behaviour 46:233–244.

Bednekoff, P. A., and S. L. Lima. 1998. Randomness, chaos and confusion in the study of antipredator vigilance. Trends in Ecology & Evolution 13:284–287.

Bejder, L., A. Samuels, H. Whitehead, H. Finn, and S. Allen. 2009. Impact assessment research: Use and misuse of habituation, sensitisation and tolerance in describing wildlife responses to anthropogenic stimuli. Marine Ecology Progress Series 395:177–185.

Berger, J. 2007. Fear, human shields and the redistribution of prey and predators in protected areas. Biology Letters 3:620–623.

Blair, H. B., N. D. Merchant, A. S. Friedlaender, D. N. Wiley, and S. E. Parks. 2016. Evidence for ship noise impacts on humpback whale foraging behaviour. Biology Letters 12.

Brown, C. L., A. R. Hardy, J. R. Barber, K. M. Fristrup, K. R. Crooks, and L. M. Angeloni. 2012. The effect of human activities and their associated noise on ungulate behavior. PLoS ONE 7:38–40.

Buxton, R. T., M. F. McKenna, E. Brown, R. Ohms, A. Hammesfahr, L. M. Angeloni, K. R. Crooks, and G. Wittemyer. 2020. Varying behavioral responses of wildlife to motorcycle traffic. Global Ecology and Conservation 21.

Buxton, R. T., M. F. McKenna, D. Mennitt, K. M. Fristrup, K. R. Crooks, L. M. Angeloni, and G. Wittemyer. 2017. Noise pollution is pervasive in U.S. protected areas. Science 356:531–533.

Cardoso, G. C., Y. Hu, and C. D. Francis. 2018. The comparative evidence for urban species sorting by anthropogenic noise. Royal Society Open Science 5:172059.

Castaneda, E., V. R. Leavings, R. F. Noss, and M. K. Grace. 2020. The effects of traffic noise on tadpole behavior and development. Springer Verlag.

Ciuti, S., J. M. Northrup, T. B. Muhly, S. Simi, M. Musiani, J. A. Pitt, and M. S. Boyce. 2012. Effects of Humans on Behaviour of Wildlife Exceed Those of Natural Predators in a Landscape of Fear. PLoS ONE 7.

Clevenger, A. P., and N. Waltho. 2005. Performance indices to identify attributes of highway crossing structures facilitating movement of large mammals. Biological conservation 121:453–464.

Creel, S., and D. Christianson. 2008. Relationships between direct predation and risk effects. Trends in Ecology and Evolution 23:194–201.

Creel, S., and J. A. Winnie. 2005. Responses of elk herd size to fine-scale spatial and temporal variation in the risk of predation by wolves. Animal Behaviour 69:1181–1189.

Darimont, C. T., C. H. Fox, H. M. Bryan, and T. E. Reimchen. 2015. The unique ecology of human predators. Science 349:858–860.

Dominoni, D. M., W. Halfwerk, E. Baird, R. T. Buxton, E. Fernández-Juricic, K. M. Fristrup, M. F. McKenna, D. J. Mennitt, E. K. Perkin, B. M. Seymoure, D. C. Stoner, J. B. Tennessen, C. A. Toth, L. P. Tyrrell, A. Wilson, C. D. Francis, N. H. Carter, and J. R. Barber. 2020. Why conservation biology can benefit from sensory ecology. Nature Ecology and Evolution 4:502–511.

Dröge, E., S. Creel, M. S. Becker, and J. M'Soka. 2017. Risky times and risky places interact to affect prey behaviour /631/158/856 /631/601/18 article. Nature Ecology and Evolution 1:1123–1128.

Dulac, J. 2013. Global land transport infrastructure requirements - Estimating road and railway infrastructure capacity and costs to 2050. International Energy Agency:54.

Francis, C. D., and J. R. Barber. 2013. A framework for understanding noise impacts on wildlife : an urgent conservation priority.

Francis, C. D., N. J. Kleist, and P. Catherine. 2012. Noise pollution alters ecological services : enhanced pollination and disrupted seed dispersal:2727–2735.

Friard, O., and M. Gamba. 2016. BORIS: a free, versatile open-source event-logging software for video/audio coding and live observations. Methods in Ecology and Evolution 7:1325–1330.

Frid, A., and L. Dill. 2002. Human-caused disturbance as a form of predation risk. Journal of Wildlife Management 78:58–67.

Gaynor, K. M., J. S. Brown, A. D. Middleton, M. E. Power, and J. S. Brashares. 2019. Landscapes of Fear: Spatial Patterns of Risk Perception and Response. Trends in Ecology and Evolution 34:355–368.

Gaynor, K. M., M. J. Cherry, S. L. Gilbert, M. T. Kohl, C. L. Larson, T. M. Newsome, L. R. Prugh, and J. P. Suraci. 2020. An applied ecology of fear framework : linking theory to conservation practice:1–14.

Gaynor, K. M., C. E. Hojnowski, N. H. Carter, and J. S. Brashares. 2018. The influence of human disturbance on wildlife nocturnality 1235:1232–1235.

Gill, J. A., K. Norris, and W. J. Sutherland. 2001. Why behavioural responses may not reflect the population consequences of human disturbance. Biological Conservation 97:265–268.

Hammond, T. T., C. A. Ortiz-Jimenez, and J. E. Smith. 2020. Anthropogenic Change Alters Ecological Relationships via Interactive Changes in Stress Physiology and Behavior within and among Organisms. Integrative and comparative biology 60:57–69.

IUCN. 2019. The IUCN Red List of Threatened Species.

Koch, M., and H. U. Schnitzler. 1997. The acoustic startle response in rats - Circuits mediating evocation, inhibition and potentiation. Behavioural Brain Research 89:35–49.

Kuijper, D. P. J., J. W. Bubnicki, M. Churski, B. Mols, and P. Van Hooft. 2015. Context dependence of risk effects : wolves and tree logs create patches of fear in an old-growth forest. Behavioral Ecology 26:1558–1568.

Kuijper, D. P. J., E. Sahlén, B. Elmhagen, S. Chamaillé-Jammes, H. Sand, K. Lone, and J. P. G. M. Cromsigt. 2016. Paws without claws? Ecological effects of large carnivores in anthropogenic landscapes. Proceedings of the Royal Society B: Biological Sciences 283.

Lashley, M. A., M. C. Chitwood, M. T. Biggerstaff, D. L. Morina, C. E. Moorman, and C. S. DePerno. 2014. White-tailed deer vigilance: The influence of social and environmental factors. PLoS ONE 9:1–6.

Laundré, J. W., L. Hernández, and K. B. Altendorf. 2001. Wolves, elk, and bison: reestablishing the “landscape of fear” in Yellowstone National Park, U.S.A. Canadian Journal of Zoology 79:1401–1409.

Laurance, W. F., G. R. Clements, S. Sloan, C. S. O’Connell, N. D. Mueller, M. Goosem, O. Venter, D. P. Edwards, B. Phalan, A. Balmford, R. Van Der Ree, and I. B. Arrea. 2014. A global strategy for road building. Nature 513:229–232.

Le, M.-L. T., C. M. Garvin, J. R. Barber, and C. D. Francis. 2019. Natural sounds alter California ground squirrel, Otospermophilus beecheyi, foraging, vigilance and movement behaviours. Animal Behaviour 157:51–60.

Lima, S. L., and P. A. Bednekoff. 1999. Temporal variation in danger drives antipredator behavior: The predation risk allocation hypothesis. American Naturalist 153:649–659.

Magnhagen, C., K. Johansson, and P. Sigray. 2017. Effects of motorboat noise on foraging behaviour in Eurasian perch and roach: A field experiment. Marine Ecology Progress Series 564:115–125.

McClure, C. J. W., H. E. Ware, J. Carlisle, G. Kaltenecker, and J. R. Barber. 2013. An experimental investigation into the effects of traffic noise on distributions of birds: avoiding the phantom road. Proceedings of the Royal Society B: Biological Sciences

280:20132290–20132290.

Meillère, A., F. Brischoux, and F. Angelier. 2015. Impact of chronic noise exposure on antipredator behavior : an experiment in breeding house sparrows. International Society for Behavioral Ecology 00:1–9.

Moll, R. J., K. M. Redilla, T. Mudumba, A. B. Muneza, S. M. Gray, L. Abade, M. W. Hayward, J. J. Millspaugh, and R. A. Montgomery. 2017. The many faces of fear: a synthesis of the methodological variation in characterizing predation risk. Journal of Animal Ecology 86:749–765.

Mtui, E. K. 2014. Road constraints on impala (Aepyceros melampus) behavior. Norwegian University of Science and Technology.

Nedelec, S. L., S. C. Mills, D. Lecchini, B. Nedelec, S. D. Simpson, and A. N. Radford. 2016. Repeated exposure to noise increases tolerance in a coral reef fish. Environmental Pollution 216:428–436.

Neo, Y. Y., J. Hubert, L. J. Bolle, H. V. Winter, and H. Slabbekoorn. 2018. European seabass respond more strongly to noise exposure at night and habituate over repeated trials of sound exposure. Environmental Pollution 239:367–374.

Owen, M. A., R. R. Swaisgood, and D. T. Blumstein. 2017. Contextual influences on animal decision-making: Significance for behavior-based wildlife conservation and management. Integrative Zoology 12:32–48.

Prugh, L. R., K. J. Sivy, P. J. Mahoney, T. R. Ganz, M. A. Ditmer, M. van de Kerk, S. L. Gilbert, and R. A. Montgomery. 2019. Designing studies of predation risk for improved inference in carnivore-ungulate systems. Biological Conservation 232:194–207.

Quinn, J. L., M. J. Whittingham, S. J. Butler, W. Cresswell, J. L. Quinn, M. J. Whittingham, S. J. Butler, W. Cresswell, and W. Noise. 2006. Predation Risk Compensation and Vigilance in the Chaffinch Fringilla coelebs 37:601–608.

van der Ree, R., D. Heinze, M. McCarthy, and I. Mansergh. 2009. Wildlife tunnel enhances population viability. Ecology and Society 14.

Roberts, G. 1996. Why individual vigilance declines as group size increases. Animal Behaviour 51:1077–1086.

Rogers, L. L. 1992. Watchable wildlife: the black bear. The Station.

Rytwinski, T., and L. Fahrig. 2015. The impacts of roads and traffic on terrestrial animal populations. Pages 237–246 Handbook of Road Ecology.

Rytwinski, T., K. Soanes, J. A. G. Jaeger, L. Fahrig, S. Findlay, J. Houlahan, R. Van Der Ree, and E. A. Van Der Grift. 2016. How Effective Is Road Mitigation at Reducing Road-Kill ? A Meta-Analysis:1–25.

Schmitz, O. J., C. C. Wilmers, S. J. Leroux, C. E. Doughty, T. B. Atwood, M. Galetti, A. B. Davies, and S. J. Goetz. 2018. Animals and the zoogeochemistry of the carbon cycle. Science 362.

Seidler, R. G., D. S. Green, and J. P. Beckmann. 2018. Highways, crossing structures and risk: Behaviors of Greater Yellowstone pronghorn elucidate efficacy of road mitigation. Global Ecology and Conservation 15.

Shannon, G., L. M. Angeloni, G. Wittemyer, K. M. Fristrup, and K. R. Crooks. 2014a. Road traffic noise modifies behaviour of a keystone species 94:135–141.

Shannon, G., L. S. Cordes, A. R. Hardy, L. M. Angeloni, and K. R. Crooks. 2014b. Behavioral responses associated with a human-mediated predator shelter. PLoS ONE 9.

Shannon, G., K. R. Crooks, G. Wittemyer, K. M. Fristrup, and L. M. Angeloni. 2016. Road noise causes earlier predator detection and flight response in a free-ranging mammal. Behavioral Ecology 27:1370–1375.

Siemers, M., and A. Schaub. 2011. Hunting at the highway : traffic noise reduces foraging efficiency in acoustic predators:1646–1652.

Smith, J. A., J. P. Suraci, M. Clinchy, A. Crawford, D. Roberts, L. Y. Zanette, and C. C. Wilmers. 2017. Fear of the human ‘super predator’ reduces feeding time in large carnivores. Proceedings of the Royal Society B: Biological Sciences 284.

Stankowich, T. 2008. Ungulate flight responses to human disturbance: A review and meta-analysis. Biological Conservation 141:2159–2173.

Støen, O. G., A. Ordiz, A. L. Evans, T. G. Laske, J. Kindberg, O. Fröbert, J. E. Swenson, and J. M. Arnemo. 2015. Physiological evidence for a human-induced landscape of fear in brown bears (Ursus arctos). Physiology and Behavior 152:244–248.

Strano, E., F. Simini, M. De Nadai, T. Esch, and M. Marconcini. 2020. Precise mapping, spatial structure and classification of all the human settlements on Earth:1–43.

Sueur, J., T. Aubin, C. Simonis, L. Lellouch, E. C. Brown, M. Depraetere, C. Desjonqueres, F. Fabianek, A. Gasc, E. Kasten, S. LaZerte, J. Lees, J. Marchal, A. Mikulec, S. Pavoine, D. Pinaud, A. Stotz, L. J. Villanueva-Rivera, Z. Ross, C. G. Witthoft, and H. Zhivomirov. 2020. Package “seewave” Type Package Title Sound Analysis and Synthesis.

Suraci, J. P., M. Clinchy, L. Y. Zanette, and C. C. Wilmers. 2019. Fear of humans as apex predators has landscape-scale impacts from mountain lions to mice. Ecology Letters 22:1578–1586.

Suraci, J. P., B. A. Nickel, and C. C. Wilmers. 2020. Fine-scale movement decisions by a large carnivore inform conservation planning in human-dominated landscapes. Landscape Ecology 35:1635–1649.

Tidau, S., and M. Briffa. 2019. Distracted decision makers: Ship noise and predation risk change shell choice in hermit crabs. Behavioral Ecology 30:1157–1167.

Ujvári, M., H. J. Baagøe, and A. B. Madsen. 2004. Effectiveness of acoustic road markings in reducing deer-vehicle collisions: A behavioural study. Wildlife Biology 10:155–159.

Voellmy, I. K., J. Purser, D. Flynn, P. Kennedy, S. D. Simpson, and A. N. Radford. 2014. Acoustic noise reduces foraging success in two sympatric fish species via different mechanisms. Animal Behaviour 89:191–198.

Wale, M. A., S. D. Simpson, and A. N. Radford. 2013. Noise negatively affects foraging and antipredator behaviour in shore crabs. Animal Behaviour 86:111–118.

Walsh, E. P., G. Arnott, and H. P. Kunc. 2017. Noise affects resource assessment in an invertebrate. Biology Letters 13.

Walthers, A. R., and C. A. Barber. 2020. Traffic noise as a potential stressor to offspring of an urban bird, the European Starling. Journal of Ornithology 161:459–467.

Ware, H. E., C. J. W. McClure, J. D. Carlisle, and J. R. Barber. 2015. A phantom road experiment reveals traffic noise is an invisible source of habitat degradation. Proceedings of the National Academy of Sciences 112:12105–12109.

Warren, P. S., M. Katti, M. Ermann, and A. Brazel. 2006. Urban bioacoustics: it's not just noise. Animal behaviour 71:491–502.

Weisenberger, M. E., P. R. Krausman, M. C. Wallace, D. W. De Young, and O. E. Maughan. 1996. Effects of Simulated Jet Aircraft Noise on Heart Rate and Behavior of Desert Ungulates. The Journal of Wildlife Management 60:52.

Wisniewska, D. M., M. Johnson, J. Teilmann, U. Siebert, A. Galatius, R. Dietz, and P. T. Madsen. 2018. High rates of vessel noise disrupt foraging in wild harbour porpoises (Phocoena phocoena). Proceedings of the Royal Society B: Biological Sciences 285.

Zanette, L. Y., and M. Clinchy. 2019. Ecology of fear. Current Biology 29:R309–R313.

Tables

Table 3.1. The relationship (coefficient estimate, standard error and *z*-value) between the decision-making event response variable (flight or entry) and the variables from the top models (lowest AIC) for mule deer and coyotes at highway crossing structures in response to noise pollution. Difference in AIC (ΔAIC) reported for the full model and top model.

Decision-making event	**Parameter**	**Coefficient estimate**	**Standard error**	***z* value**	**AIC (ΔAIC)**
Mule deer	Instantaneous noise (2 seconds)	-0.531	0.278	-1.912	123.23 (0)
	Chronic noise	-1.115	2.082	-0.535	
	Group size				
	Time of day	0.128	0.538	0.239	
	Length of crossing structure	0.112	0.113	0.010	
	Human visitation rate	-2.114	1.932	-1.095	
Coyote	Instantaneous noise (2 seconds)	8.77415	3.354	2.616	43.20 (-6.55)
	Temperature	-1.231	0.518	-2.377	

Table 3.2. The relationship (coefficient estimate, standard error and *t*-value) between each response variable and the variables from the simplified models following step-wise removal of non-significant variables for mule deer and coyotes at highway crossing structures in response to noise pollution.

Deer	**Parameter**	**Coefficient estimate**	**Standard error**	***t* value**
Foraging	Acute noise (~20 seconds)	0.115	0.033	3.479
	Chronic noise	-0.033	0.007	-4.889
	Group size			
	Temperature	0.046	0.003	14.860
	Length of crossing structure	-0.307	0.087	-3.539
	Distance of camera from crossing structure	0.489	0.034	14.220
	Human visitation rate	-2.759	0.320	-8.617
Vigilance	Group size			
	Temperature	-0.006	0.002	-2.933
	Time of day	-0.213	0.060	-3.541
	Length of crossing structure	-0.477	0.057	-8.336
Running	Group size			
	Temperature	-0.023	0.008	-2.934
	Time of day	-1.180	0.212	-5.578
	Distance of camera from crossing structure	-0.225	0.077	-2.919
	Human visitation rate	1.831	0.483	3.790
Coyote				
Vigilance	Chronic noise	-0.096	0.026	-3.714
	Temperature	0.035	0.009	3.853

	Length of crossing structure	-0.690	0.319	-2.165
	Distance of camera from crossing structure	-0.203	0.117	-1.731
Running	Chronic noise	0.122	0.020	6.026
	Time of day	-0.654	0.225	-2.911
	Distance of camera from crossing structure	0.512	0.141	3.630

Figures

Figure 3.1. Map showing locations of crossing structures used in the study (purple dots), labelled with the intersecting highway and site name.

Figure 3.2. Landscape of fear response: Likelihood of A) coyotes and B) deer entering the crossing structure (1 = enter, 0 = repel) in response to instantaneous noise (-/+1 second) at time of decision-making event.

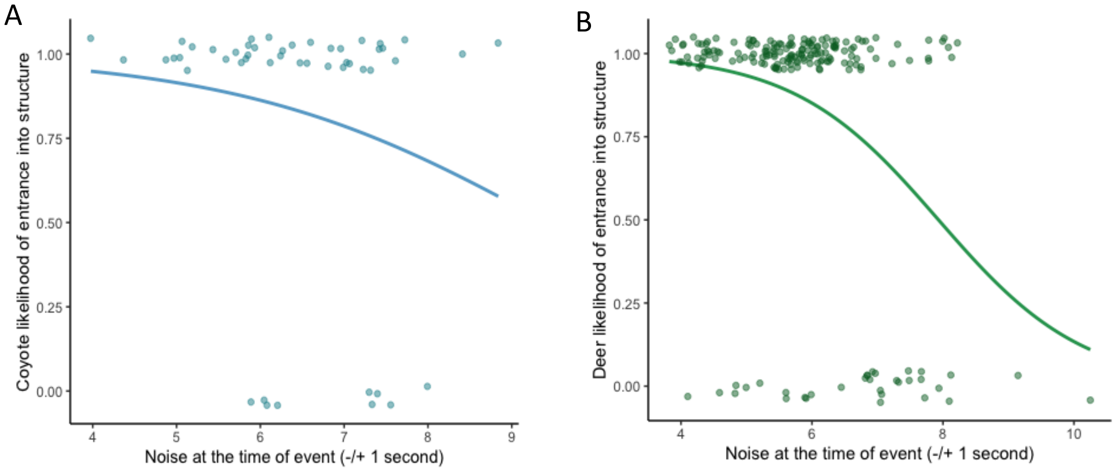

Figure 3.3. Human Shield response: mule deer foraging when exposed to acute noise (20-second duration) at highway crossing structures.

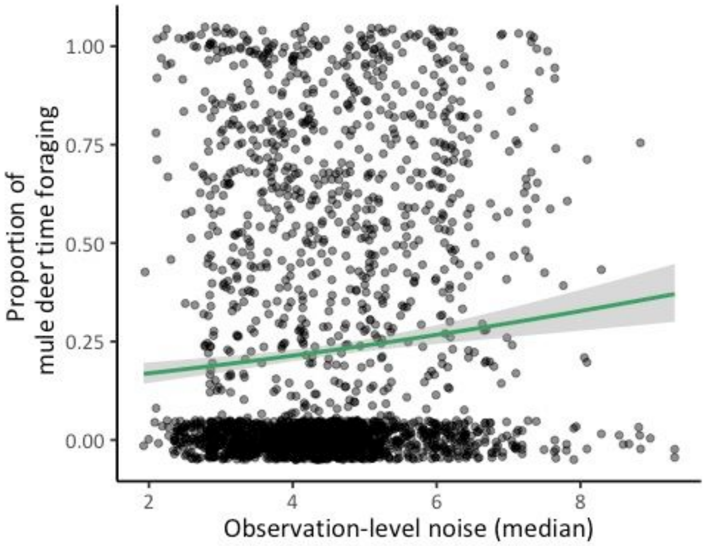

Figure 3.4. Landscape of Fear response: coyote A) vigilance and B) running when exposed to various levels of chronic noise at highway crossing structures (“site-level noise”).

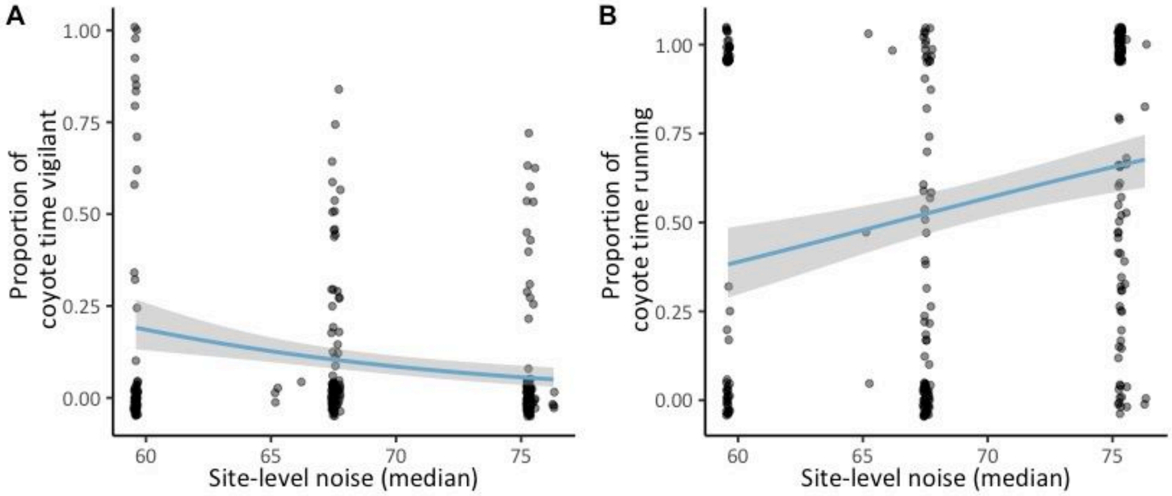

Figure 3.5. Schematic representing the various spatiotemporal levels of noise sampled at crossing structures: instantaneous noise (two seconds, camera station; yellow), acute noise (~20 seconds, camera station; dark blue) and chronic noise (one week, crossing structure; purple), and the mechanism driving responses detected at each level.

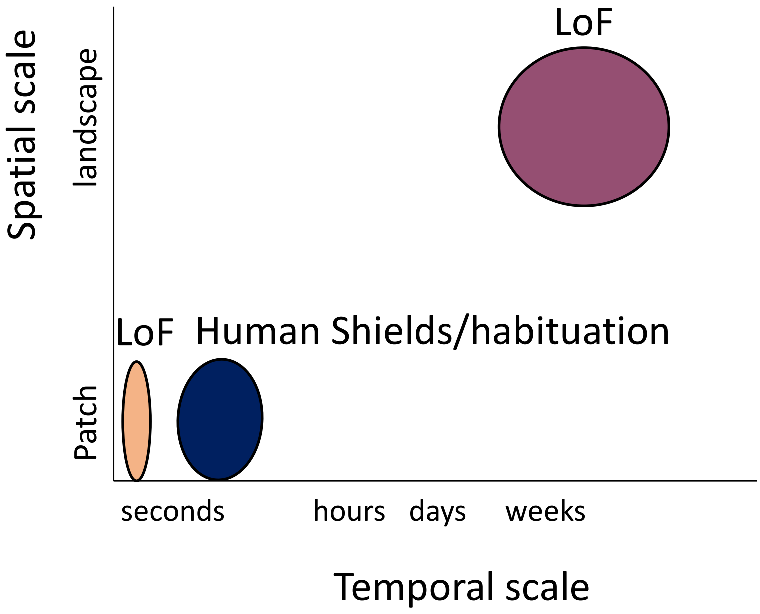

Supplement

Table S3.1. Noise levels measured at each crossing structure. C-weighting (dBC) noise measurements were used for analysis.

Site	Highway	Noise (median dBC)	Noise (Median dBA)
Andrade	I-680	75.5	52.8
Deer Crossing Structure	US 50	65.2	48.9
Gibson Road	I-5	66.2	58.1
Hirschdale	I-80	67.5	56.5
Mesa 2	SR 74	59.6	49.1
PM24	I-80	67.7	59.5
PM6	US 97	54.2	43
Sheep Rock	US 97	55.4	-
Soda Springs	I-80	75.3	61.8
Unknown Bridge	I-80	76.3	64.3

ProQuest LLC
789 East Eisenhower Parkway
P.O. Box 1346
Ann Arbor, MI 48106 - 1346